Supporting Information

Structural diversification of bioactive bibenzyls through modular co-culture leading to the discovery of a novel neuroprotective agent

/

Table of Contents

Supplementary Material and Methods

1,1-Diphenyl-2-picrylhydrazyl (DPPH) assay

1,1-Diphenyl-2-picrylhydrazyl (DPPH) was weighed and dissolved in anhydrous ethanol with 1×10^{-4} mol/L. 100 μL of different concentrations of test solution and 100 μL DPPH ·solution were added to the 96-well plate, and the commonly used antioxidant vitamin C was selected as the positive control (A_1). At the same time, the different concentration of the test solution without DPPH ·(100 μL anhydrous ethanol instead of DPPH ·solution) was used as the control to eliminate the interference of the color of the test product itself on the test results (A_2). In addition, DPPH ·negative control (A_0) was set (100 μL anhydrous ethanol was used instead of the test sample). The 96-well plate was put into a microplate reader, oscillated for 1 min, and stored in this condition (room temperature, away from light) for 30 min. Then the absorbance value was measured at 517 nm.

$$\text{DPPH clearance rate (\%)} = [A_0-(A_1-A_2)]/A_0 \times 100\% \quad \text{(S1)}$$

Pyrogallol autoxidation assay

180 μL of 0.05 mol/L Tris-HCl buffer solution (pH 8.2) was added to the 96-well plate, then 40 μL of sample solution (vitamin C was selected as the positive control) and 16 μL of 9 mmol/L pyrogallol solution were added. 5 min later, 8 μL of 3 mol/L HCl solution was added to terminate the reaction, and the absorbance was measured at 299 nm (A_1). Model control group (A_0) replaced the sample solution with 40 μL water; Reference solution control group ($A_{1'}$) added 40 μL of sample solution to 180 μL of 0.05 mol/ L Tris-HCl buffer solution, and then added 16 μL of water after fully mixing. In blank control group (A_2), pyrogallol and sample solution were replaced with 56 μL water.

$$O_2^{-}\cdot\text{clearance rate (\%)} = [A_0-(A_1-A_{1'}) + A_2]/A_0] \times 100\% \quad \text{(S2)}$$

Fenton reaction

30 μL of 0.75 mmol/L *o*-diphenanthrene solution was added to the 96-well plate. Then 60 μL PBS solution (pH 7.4) and 30 μL distilled water were added. After fully mixing, 30 μL of 0.75 mmol/L ferrous sulfate solution was added. After watering bath at 37 ℃ for 60 minutes, the absorbance was measured at 536 nm (A_0). The above procedure was repeated with 30 μL distilled water instead of H_2O_2 to measure absorbance (A_1), then repeated with 30 μL test solution instead of 30 μL distilled water to determine absorbance (A_2); Only PBS solution and test solution were added, and the other reagents were supplemented with distilled water. The above procedure was repeated to measure the absorbance (A_3); only PBS solution was added, other reagents with distilled water was replaced to supplement. The above operation was repeated, and the absorbance(A_4) was measured.

$$\text{OH clearance rate (\%)} = [(A_2 - A_3 - A_0 + A_4)/(A_1 - A_0)] \times 100\% \quad \text{(S3)}$$

Oxygen radical absorbance capacity (ORAC) assay

20 μL of sample solution (vitamin C was selected as the positive control) was added to each well of the 96-well plate, then added 20 μL of 75 mmol/L potassium phosphate buffer and 140 μL of 18.3 mmol/L AAPH, and finally added 20 μL of 630 nmol/L sodium fluorescein to start the reaction. The 96-well plate was quickly placed in a fluorescence microplate reader (preset temperature 37 ℃) to start the measurement, and a point was measured every 2 min until the fluorescence intensity attenuated to a straight line. The antioxidant capacity of compounds could be reflected by comparing the protected integral area net AUC on the fluorescence decay curve (the integral area under the fluorescence decay curve minus the area under the blank curve without antioxidant).

Determination of 8-hydroxy-2′-deoxyguanosine (8-OHDG)

The level of 8-OHDG was detected following the ELISA kit instruction (Cusabio, Wuhan, China). 100 μL standard or the supernatant of brain tissue homogenate was added per well, and incubated for 2 h at 37 ℃. Then 100 μL Biotin-antibody was added to each well after removing the liquid, and incubated for 1 h at 37 ℃. Each well was aspirated and washed, and the process was repeated two times for a total of three washes. Then the steps were repeated using HRP-avidin before a total of five washes. At last, 90 μL TMB substrate was added and incubated for 15 min at 37 °C and 50 μL Stop solution to stop the reaction. The optical density of each well was determined within 5 min by using a microplate reader set to 450 nm.

Determination of Protein Carbonyl

Carbonylation of proteins was detected by Protein Carbonyl Colorimetric Assay. The supernatant of brain tissue homogenate was transferred to a clean centrifuge tube, and streptomycin sulfate with 10% volume fraction was dropped, fully mixed, and shaken intermittently at room temperature for 10 min. After centrifugation at 11,000 × g for 5 min, 100 μL supernatant was added 400 μL of 10 mmol/ L DNPH (dissolved in 2 mol/ L HCl). A blank control group was set, which was 2 mol/L HCl solution without DNPH. Each reaction system was placed in the dark for 1 h and swirled once every 10 min. After the reaction, 500 μL of 0.2 kg/L trichloroacetic acid (TCA) solution was added to precipitate the protein hydrazone derivative. Centrifugation was performed at 4 ℃ at 12,000 × g for 15 min, and the supernatant was discarded. The precipitation was washed with 1 mL ethanol and ethyl acetate mixture (V/V = 1:1) for 3 times, and the final precipitation was dissolved with 1.25 mL of 6 mol/L guanidine hydrochloride (37 ℃ for 15 min). After centrifugation at 12,000 × g for 15 min, the absorbance value of supernatant was measured at 370 nm.

Quantitative RT-PCR

The rat brain tissue was homogenized with Trizol reagent (1 mL for 100 mg of tissue, TransGen Biotech, Cat ET111). 1 mL of homogenate was mixed with 200 μL chloroform in a centrifuge tube and centrifuged at 10,000 × g for 15 min at 4 ℃. The supernatant was then mixed with 500 μL of isopropyl alcohol in a new 1.5 mL centrifuge tube and centrifuged at 10,000 × *g* for 10 min at 4 ℃. After discarding the supernatant, the precipitate was rinsed with 1 mL of 75% absolute ethanol (750 μL absolute ethanol and 250 μL of DEPC water). After centrifugation at 10,000 × g for 5 min at 4 ℃, the supernatant was discarded and the RNA was resuspended in 50 μL of DEPC water. After uniform quantification, mRNA was reverse transcribed into cDNA using Revert Aid First Strand cDNA Synthesis Kit (Yeasen, Cat 11141ES60). cDNA was generated by reverse transcription at 25 ℃ for 5 min, 55 ℃ for 15 min and 85 ℃ for 5 min. The qRT-PCR conditions were as follows: 95 ℃ for 30 s, followed by 40 cycles of 95 ℃ for 10 s, and 60 ℃ for 30 s. The primer sequences used for qRT-PCR are shown in **Table S4**. The relative expression of objective mRNA was normalized to β-actin mRNA and calculated using the $2^{-\Delta\Delta CT}$ method.

Western Blot

Protein samples from operative hemispheres of rats and SK-N-SH were prepared using RIPA lysis buffer supplemented with complete EDTA-free protease inhibitor mixtures (4693116001, Roche, Indianapolis, IN) and phosphatase inhibitor mixtures (04906845001, Roche, Indianapolis, IN). Protein samples were separated on SDS-polyacrylamide gels and transferred to PVDF membranes. The membrane was blocked with 5% nonfat milk for 2 h and subsequently incubated with the following primary antibodies overnight at 4 ℃: anti-β-actin (1:2000, ZSGB-BIO, TA-09), anti-Aifm3 (1:500, proteintech, 14778-1-AP), anti-Nrf-2 (1:2000, proteintech, 16396-1-AP), anti-HO-1 (1:2000, Abcam, ab189491), anti-NQO-1 (1:2000, Abcam, ab80588). Then anti-mouse or anti-rabbit IgG-HRP (1:2000, ZSGB-BIO, ZB-2301; ZB-2305) were used as secondary antibodies for 2 h at room temperature, signals were detected using Image Quant LAS 500 (GE Healthcare). Three samples per group were used for western blot analysis.

Supplementary Tables

Table S1. Genes used in this study.

Gene	Full name	Source organism	Source
DoBBS1	Bibenzyl synthase	*Dendrobium officinale*	This study
DoBBS2	Bibenzyl synthase	*D. officinale*	This study
DoBBS3	Bibenzyl synthase	*D. officinale*	This study
DoBBS4	Bibenzyl synthase	*D. officinale*	This study
DoBBS5	Bibenzyl synthase	*D. officinale*	This study
DoBBS6	Bibenzyl synthase	*D. officinale*	This study
DoBBS7	Bibenzyl synthase	*D. officinale*	This study
DoBBS8	Bibenzyl synthase	*D. officinale*	This study
DoBBS9	Bibenzyl synthase	*D. officinale*	This study
DoOMT1	*O*-methyltransferase	*D. officinale*	This study
DoOMT2	*O*-methyltransferase	*D. officinale*	This study
DoOMT3	*O*-methyltransferase	*D. officinale*	This study
DoOMT4	*O*-methyltransferase	*D. officinale*	This study
DoOMT5	*O*-methyltransferase	*D. officinale*	This study
DoOMT6	*O*-methyltransferase	*D. officinale*	This study
DoOMT7	*O*-methyltransferase	*D. officinale*	This study
DoOMT8	*O*-methyltransferase	*D. officinale*	This study
DoOMT9	*O*-methyltransferase	*D. officinale*	This study
DoOMT10	*O*-methyltransferase	*D. officinale*	This study
DoOMT11	*O*-methyltransferase	*D. officinale*	This study
metK	*S*-adenosylmethionine synthetase	*Escherichia. coli*	Markham et al[1].
PsPT1	Prenyltransferase	*Periconia* sp. F-31	This study
UGT71E5	Glycosyltransferase	*Carthamus tinctorius*	Xie et al[2].
At4CL1	4-coumarate coenzyme A ligase	*Aradopsis thaliana*	Ehlting et al[3].
AAE13	Malonyl-CoA synthase	*A. thaliana*	Chen et al[4].
MatC	malonate carrier protein	*Rhizobium trifolii*	An et al[5].
MK	Mevalonate kinase	*Staphylococcus aureus*	Wang et al[6].
PMK	Phosphomevalonate kinase	*S. aureus*	Wang et al[6].
PMD	Mevalonate pyrophosphate decarboxylase	*S. aureus*	Wang et al[6].
IDI	IPP isomerase	*Bacillus subtilis*	Wang et al[6].
AACT	Acetoacetyl-CoA thiolase	*E. coli*	Wang et al[6].
HMGS	HMG-CoA synthase	*Enterococcus. faecalis*	Wang et al[6].
HMGR	Truncated HMG-CoA reductase	*E. faecalis*	Wang et al[6].

Table S2. Plasmids used in this study.

Plasmids	Detailed information	Source
pET-28a	T7 promoters, pBR322 ori, Kan^R	Novagen
pET-21c	T7 promoters, pBR322 ori, Amp^R	Novagen
pACYCDuet-1	Double T7 promoters, p15A ori, Cm^R	Novagen
pETDuet-1	Double T7 promoters, ColE1 ori, Amp^R	Novagen
pCDFDuet-1	Double T7 promoters, CDF ori, Sm^R	Novagen
p01	pET-28a-*DoBBS1*	This study
p02	pET-28a-*DoBBS2*	This study
p03	pET-28a-*DoBBS3*	This study
p04	pET-28a-*DoBBS4*	This study
p05	pET-28a-*DoBBS5*	This study
p06	pET-28a-*DoBBS6*	This study
p07	pET-28a-*DoBBS7*	This study
p08	pET-28a-*DoBBS8*	This study
p09	pET-28a-*DoBBS9*	This study
p10	pET-28a-*DoOMT1*	This study
p11	pET-28a-*DoOMT2*	This study
p12	pET-28a-*DoOMT3*	This study
p13	pET-28a-*DoOMT4*	This study
p14	pET-28a-*DoOMT5*	This study
p15	pET-28a-*DoOMT6*	This study
p16	pET-28a-*DoOMT7*	This study
p17	pET-28a-*DoOMT8*	This study
p18	pET-28a-*DoOMT9*	This study
p19	pET-28a-*DoOMT10*	This study
p20	pET-28a-*DoOMT11*	This study
p21	pCDFDuet-1-*metK*	This study
p22	pETDuet-1-*AAE13-MatC*	This study
p23	pCDFDuet-1-*DoBBS8*	This study
p24	pACYCDuet-1-*At4CL1*	This study
p25	pCDFDuet-1-*PsPT1*	This study
p26	pET-28a-*UGT71E5*	This study
pXL13	pET-28a-*MK-PMK-PMD-IDI*	This study
pXL17	pET-21c-*AACT-HMGS-HMGR*	This study

Table S3. Strains used in this study.

Strains	Detailed information	Source
E01	*Trans*etta (DE3): p01	This study
E02	*Trans*etta (DE3): p02	This study
E03	*Trans*etta (DE3): p03	This study
E04	*Trans*etta (DE3): p04	This study
E05	*Trans*etta (DE3): p05	This study
E06	*Trans*etta (DE3): p06	This study
E07	*Trans*etta (DE3): p07	This study
E08	*Trans*etta (DE3): p08	This study
E09	*Trans*etta (DE3): p09	This study
E10	*Trans*etta (DE3): p10	This study
E11	*Trans*etta (DE3): p11	This study
E12	*Trans*etta (DE3): p12	This study
E13	*Trans*etta (DE3): p13	This study
E14	*Trans*etta (DE3): p14	This study
E15	*Trans*etta (DE3): p15	This study
E16	*Trans*etta (DE3): p16	This study
E17	*Trans*etta (DE3): p17	This study
E18	*Trans*etta (DE3): p18	This study
E19	*Trans*etta (DE3): p19	This study
E20	*Trans*etta (DE3): p20	This study
E-DoBBS8	BL21(DE3): p22, p23, p24	This study
E-DoOMT1	BL21(DE3): p10, p21	This study
E-DoOMT6	BL21(DE3): p15, p21	This study
E-PsPT1	BL21(DE3): p25, pXL13, pXL17	This study
E-UGT71E5	*Trans*etta (DE3): p26	Xie et al[2].

Table S4. Primers used in this study.

Primer	Sequence (5′→3′)
DoBBS1-F	CAGCAAATGGGTCGCGGATCCATGCCGAGCCTTGAATCCATCAG
DoBBS1-R	GTGGTGGTGGTGGTGCTCGAGTCAGAGATGGACACTGCGTAGAAC
DoBBS2-F	CAGCAAATGGGTCGCGGATCCATGCCGAGCCTTGAATCCATCAG
DoBBS2-R	GTGGTGGTGGTGGTGCTCGAGTCAGAGATGGACACTGCGTAGAAC
DoBBS3-F	CAGCAAATGGGTCGCGGATCCATGCCGAGCCTTGAATCCATCAG
DoBBS3-R	GTGGTGGTGGTGGTGCTCGAGTCAGAGATGGACACTGCGTAGAAC
DoBBS4-F	CAGCAAATGGGTCGCGGATCCATGCCGAGCCTTGAATCCATCAG
DoBBS4-R	GTGGTGGTGGTGGTGCTCGAGTCAGAGATGGACACTGCGTAGAAC
DoBBS5-F	CAGCAAATGGGTCGCGGATCCATGCCGAGCCTTGAATCCATCAG
DoBBS5-R	GTGGTGGTGGTGGTGCTCGAGTCAGAGAGGGACACTGCGTAGAAC
DoBBS6-F	CAGCAAATGGGTCGCGGATCCATGCCGAGCCTTGAATCCATCAG
DoBBS6-R	GTGGTGGTGGTGGTGCTCGAGTCAGAGAGGGACACTGCGTAGAAC
DoBBS7-F	CAGCAAATGGGTCGCGGATCCATGAAAGCTGTTAGAAAAGTAAC
DoBBS7-R	GTGGTGGTGGTGGTGCTCGAGTCAAACAAGAGGAGCGCTACGAAG
DoBBS8-F	CAGCAAATGGGTCGCGGATCCATGCCGAGCCTTGAATCCATCAA
DoBBS8-R	GTGGTGGTGGTGGTGCTCGAGTCAAATTGGAACACTGCGGAGGAT
DoBBS9-F	CAGCAAATGGGTCGCGGATCCATGCCGAGCCTTGAATCCATCAA
DoBBS9-R	GTGGTGGTGGTGGTGCTCGAGTCAAATTGGAACACTGCGGAGGAT
DoOMT1-F	CAGCAAATGGGTCGCGGATCCATGGATTCAGAATCTCATCAG
DoOMT1-R	GTGGTGGTGGTGGTGCTCGAGTTTGCTCAACTCCATTATCCAAGC
DoOMT2-F	CAGCAAATGGGTCGCGGATCCATGGGCAGTTACAACGCCACCG
DoOMT2-R	GTGGTGGTGGTGGTGCTCGAGCTTGATGAATTCCATAACCCAAC
DoOMT3-F	CAGCAAATGGGTCGCGGATCCATGGGTTCAGAATCTCATAAAC
DoOMT3-R	GTGGTGGTGGTGGTGCTCGAGTTTGCTCAACTCCATTATCCAAGC
DoOMT4-F	CAGCAAATGGGTCGCGGATCCATGGCGGCCTCCGGCGGAGAAAT
DoOMT4-R	GTGGTGGTGGTGGTGCTCGAGCTTCTGGAACTCTAGAACAGTA
DoOMT5-F	CAGCAAATGGGTCGCGGATCCATGCCAGAATTAAGCAATAAAAC
DoOMT5-R	GTGGTGGTGGTGGTGCTCGAGAATCCAAGCTTCTATGACATGC
DoOMT6-F	CAGCAAATGGGTCGCGGATCCATGGACGGTGATGATCTCTCC
DoOMT6-R	GTGGTGGTGGTGGTGCTCGAGGACGACGCGGCGGCAAATCGTG
DoOMT7-F	CAGCAAATGGGTCGCGGATCCATGGACGTTGATGATCTCTCCAC
DoOMT7-R	GTGGTGGTGGTGGTGCTCGAGGACGACGCGGCGGCAAATCGTG
DoOMT8-F	CAGCAAATGGGTCGCGGATCCATGGCTAATCCTGGTAGAATTTTC
DoOMT8-R	GTGGTGGTGGTGGTGCTCGAGAGCAACCCGCCTACAAATGG
DoOMT9-F	CAGCAAATGGGTCGCGGATCCATGGCGATATCACCTCCGTCCC
DoOMT9-R	GTGGTGGTGGTGGTGCTCGAGCTCCCTTTTGCGGCAGATTGTC
DoOMT10-F	CAGCAAATGGGTCGCGGATCCATGGCGACCGCCACCGCGGAGG

DoOMT10-R	GTGGTGGTGGTGGTGCTCGAGGCTAACACGGCGGCAGAGAGTA
DoOMT11-F	CAGCAAATGGGTCGCGGATCCATGCAGTGCCTATTGCAGAGTC
DoOMT11-R	GTGGTGGTGGTGGTGCTCGAGTTTGATTCGCCTGCAAATGGTG
pACYC-*At4CL1*-F	GCAGATCTCAATTGGATGGCGCCACAAGAACAAGC
pACYC-*At4CL1*-R	ATCGCGTGGCCGGCCTCACAATCCATTTGCTAG
pCDF-*DoBBS8*-F	GCAGATCTCAATTGGATGCCGAGCCTTGAATCC
pCDF-*DoBBS8*-R	ATCGCGTGGCCGGCCTTAAATTGGAACACT
pETD-*MatC*-F	GCAGATCTCAATTGGATGGGTATTGAACTGC
pETD-*MatC*-R	ATCGCGTGGCCGGCCTTAAACCAGACCCGG
pETD-*AAE13*-F	GCAGGTCGACAAGCTTATGGAAGTGTTTAAAGC
pETD-*AAE13*-R	CCGCTCGACTTAAGCATTATTCTTGATTTTCCAGAG
pCDF-*metK*-F	ATGGCAGATCTCAATTGGATGGCAAAACACCTTTTTACG
pCDF-*metK*-R	GCGATCGCGTGGCCGGCCGATATTTACTTCAGACCGGCAG
pCDF-*PsPT1*-F	ATGGCAGATCTCAATTGGATGTCTCACACCGTCGT
pCDF-*PsPT1*-R	GCGATCGCGTGGCCGGCCGATATCTAGTTGGGGAGATAG
β-actin-F	TGAAAAGATGACCCAGGACTCTC
β-actin-R	TGATCTCATCTGGGAAAGAGCA
Aifm 3-F	CAGGACTGTGTGGAGGCTAC
Aifm 3-R	GGGACAGCACACCTTTCACC
Bax-F	AGAGGATGATTGCTGATGTGG
Bax-R	CCCAGTTGAAGTTGCCGT
Bcl-2-F	GATAACGGAGGCTGGGATGC
Bcl-2-R	ATGCACCCAGAGTGATGCAG
Caspase-3-F	GAGCTTGGAACGCGAAGAAA
Caspase-3-R	AGTCCATCGACTTGCTTCCA
Cytochrome c-F	CCAGCCCGGACCGAATTTA
Cytochrome c-R	CTGTCTTCCGCCCAAACAGA

Table S5. Evaluation the neuroprotective effect of the bibenzyl derivatives on the damaged cells induced by glutamate.

Group	Drug concentration	Relative survival rate (%)			Improved survival rate (%)	*P* value
Control		100	100	100	-	-
Model	29 mM	62.53	63.02	65.01	-	0.000
Resveratrol	10 μM	72.80	78.16	75.45	18.83	0.017
12	10 μM	71.21	72.30	76.29	**15.32**	0.006
13	10 μM	65.95	72.23	76.19	12.43	0.076
9	10 μM	65.45	70.90	72.09	9.36	0.061
4	10 μM	64.05	68.10	73.73	7.97	0.133
15	10 μM	65.34	67.50	67.75	5.27	0.028
1	10 μM	64.08	67.35	66.91	4.08	0.098
10	10 μM	63.89	67.50	66.64	3.93	0.131
20	10 μM	64.19	66.35	67.41	3.88	0.036
21	10 μM	62.94	65.22	66.38	2.08	0.126
14	10 μM	63.55	64.37	63.87	0.67	0.654
7	10 μM	60.63	62.85	65.73	-0.74	0.613
22 and **23**	10 μM	58.92	62.52	66.06	-1.65	0.534
16	10 μM	60.68	62.15	63.99	-1.98	0.054
19	10 μM	59.06	59.69	63.89	-4.19	0.074
11	10 μM	59.39	54.87	57.91	-9.63	0.057

Table S6. HPLC methods used in this study.

Method	Solvent A	Solvent B	Gradient	
1	0.1% formic acid aqueous solution	Acetonitrile	15–45% B, 25 min; 45–100% B, 10 min; 100% B, 5 min	Analysis for bibenzyl derivatives
2	0.1% trifluoroacetic acid aqueous solution	Acetonitrile	0% B, 5 min; 0–40% B, 20 min; 40–100% B, 3 min; 100% B, 3 min	Analysis for the CoA derivatives
3	ddH_2O	Acetonitrile	20–40% B, 20 min; 40–100% B, 5 min; 100% B, 5 min	Preparation for the methylated bibenzyl derivatives
4	0.1% formic acid aqueous solution	Acetonitrile	15–40% B, 20 min; 40–100% B, 5 min; 100% B, 5 min	Preparation for the prenylated bibenzyl derivatives
5	ddH_2O	Acetonitrile	15–30% B, 15 min; 30–100% B, 5 min; 100% B, 5min	Preparation for the glycosylated bibenzyl derivatives
6	ddH_2O	Acetonitrile	15–45% B, 25 min; 45–100% B, 2 min; 100% B, 5min	Preparation for the methylated/ prenylated and glycosylated bibenzyl derivatives

Supplementary Figures

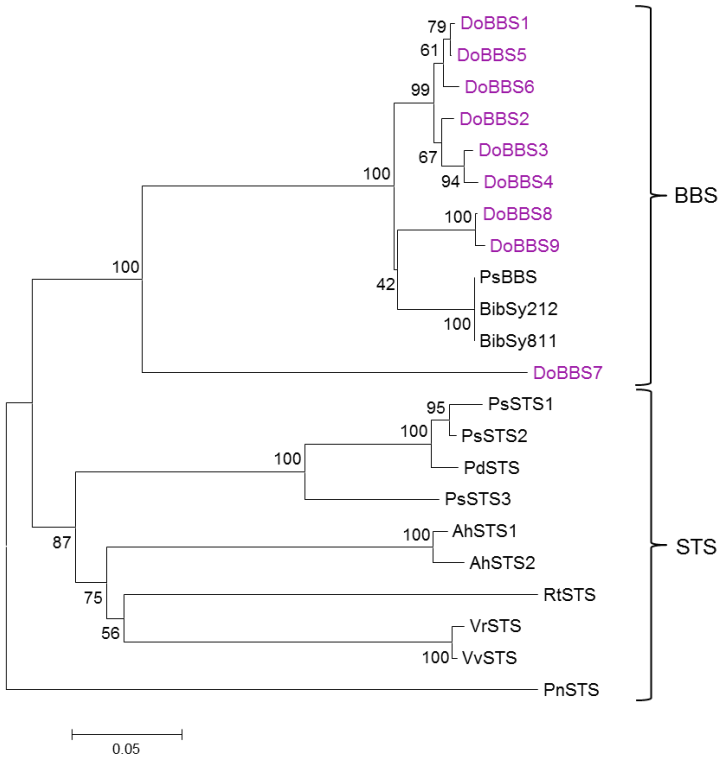

Figure S1. Phylogenetic analysis of DoBBSs with plant bibenzyl synthases (BBSs) and stilbene synthases (STSs). The results were calculated using the MEGA version 6 software. Method: Neighbor-joining, Bootstrap: 1000. The branch lengths represent relative genetic distances. The protein sequences and corresponding accession numbers that were used for this comparasion are as follows: PsBBS (P53416); BibSy212 (CAA56276); BibSy811 (CAA56277); PsSTS1 (AAB24341); PsSTS2 (CAA43165); PdSTS (BAA94953); PsSTS3 (P48407); AhSTS1 (BAA78617); AhSTS2 (P20178); VrSTS1 (AAF00586); VvSTS (CAA54221); RtSTS (AAP13782); PnSTS (BAA87925).

Figure S2. Multiple alignment of DoBBSs and reported BBS, STS from plants. C164-H303-N336 are the conserved catalytic triad motif in PKSs.

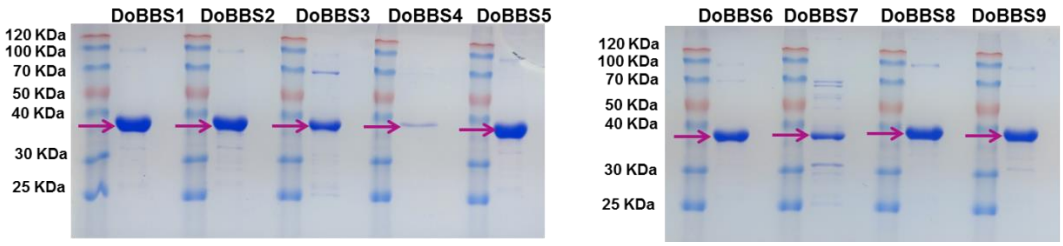

Figure S3. SDS-PAGE analysis of purified proteins of DoBBSs.

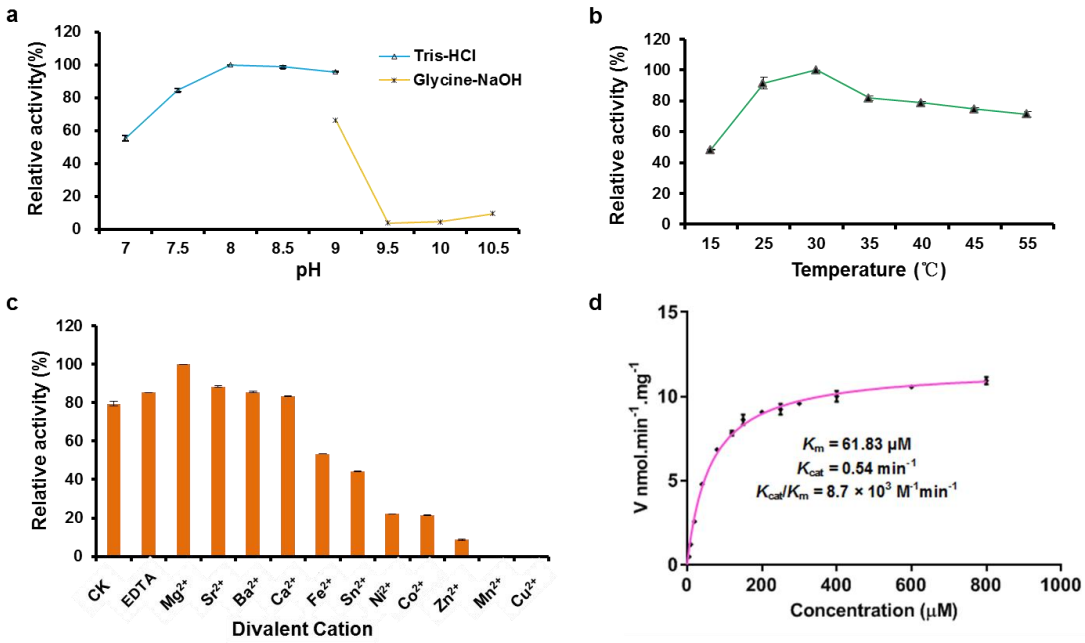

Figure S4. Biochemical characterization of DoBBS8. Effects of (a) pH of buffers, (b) temperature, (c) divalet metal ions on enzyme activity of DoBBS8 with *p*-hydroxyphenylpropionyl-CoA as the starter unit and malonyl-CoA as the extender unit. (d) Kinetic analysis of DoBBS8 towards *p*-hydroxyphenylpropionyl-CoA. The error bars show the SD (n = 2).

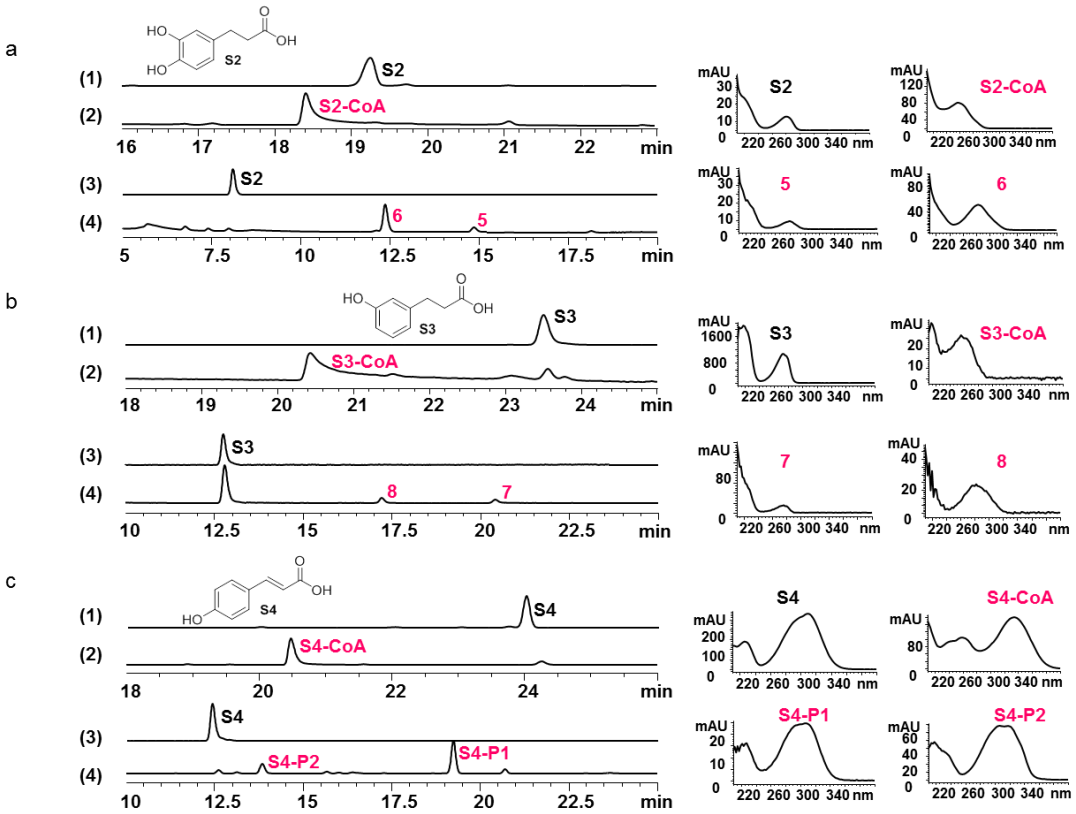

Figure S5. Substrate promiscuity of the purified DoBBS8. HPLC analysis of the enzymatic reactions with the substrate of **S2** (a)/**S3** (b)/**S4** (c); HPLC analysis (λ = 254 nm) of (1) the standards **S2–S4**, (2) the enzymatic reactions catalyzed by the purified At4CL1 with CoA and **S2–S4** as substrates on the Tosoh TSK gel ODS column; HPLC analysis (λ = 280 nm) of (3) the standards **S2–S4**, (4) the casade reactions catalyzed by the purified At4CL2, AAE13 and DoBBS8, with malonic acid, CoA, and **S2–S4** as substrates on the Shiseido Capcell Pak C18 MGIII column.

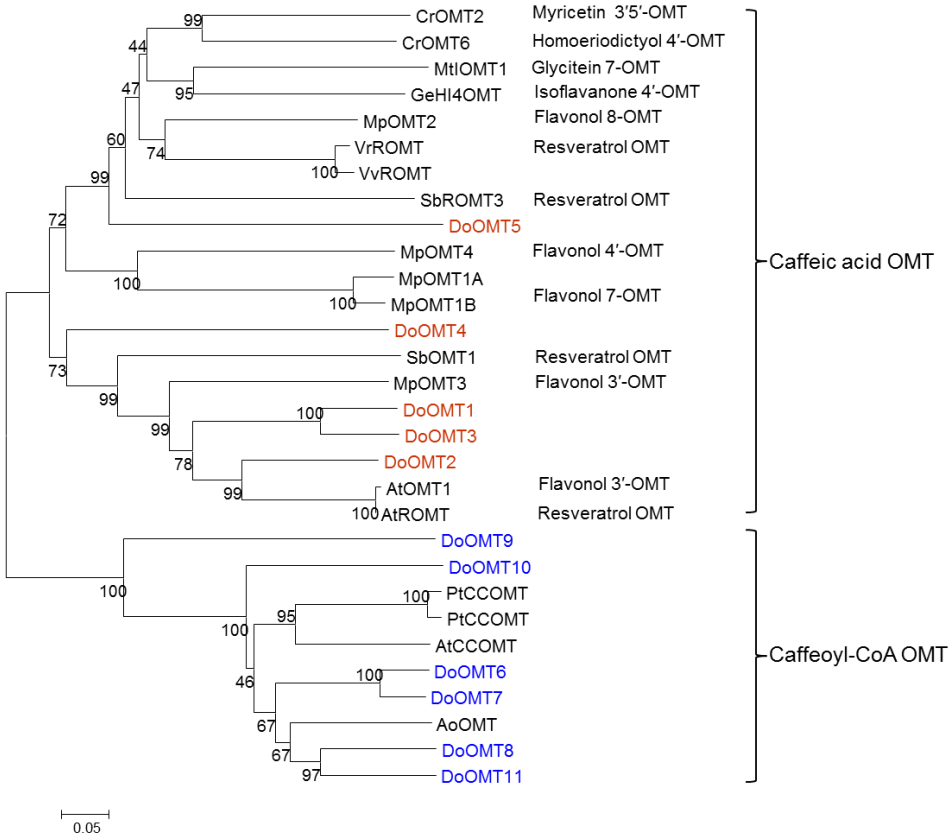

Figure S6. Phylogenetic analysis of DoOMTs with plant OMTs. The results were calculated using the MEGA version 6 software. Method: Neighbor-joining, Bootstrap: 1000. The branch lengths represent relative genetic distances. The protein sequences and corresponding accession numbers that were used for this comparasion are as follows: AtOMT1 (U70424); CrOMT2 (AY127568); CrOMT6 (AY343490); MpOMT1A (AY337457); MpOMT1B (AY337458); MpOMT2 (AY337459); MpOMT3 (AY337460); MpOMT4 (AY337461); MtIOMT1 (AY942159); GeHI4′OMT (AB091684); AtROMT (AY062837); VrROMT (JX673941); SbOMT1 (EF189707); SbROMT3 (JX673942); VvROMT (NM_001281115); AoOMT (XP_020252875); PtCCOMT (XP_002312473); AtCCOMT (NP_564916); PtCCOMT (AFZ78549).

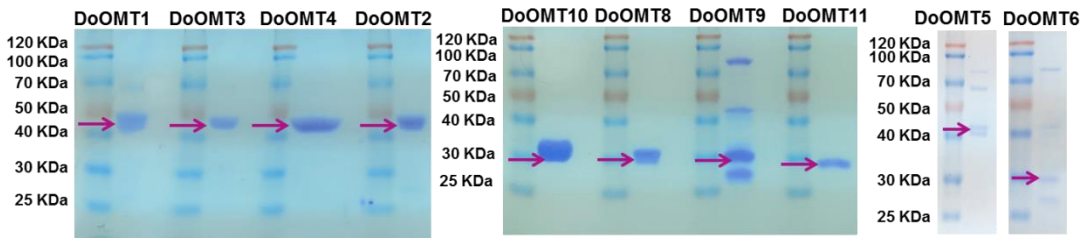

Figure S7. SDS-PAGE analysis of purified proteins of DoOMTs.

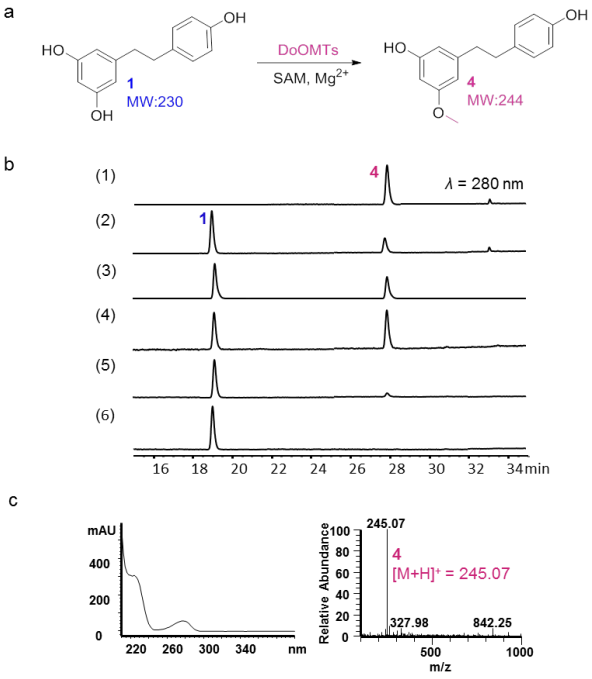

Figure S8. Functional characterization of DoOMTs. (a) Enzymatic reaction catalyzed by DoOMTs; (b) HPLC analysis (λ = 280 nm) of the reactions with (1) DoOMT1, (2) DoOMT2, (3) DoOMT3, (4) DoOMT4, (5) DoOMT5, (6) boiled DoOMT1; (c) UV and MS spectra of product **4** at positive mode.

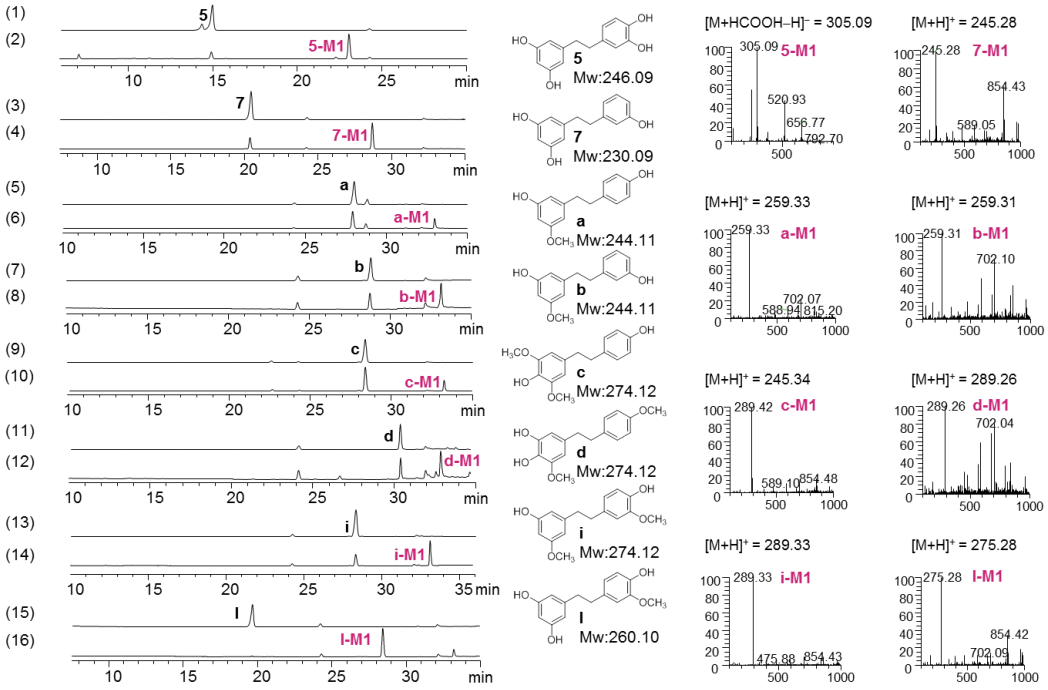

Figure S9. Substrate promiscuity analysis of the purified DoOMT1. HPLC-MS analysis (λ = 280 nm) of the standard substrates of (1) **5**, (3) **7**, (5) **a**, (7) **b**, (9) **c**, (11) **d**, (13) **i**, (15) **l**, and the reactions catalyzed by DoOMT1 with substrates of (2) **5**, (4) **7**, (6) **a**, (8) **b**, (10) **c**, (12) **d**, (14) **i**, (16) **l**.

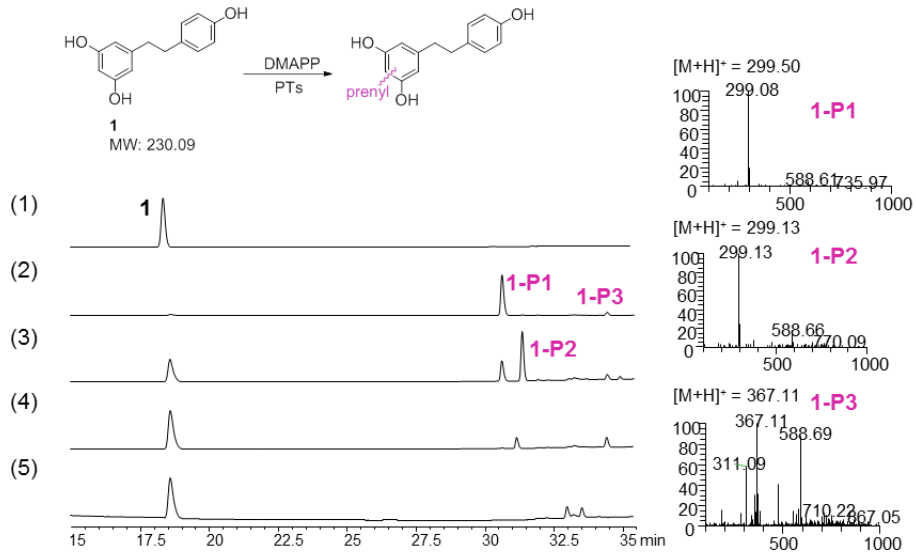

Figure S10. Screening for bibenzyl prenyltransferases. HPLC-MS analysis (λ = 280 nm) of the standard substrate of (1) **1**, and the reactions catalyzed by (2) PsPT1, (3) ScPT1, (4) AtaPT[7], (5) PsPT2.

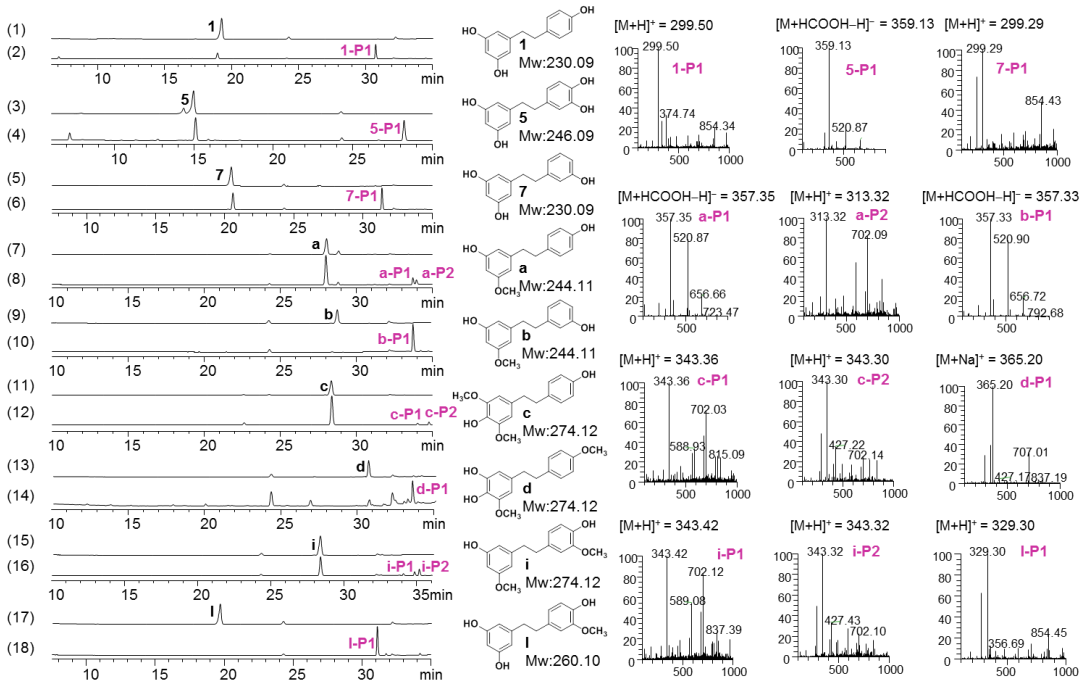

Figure S11. Substrate promiscuity analysis of the purified PsPT1. HPLC-MS analysis (λ = 280 nm) of the standard substrates of (1) **1**, (3) **5**, (5) **7**, (7) **a**, (9) **b**, (11) **c**, (13) **d**, (15) **i**, (17) **l**, and the reactions catalyzed by PsPT1 with substrates of (2) **1**, (4) **5**, (6) **7**, (8) **a**, (10) **b**, (12) **c**, (14) **d**, (16) **i**, (18) **l**.

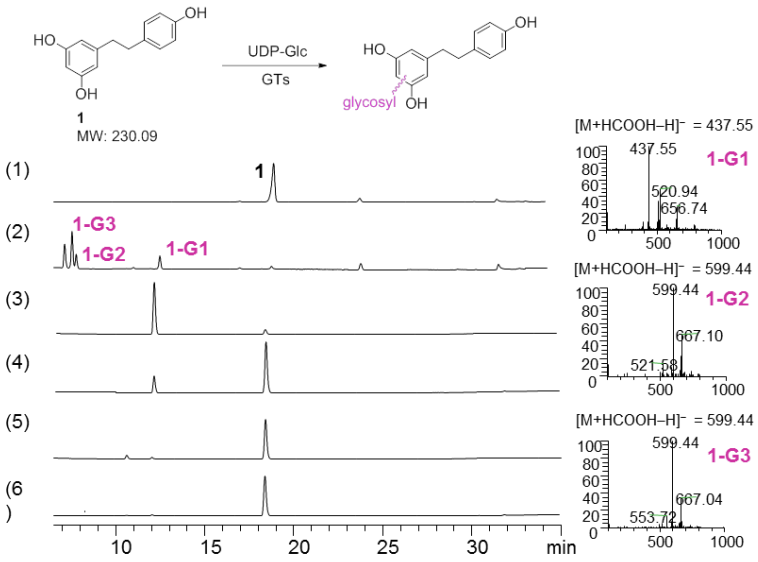

Figure S12. Screening for bibenzyl glycosyltransferases. HPLC-MS analysis (λ = 280 nm) of the standard substrate of (1) **1**, and the reactions catalyzed by (2) UGT71E5[2], (3) MiCGT[8], (4) UGT73AE1[9], (5) UGT88B2[10], (6) MiCGTb[11,12].

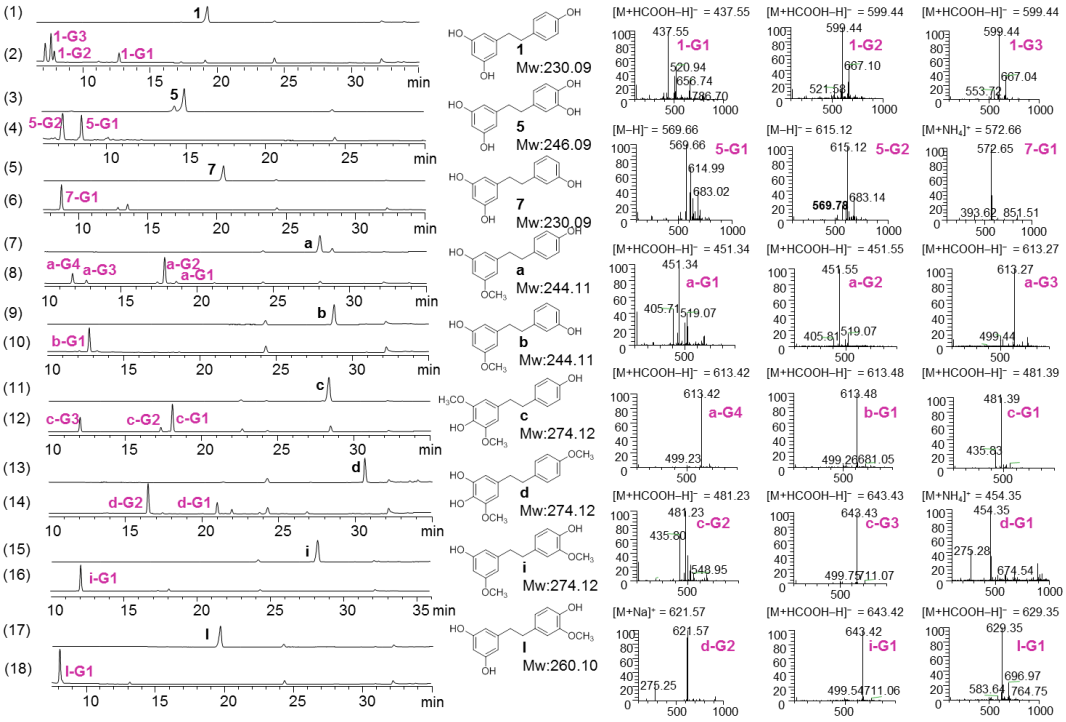

Figure S13. Substrate promiscuity analysis of the purified UGT71E5. HPLC-MS analysis (λ = 280 nm) of the standard substrates of (1) **1**, (3) **5**, (5) **7**, (7) **a**, (9) **b**, (11) **c**, (13) **d**, (15) **i**, (17) **l**, and the reactions catalyzed by UGT71E5 with substrates of (2) **1**, (4) **5**, (6) **7**, (8) **a**, (10) **b**, (12) **c**, (14) **d**, (16) **i**, (18) **l**.

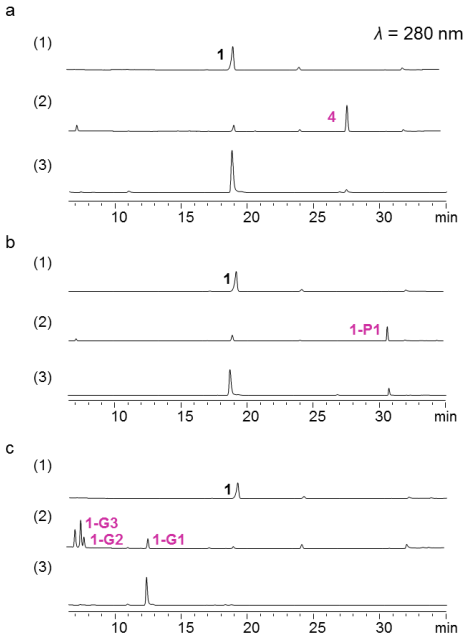

Figure S14. Functional identification of the modular post-modifying strains. HPLC analysis (λ = 280 nm) of (1) the standard substrate of **1**, (2) the enzymatic reactions catalyzed by a) DoOMT1, b) PsPT1, c) UGT71E5, (3) the whole-cell reactions catalyzed by a) the methylation strain *E-DoOMT1*, b) the prenylation strain *E-PsPT1*, c) the glycosylation strain *E-UGT71E5*, with substrate **1** as the starting material.

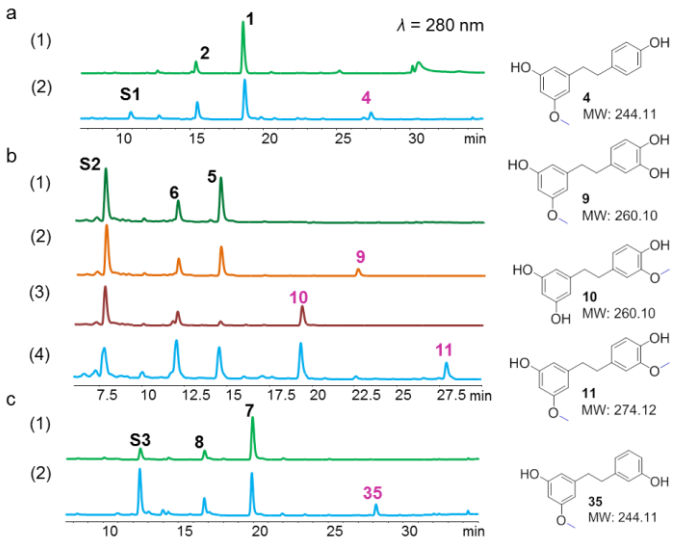

Figure S15. The whole-cell synthesis of methylated bibenzyl derivatives. HPLC analysis (λ = 280 nm) of the reactions with malonic acid and (a) **S1**, (b) **S2**, (c) **S3** as the starting materials; The whole-cell reactions catalyzed by (1) *E-DoBBS8*, (2) the co-culture of *E-DoBBS8* and the methylation strain *E-DoOMT1*, (3) the co-culture of *E-DoBBS8* and the methylation strain *E-DoOMT6*, (4) the co-culture of *E-DoBBS8* and the methylation strains *E-DoOMT1*and *E-DoOMT6*.

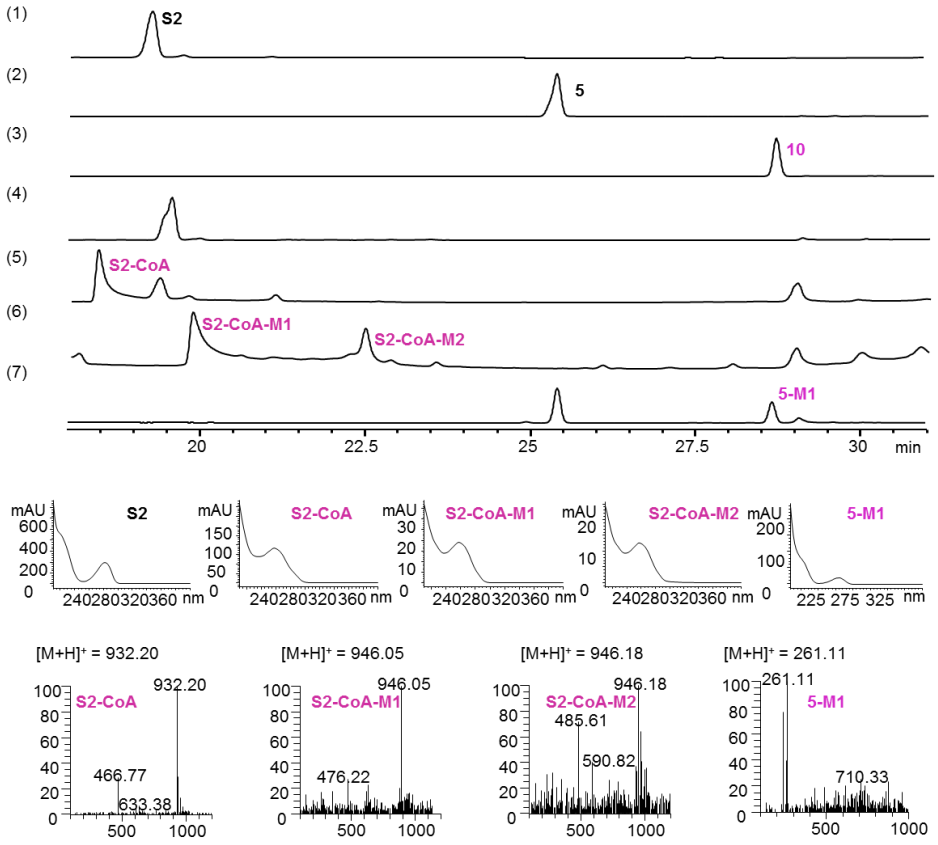

Figure S16. Functional identification of the enzyme activity of the purified DoOMT6. HPLC analysis (λ = 280 nm) of the standard substrates of (1) **S2**; (2) **5**; and (3) **10**; (4) HPLC analysis (λ = 254 nm) of the enzymatic reaction catalyzed by DoOMT6, with **S2** and SAM as substrates; (5) HPLC analysis (λ = 254 nm) of the enzymatic reaction catalyzed by At4CL1, with **S2** and CoA as substrates; (6) HPLC analysis (λ = 254 nm) of the cascade reaction catalyzed by At4CL1 and DoOMT6, with **S2**, CoA and SAM as substrates; (7) HPLC analysis (λ = 254 nm) of the enzymatic reaction catalyzed by DoOMT6, with **5** and SAM as substrates.

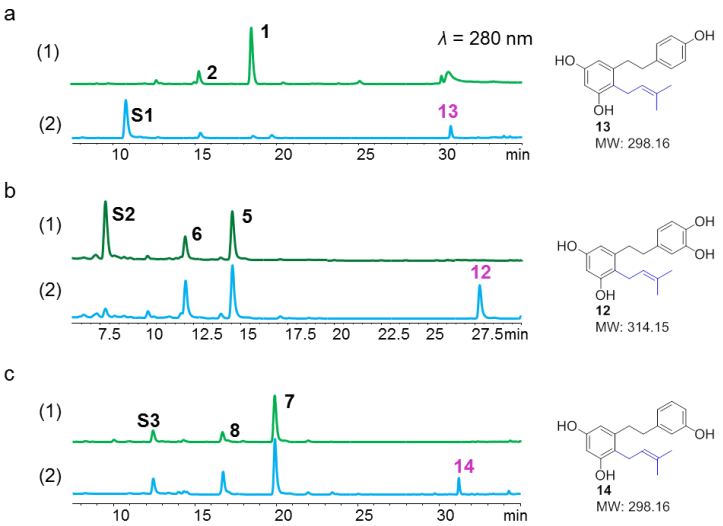

Figure S17. The whole-cell synthesis of prenylated bibenzyl derivatives. HPLC analysis (λ = 280 nm) of the reactions with malonic acid and (a) **S1**, (b) **S2**, (c) **S3** as the starting materials; The whole-cell reactions catalyzed by (1) *E-DoBBS8*, (2) the co-culture of *E-DoBBS8* and the prenylation strain *E-PsPT1*.

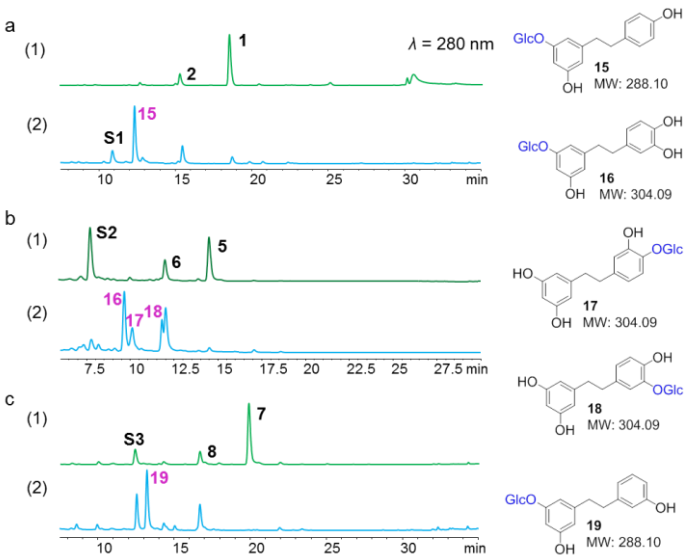

Figure S18. The whole-cell synthesis of glycosylated bibenzyl derivatives. HPLC analysis (λ = 280 nm) of the reactions with malonic acid and (a) **S1**, (b) **S2**, (c) **S3** as the starting materials; The whole-cell reactions catalyzed by (1) *E-DoBBS8*, (2) the co-culture of *E-DoBBS8* and the glycosylation strain *E-UGT71E5*.

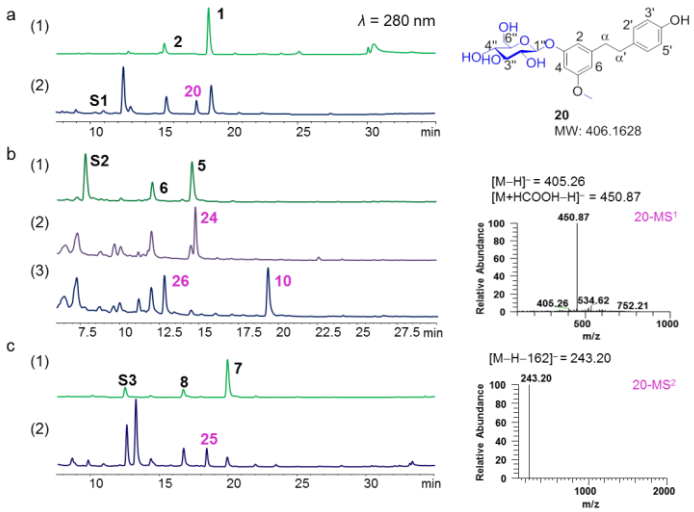

Figure S19. The whole-cell synthesis of methylated and glycosylated bibenzyl derivatives. HPLC-MS analysis (λ = 280 nm) of the reactions with malonic acid and (a) **S1**, (b) **S2**, (c) **S3** as the starting materials; The whole-cell reactions catalyzed by (1) *E-DoBBS8*, (2) the co-culture of *E-DoBBS8*, the glycosylation strain *E-UGT71E5* and the methylation strain *E-DoOMT1*, (3) the co-culture of *E-DoBBS8*, the glycosylation strain *E-UGT71E5* and the methylation strain *E-DoOMT6*.

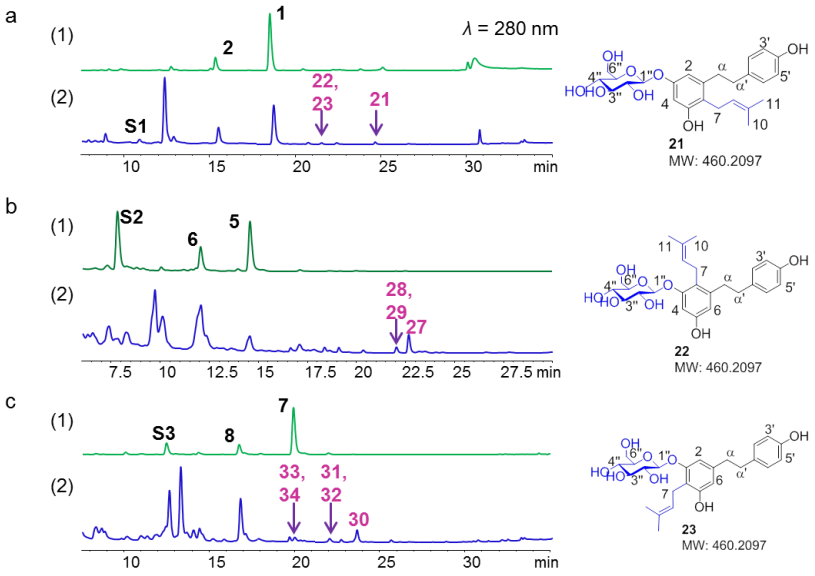

Figure S20. The whole-cell synthesis of prenylated and glycosylated bibenzyl derivatives. HPLC analysis (λ = 280 nm) of the reactions with malonic acid and (a) **S1**, (b) **S2**, (c) **S3** as the starting materials; The whole-cell reactions catalyzed by (1) *E-DoBBS8*, (2) the co-culture of *E-DoBBS8* and the glycosylation strain *E-UGT71E5* and the prenylation strain *E-PsPT1*.

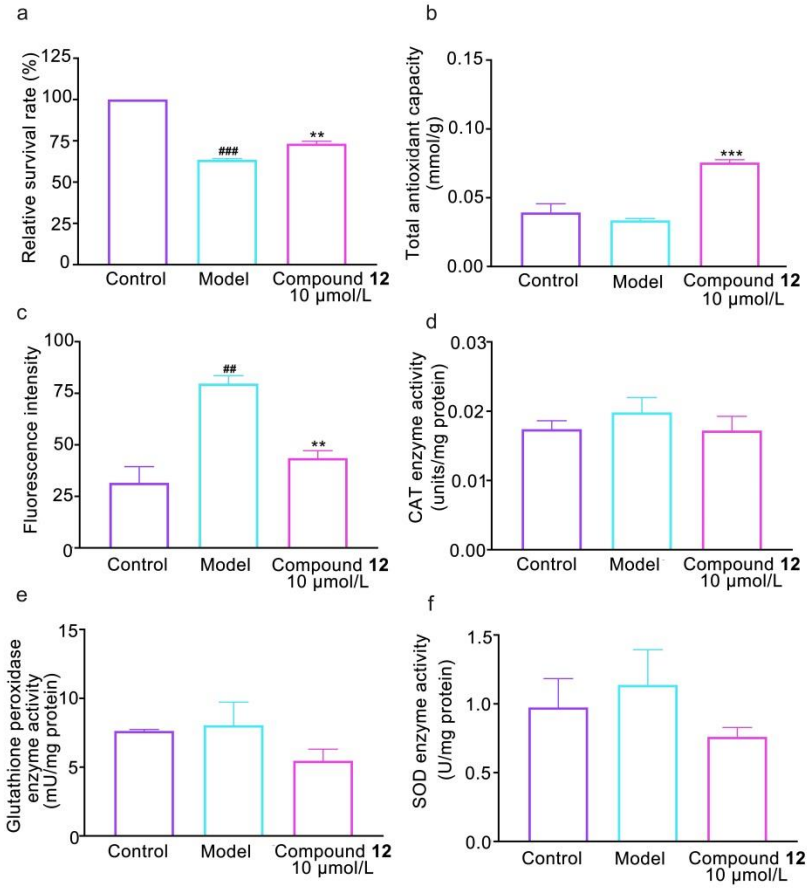

Figure S21. Effects of compound 12 on cell survival and the levels of ROS, total antioxidant capacity, CAT, GSH-Px and SOD in SK-N-SH cells after glutamate injury. (a) Relative survival rate after glutamate injury (n = 3). (b) The level of total antioxidant capacity after glutamate injury (n = 3). (c) The level of ROS after glutamate injury (n = 3). (d) The level of CAT after glutamate injury (n = 6). (e) The level of GSH-Px after glutamate injury (n = 3). (f) The level of SOD after glutamate injury (n = 3). Data were shown as mean ± SEM, $^{\#\#}P$<0.01, $^{\#\#\#}P$<0.001 vs the control group, $^{*}P$<0.05, $^{**}P$<0.01 and $^{***}P$<0.001 *vs* the model group.

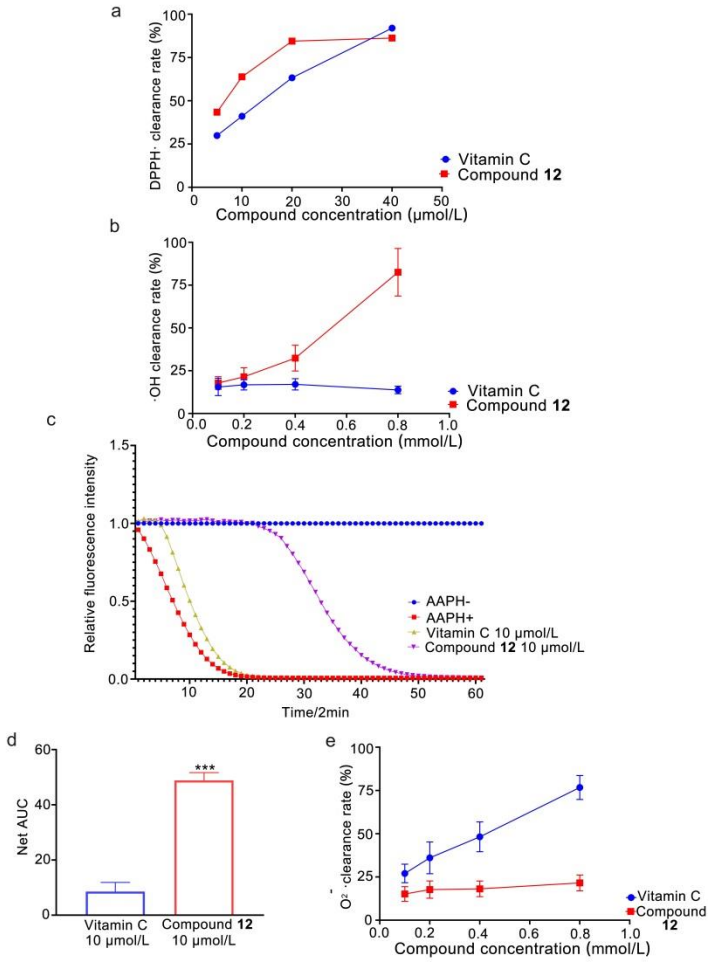

Figure S22. Scavenging effects of compound 12 on free radicals *in vitro*. The clearance rate of compound **12** and vitamin C for DPPH·(a), ·OH (b), oxidative radical (c–d), and O_2^{-}·(e), Data were shown as mean ± SEM, $^{***}P<0.001$ *vs* the vitamin C, $n = 3$.

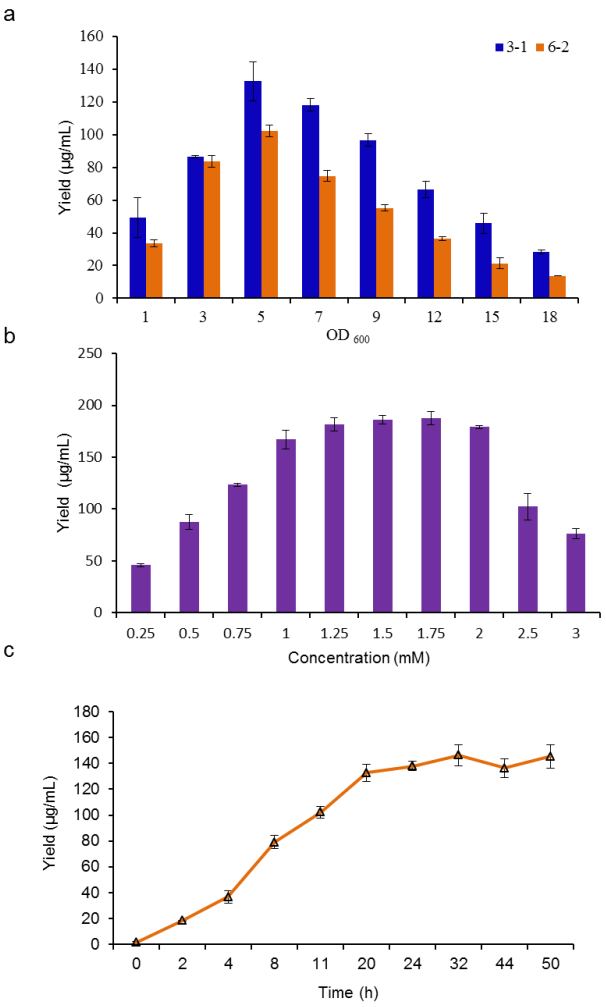

Figure S23. Optimizing the reaction conditions of whole-cell system of *E-DoBBS8*. (a). Effects of OD_{600} on the yield of product **1**. **3-1** means that the final concentration of malonic acid was at 3 mmol/L, **S1** was at 1 mmol/L. **6-2** means that the final concentration of malonic acid was at 6 mmol/L, **S1** was at 2 mmol/L. (b). Effects of the **S1** concentration on the yield of product **1**. The concentration of malonic acid was kept at three times of **S1**. (c) The time course for whole-cell reaction of *E-DoBBS8*. The error bars show the SD (n = 2).

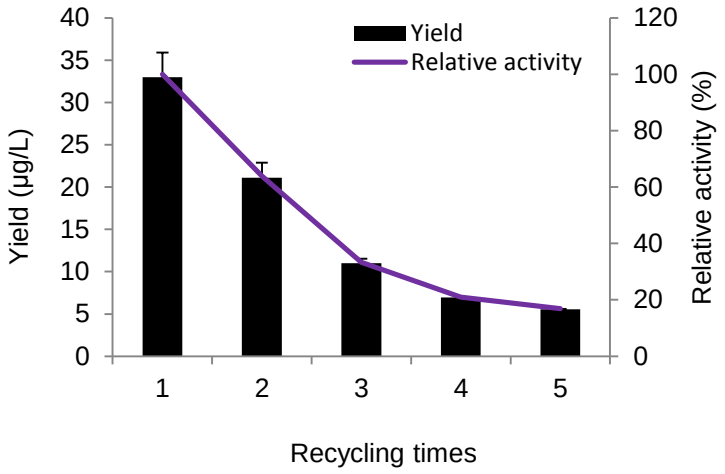

Figure S24. Recycling biosynthesis of compound 12. The error bars show the SD (*n* = 3).

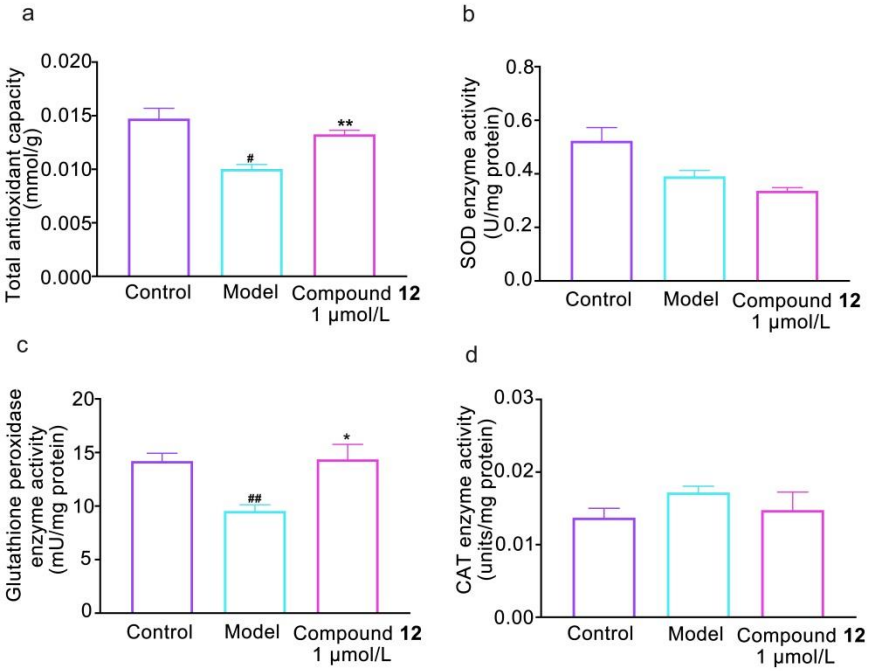

Figure S25. The effects of compound 12 on damaged cells induced by OGD/R. (a) The level of total antioxidant capacity after OGD/R injury. (b) The activities of SOD after OGD/R injury. (c) The activities of GSH-Px after OGD/R injury. (d) The activities of CAT after OGD/R injury. Data were shown as mean ± SEM, $^{\#}P<0.05$, $^{\#\#}P<0.01$ *vs* the control group, $^{*}P<0.05$ and $^{**}P<0.01$ *vs* the model group, $n = 3$.

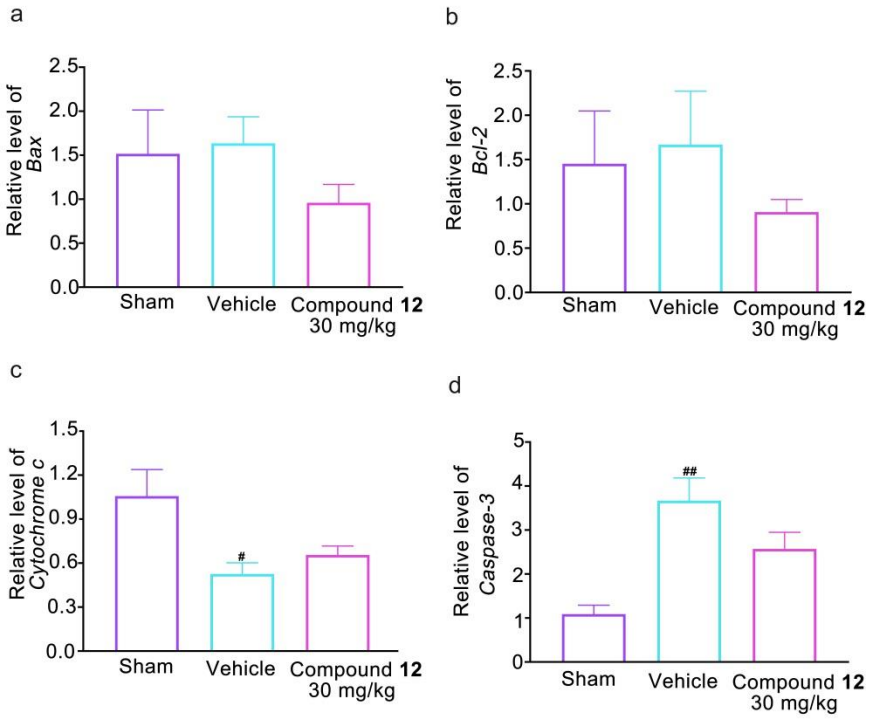

Figure S26. Compound 12 had no effect on apoptosis-related genes expressions. (a) The level of *Bax* mRNA. (b) The level of *Bcl-2* mRNA. (c) The level of *Cytochrome c* mRNA. (d) The level of *Caspase-3* mRNA. Data were shown as mean ± SEM, $^{\#}P<0.05$, $^{\#\#}P<0.001$ *vs* the sham group, $n = 5$.

Supplementary spectroscopic data of bibenzyl derivatives (1–23).

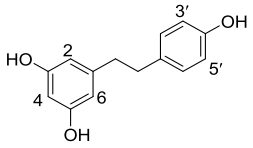

1
MW: 230.09

3,4′,5-Trihydroxybibenzyl (1): $C_{14}H_{14}O_3$, ESI-MS *m/z* 231.05 $[M+H]^+$; ^{1}H NMR (DMSO-d_6, 400 MHz): δ_H 9.13 (s, 4′-OH), 9.04 (s, 2H, 3, 5-OH), 6.98 (d, *J* = 8.4 Hz, 2H, H-2′, 6′), 6.64 (d, *J* = 8.4 Hz, 2H, H-3′, 5′), 6.05 (d, *J* = 2.1 Hz, 2H, H-2, 6), 6.01 (t, *J* = 2.1 Hz, H-4), 2.63 (m, overlapped, 4H, H-α, α′); ^{13}C NMR (DMSO-d_6, 100 MHz): δ_C 158.2 (C-3, 5), 155.3 (C-4′), 143.6 (C-1), 131.7 (C-1′), 129.1 (C-2′, 6′), 115.0 (C-3′, 5′), 106.4 (C-2, 6), 100.1 (C-4), 37.6 (C-α), 36.1 (C-α′).[13]

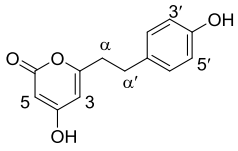

2
MW: 232.07

Dihydrobisnoryangonin (2): $C_{13}H_{12}O_4$, ESI-MS *m/z* 232.96 $[M+H]^+$; ^{1}H NMR (DMSO-d_6, 400 MHz): δ_H 7.00 (d, *J* = 8.40 Hz, 2H, H-2′, 6′), 6.65 (d, *J* = 8.36 Hz, 2H, H-3′, 5′), 5.76 (d, *J* = 2.00 Hz, H-3), 5.00 (d, *J* = 2.08 Hz, H-5), 2.74 (t, *J* = 8.08 Hz, 2H, H-α), 2.62 (t, *J* = 8.08 Hz, 2H, H-α′); ^{13}C NMR (DMSO-d_6, 100 MHz): δ_C 167.8 (C-4), 164.6 (C-2), 164.4 (C-6), 155.6 (C-4′), 130.3 (C-1′), 129.1 (C-2′, 6′), 115.1 (C-3′, 5′), 101.6 (C-3), 87.7 (C-5), 34.9 (C-α), 31.4 (C-α′).[14]

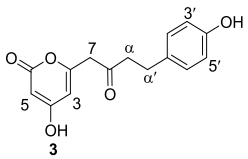

3
MW: 274.08

4-Hydroxy-6-[4-(4-hydroxyphenyl)-2-oxobutyl]-2*H*-pyran-2-one (3): $C_{15}H_{14}O_5$, ESI-MS *m/z* 275.06 $[M+H]^+$; ^{1}H NMR (DMSO-d_6, 400 MHz): δ_H 6.97 (d, *J* = 8.4 Hz, 2H, H-2′, 6′), 6.64 (d, *J* = 8.4 Hz, 2H, H-3′, 5′), 5.68 (s, H-3), 4.71 (s, H-5), 3.56 (s, H-7), 2.74 (t, *J* = 7.2 Hz, 2H, H-α), 2.66 (t, *J* = 7.2 Hz, 2H, H-α′).[15,16]

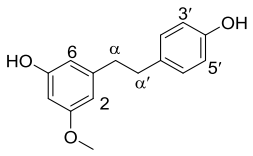

4
MW: 244.11

3-Methoxy-4′,5-dihydroxybibenzyl (4): $C_{15}H_{16}O_3$, ESI-MS *m/z* 245.07 $[M+H]^+$; ^{1}H NMR (DMSO-d_6, 400 MHz): δ_H 9.26 (s, 5-OH), 9.13 (s, 4′-OH), 7.00 (d, *J* = 8.4 Hz, 2H, H-2′, 6′), 6.65 (d, *J* = 8.4 Hz, 2H, H-3′, 5′), 6.21 (d, *J* = 2.2 Hz, 2H, H-2, 6), 6.14 (t, *J* = 2.2 Hz, H-4), 3.65 (s, 3H, 3-OMe), 2.68 (m, overlapped, 4H, H-α, α′); ^{13}C NMR (DMSO-d_6, 100 MHz): δ_C 160.3 (C-3), 158.3 (C-5), 155.3 (C-4′), 143.8 (C-1), 131.6 (C-1′), 129.1 (C-2′, 6′), 115.0 (C-3′, 5′), 107.9 (C-2), 104.9 (C-6), 98.7 (C-4), 54.8 (3-OMe), 37.7 (C-α), 36.0 (C-α′).[17]

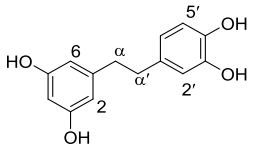

5
MW: 246.09

3,3′,4′,5-Tetrahydroxybibenzyl (5): $C_{14}H_{14}O_4$, ESI-MS *m/z* 290.91 $[M+HCOOH–H]^-$; ^{1}H NMR (DMSO-d_6, 400 MHz): δ_H 9.01 (s, 2H, 3, 5-OH), 8.66 (s, 3′-OH), 8.59 (s, 4′-OH), 6.60 (d, *J* = 8.0 Hz, H-5′), 6.58 (d, *J* = 1.8 Hz, H-2′), 6.44 (dd, *J* = 1.8, 8.0 Hz, H-6′), 6.05 (d, *J* = 1.9 Hz, 2H, H-2, 6), 6.01 (t, *J* = 1.9 Hz, H-4), 2.59 (m, overlapped, 4H, H-α, α′); ^{13}C NMR (DMSO-d_6, 100 MHz): δ_C 158.2 (C-3, 5), 144.9 (C-3′), 143.7 (C-4′), 143.2 (C-1), 132.5 (C-1′), 118.8 (C-6′), 115.7 (C-5′), 115.4 (C-2′), 106.4 (C-2, 6), 100.1 (C-4), 37.6 (C-α), 36.3 (C-α′).[18]

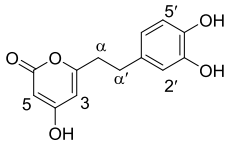

6
MW: 248.07

6-(3,4-Dihydroxyphenethyl)-4-hydroxy-2*H*-pyran-2-one (6): $C_{13}H_{12}O_5$, ESI-MS *m/z* 248.89 $[M+H]^+$; ^{1}H NMR (DMSO-d_6, 400 MHz): δ_H 6.61 (d, *J* = 8.0 Hz, H-5′), 6.57 (d, *J* = 2.0 Hz, H-2′), 6.44 (dd, *J* = 2.0, 8.0 Hz, H-6′), 5.88 (d, *J* = 2.0 Hz, H-3),

5.20 (d, J = 2.0 Hz, H-5), 2.67 (m, overlapped, 4H, H-α, α′); ^{13}C NMR (DMSO-d_6, 100 MHz): δ_C 170.8 (C-4), 166.2 (C-2), 164.4 (C-6), 145.5 (C-3′), 144.0 (C-4′), 131.3 (C-1′), 119.3 (C-6′), 116.1 (C-5′), 115.9 (C-2′), 100.5 (C-3), 88.9 (C-5), 35.3 (C-α), 31.9 (C-α′).[19]

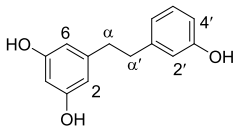

7
MW: 230.09

3,3′,5-Trihydroxybibenzyl (7): $C_{14}H_{14}O_3$, ESI-MS m/z 231.06 $[M+H]^+$; ^{1}H NMR (DMSO-d_6, 400 MHz): δ_H 9.28 (s, 3′-OH), 9.08 (s, 2H, 3, 5-OH), 7.04 (t, J = 7.7 Hz, H-5′), 6.63 (m, overlapped, 2H, H-2′, 4′), 6.56 (dd, J = 1.7, 8.0 Hz, H-6′), 6.07 (d, J = 2.0 Hz, 2H, H-2, 6), 6.02 (t, J = 2.0 Hz, H-4), 2.66 (m, overlapped, 4H, H-α, α′); ^{13}C NMR (DMSO-d_6, 100 MHz): δ_C 158.2 (C-3, 5), 157.3 (C-3′), 143.5 (C-1), 143.1 (C-1′), 129.1 (C-5′), 118.9 (C-6′), 115.2 (C-2′), 112.7 (C-4′), 106.3 (C-2, 6), 100.2 (C-4), 37.1 (C-α), 36.8 (C-α′).[20]

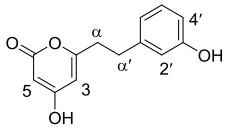

8
MW: 232.07

4-Hydroxy-6-(3-hydroxyphenethyl)-2H-pyran-2-one (8): $C_{13}H_{12}O_4$, ESI-MS m/z 232.96 $[M+H]^+$; ^{1}H NMR (DMSO-d_6, 400 MHz): δ_H 7.06 (t, J = 8.0 Hz, H-5′), 6.64-6.57 (m, overlapped, 3H, H-2′, 4′, 6′), 5.85 (d, J = 1.8 Hz, H-3), 5.11 (d, J = 1.8 Hz, H-5), 2.73 (m, overlapped, 4H, H-α, α′); ^{13}C NMR (DMSO-d_6, 100 MHz): δ_C 171.6 (C-4), 164.9 (C-2), 164.2 (C-6), 157.3 (C-3′), 141.6 (C-1′), 129.3 (C-5′), 118.9 (C-6′), 115.2 (C-2′), 113.1 (C-4′), 100.9 (C-3), 88.0 (C-5), 34.4 (C-α), 32.1 (C-α′).[21]

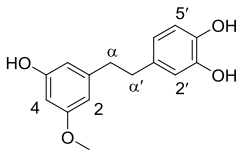

9
MW: 260.10

3-Methoxy-3′,4′,5-trihydroxybibenzyl (9): $C_{15}H_{16}O_4$, ESI-MS *m/z* 259.21 $[M–H]^-$; ^{1}H NMR (DMSO-d_6, 600 MHz): δ_H 6.61 (d, *J* = 8.0 Hz, H-5′), 6.59 (d, *J* = 2.0 Hz, H-2′), 6.44 (dd, *J* = 2.0, 8.0 Hz, H-6′), 6.21 (t, *J* = 2.0 Hz, 2H, H-2, 6), 6.13 (t, *J* = 2.0 Hz, H-4), 3.65 (s, 3H, 3-OMe), 2.64 (s, 4H, H-α, α′); ^{13}C NMR (DMSO-d_6, 100 MHz): δ_C 160.3 (C-3), 158.3 (C-5), 145.0 (C-3′), 143.9 (C-4′), 143.3 (C-1), 132.4 (C-1′), 118.8 (C-6′), 115.8 (C-5′), 115.5 (C-2′), 107.9 (C-6), 104.8 (C-2), 98.7 (C-4), 54.8 (C-3-OMe), 37.6 (C-α), 36.3 (C-α′).[22]

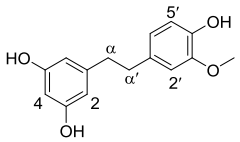

10
MW: 260.10

3′-Methoxy-3,4′,5-trihydroxybibenzyl (10): $C_{15}H_{16}O_4$, ESI-MS *m/z* 261.11 $[M+H]^+$; ^{1}H NMR (DMSO-d_6, 600 MHz): δ_H 9.03 (s, 2H, 3,5-OH), 8.64 (s, 3′-OH), 6.75 (d, *J* = 2.0 Hz, H-2′), 6.65 (d, *J* = 8.0 Hz, H-5′), 6.58 (dd, *J* = 2.0, 8.0 Hz, H-6′), 6.06 (d, *J* = 2.1 Hz, 2H, H-2, 6), 6.02 (t, *J* = 2.1 Hz, H-4), 3.72 (s, 3H, 3′-OMe), 2.65 (m, overlapped, 4H, H-α, α′); ^{13}C NMR (DMSO-d_6, 100 MHz): δ_C 158.2 (C-3, 5), 147.3 (C-3′), 144.5 (C-4′), 143.7 (C-1), 132.5 (C-1′), 120.4 (C-6′), 115.2 (C-5′), 112.6 (C-2′), 106.4 (C-2, 6), 100.1 (C-4), 55.5 (C-3′-OMe), 37.6 (C-α), 36.6 (C-α′).[23]

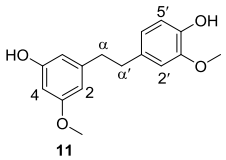

11
MW: 274.12

3,3′-Dimethoxy-4′,5-dihydroxybibenzyl (11): $C_{16}H_{18}O_4$, ESI-MS *m/z* 275.02 $[M+H]^+$; ^{1}H NMR (DMSO-d_6, 400 MHz): δ_H 6.76 (d, *J* = 1.9 Hz, H-2′), 6.65 (d, *J* = 7.9 Hz, H-5′), 6.59 (dd, *J* = 1.9, 7.9 Hz, H-6′), 6.21-6.23 (m, overlapped, 2H, H-2, 6), 6.14 (t, *J* = 2.2 Hz, H-4), 3.72 (s, 3H, 3′-OMe), 3.66 (s, 3H, 3-OMe), 2.70 (m, overlapped, 4H, H-α, α′); ^{13}C NMR (DMSO-d_6, 100 MHz): δ_C 160.3 (C-3), 158.3 (C-5), 147.3 (C-3′), 144.5 (C-4′), 143.9 (C-1), 132.4 (C-1′), 120.4 (C-6′), 115.2 (C-5′), 112.6 (C-2′), 108.0 (C-6), 104.9 (C-2), 98.7 (C-4), 55.5 (C-3′-OMe), 54.8

(C-3-OMe), 37.7 (C-α), 36.6 (C-α′).[24]

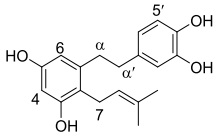

12
MW: 314.15

2-Isopentenyl-3,3′,4′,5-tetrahydroxybibenzyl (12): $C_{19}H_{22}O_4$, ESI-MS *m/z* 313.17 $[M-H]^-$; ^{1}H NMR (DMSO-d_6, 400 MHz): δ_H 6.62 (d, *J* = 8.0 Hz, H-5′), 6.58 (d, *J* = 2.0 Hz, H-2′), 6.44 (dd, *J* = 2.0, 8.0 Hz, H-6′), 6.14 (d, *J* = 2.4 Hz, H-4), 6.06 (d, *J* = 2.4 Hz, H-6), 5.00 (t, *J* = 5.4 Hz, H-8), 3.14 (d, *J* = 6.4 Hz, H-7), 2.56 (m, overlapped, 4H, H-α, α′), 1.67 (s, 3H, H-10), 1.61 (s, 3H, H-11); ^{13}C NMR (DMSO-d_6, 100 MHz): δ_C 156.2 (C-3, 5), 145.5 (C-3′), 143.7 (C-4′), 142.0 (C-1), 133.3 (C-1′), 129.3 (C-9), 125.2 (C-8), 119.1 (C-6′), 116.7 (C-2′), 116.1 (C-2), 115.9 (C-5′), 107.4 (C-6), 100.7 (C-4), 37.0 (C-α), 36.7 (C-α′), 26.0 (C-11), 24.4 (C-7), 18.3 (C-10).[25,26]

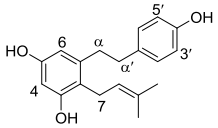

13
MW: 298.16

2-Isopentenyl-3,4′,5-trihydroxybibenzyl (13): $C_{19}H_{22}O_3$, ESI-MS *m/z* 298.99 $[M+H]^+$; ^{1}H NMR: (DMSO-d_6, 400 MHz): δ_H 9.15 (s, 3-OH), 8.98 (s, 5-OH), 8.83 (s, 4′-OH), 6.98 (d, *J* = 8.4 Hz, 2H, H-2′, 6′), 6.66 (d, *J* = 8.4 Hz, 2H, H-3′, 5′), 6.14 (d, *J* = 2.3 Hz, 2H, H-2, 6), 6.07 (d, *J* = 2.3 Hz, H-4), 4.99 (t, *J* = 6.6 Hz, H-8), 3.13 (d, *J* = 6.6 Hz, H-7), 2.60 (s, 4H, H-α, α′), 1.66 (s, 3H, H-10), 1.60 (s, 3H, H-11); ^{13}C NMR (DMSO-d_6, 100 MHz): δ_C 156.7 (C-3), 156.5 (C-5), 156.3 (C-4′), 141.4 (C-1), 132.0 (C-1′), 129.0 (C-2′, 6′), 128.8 (C-9), 124.7 (C-8), 116.3 (C-2), 115.0 (C-3′, 5′), 106.9 (C-6), 100.3 (C-4), 37.6 (C-α), 36.1 (C-α′), 25.5 (C-11), 23.9 (C-7), 17.7 (C-10).[27]

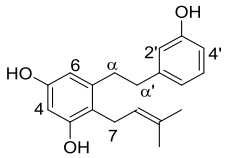

14
MW: 298.1569

2-Isopentenyl-3,3′,5-trihydroxybibenzyl (14): $C_{19}H_{22}O_4$, HR-ESI-MS: *m/z* 297.1492 $[M–H]^–$; ^{1}H NMR (DMSO-d_6, 400 MHz): δ_H 7.06 (dd, *J* = 7.7 Hz, H-5′), 6.64–6.60 (m, overlapped, 2H, H-6′, 2′), 6.57 (ddd, *J* = 0.9, 2.4, 7.7 Hz, H-5′), 6.14 (d, *J* = 2.4 Hz, H-4), 6.08 (d, *J* = 2.4 Hz, H-6), 5.00 (t, *J* = 6.6 Hz, H-8), 3.14 (d, *J* = 6.6 Hz, H-7), 2.63 (s, 4H, H-α, α′), 1.67 (s, 3H, H-10), 1.61 (s, 3H, H-11); ^{13}C NMR (DMSO-d_6, 100 MHz): δ_C 157.4 (C-3′), 155.8 (C-3), 155.6 (C-5), 143.5 (C-1′), 141.4 (C-1), 129.3 (C-9), 128.9 (C-5′), 124.8 (C-8), 118.7 (C-6′), 115.0 (C-2′), 116.3 (C-2), 112.8 (C-4′), 106.9 (C-6), 100.4 (C-4), 37.0 (C-α′), 34.7 (C-α), 25.5 (C-11), 23.8 (C-7), 17.8 (C-10).

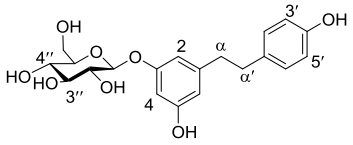

15
MW: 392.15

3-*O*-*β*-D-glucosyl-3′,5-dihydroxybibenzyl (15): $C_{20}H_{24}O_8$, ESI-MS *m/z* 391.20 $[M–H]^–$; ^{1}H NMR (DMSO-d_6, 400 MHz): δ_H 7.00 (d, *J* = 8.4 Hz, 2H, H-2′, 6′), 6.65 (d, *J* = 8.4 Hz, 2H, H-3′, 5′), 6.25 (m, overlapped, 2H, H-2, 6), 6.34 (t, *J* = 1.7 Hz, H-4), 4.73 (d, *J* = 7.6 Hz, H-1″), 3.68 (dd, *J* = 2.0, 11.8 Hz, H-6″a), 3.47 (dd, *J* = 5.40 Hz, 11.8 Hz, H-6″b), 3.25–3.13 (m, overlapped, 4H, H-2″-5″), 2.68 (m, overlapped, 4H, H-α, α′); ^{13}C NMR (DMSO- d_6, 100 MHz): δ_C 158.5 (C-3), 158.1 (C-5), 156.4 (C-4′), 143.7 (C-1), 131.6 (C-1′), 129.1 (C-2′, 6′), 115.0 (C-3′, 5′), 109.1 (C-6), 107.2 (C-2), 101.1 (C-4), 100.4 (C-1″), 77.0 (C-3″), 76.7 (C-5″), 73.2 (C-2″), 69.7 (C-4″), 60.6 (C-6″), 37.6 (C-α), 36.0 (C-α′).[28]

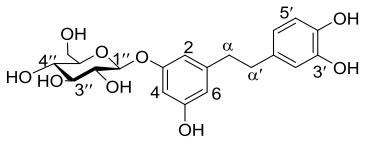

16
MW: 408.1420

3-*O*-*β*-D-glucosyl-3′,4′,5-trihydroxybibenzyl (16): $C_{20}H_{24}O_9$, HR-ESI-MS: *m/z* 407.1343 $[M–H]^–$; ESI-MS *m/z* 407.50 $[M–H]^–$; ^{1}H NMR (DMSO-d_6, 400 MHz): δ_H

6.60 (d, *J* = 8.0 Hz, H-5′), 6.59 (d, *J* = 2.0 Hz, H-2′), 6.44 (dd, *J* = 2.0, 8.0 Hz, H-6′), 6.34 (dd, *J* = 1.7, 1.7 Hz, H-6), 6.26–6.25 (m, overlapped, 2H, H-2, 4), 4.74 (d, *J* = 7.7 Hz, H-1″), 3.68 (dd, *J* = 2.0, 12.0 Hz, H-6″a), 3.48 (dd, *J* = 5.4, 12.0 Hz, H-6″b), 3.25–3.16 (m, overlapped, 4H, H-2″–5″), 2.64 (s, 4H, H-α, α′); ^{13}C NMR (DMSO-d_6, 100 MHz): δ_C 158.5 (C-3), 158.1 (C-5), 145.1 (C-3′), 143.7 (C-1), 143.3 (C-4′), 132.4 (C-1′), 118.8 (C-6′), 115.9 (C-2′), 115.4 (C-5′), 109.1 (C-2), 107.2 (C-6), 101.1 (C-4), 100.4 (C-1″), 77.0 (C-3″), 76.2 (C-5″), 73.2 (C-2″), 69.7 (C-4″), 60.6 (C-6″), 37.6 (C-α), 36.2 (C-α′).

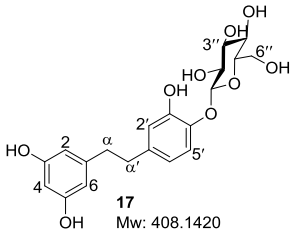

17 Mw: 408.1420

4′-*O*-*β*-D-glucosyl-3,3′,5-trihydroxybibenzyl (17): $C_{20}H_{24}O_9$, HR-ESI-MS: *m*/*z* 407.1342 $[M–H]^–$; ESI-MS *m*/*z* 407.65 $[M–H]^–$; ^{1}H NMR (DMSO-d_6, 400 MHz): δ_H 6.99 (d, *J* = 8.2 Hz, H-5′), 6.66 (d, *J* = 2.0 Hz, H-2′), 6.56 (dd, *J* = 2.0, 8.2 Hz, H-6′), 6.06 (d, *J* = 2.2 Hz, 2H, H-2, 6), 6.01 (dd, *J* = 2.2, 2.2 Hz, H-4), 4.61 (d, *J* = 7.6 Hz, H-1″), 3.72 (dd, *J* = 2.1, 11.8 Hz, H-6″a), 3.47 (dd, *J* = 5.8, 11.8 Hz, H-6″b), 3.27–3.15 (m, overlapped, 4H, H-2″–5″), 2.66 (s, 4H, H-α, α′); ^{13}C NMR (DMSO-d_6, 100 MHz): δ_C 158.3 (C-3, 5), 146.8 (C-3′), 143.6 (C-4′), 143.5 (C-1), 136.6 (C-1′), 119.0 (C-6′), 116.9 (C-5′), 116.0 (C-2′), 106.3 (C-2, 6), 102.9 (C-1″), 100.2 (C-4), 77.1 (C-3″), 75.9 (C-5″), 73.3 (C-2″), 69.8 (C-4″), 60.8 (C-6″), 37.3 (C-α), 36.2 (C-α′).

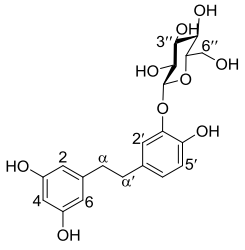

18
Mw: 408.1420

3′-*O*-*β*-D-glucosyl-3,4′,5-trihydroxybibenzyl (18): $C_{20}H_{24}O_9$, HR-ESI-MS: *m*/*z* 407.1343 $[M–H]^–$; ESI-MS *m*/*z* 407.56 $[M–H]^–$; ^{1}H NMR (DMSO-d_6, 400 MHz): δ_H 7.00 (d, *J* = 1.5 Hz, H-2′), 6.72–6.67 (m, overlapped, 2H, H-5′, 6′), 6.06 (d, *J* = 2.2 Hz,

2H, H-2, 6), 6.01 (dd, *J* = 2.2, 2.2 Hz, H-4), 4.61 (d, *J* = 7.5 Hz, H-1″), 3.72 (dd, *J* = 2.1, 11.8 Hz, H-6″a), 3.49 (dd, *J* = 5.7, 11.8 Hz, H-6″b), 3.29–3.16 (m, overlapped, 4H, H-2″–5″), 2.66 (m, overlapped, 4H, H-α, α′); ^{13}C NMR (DMSO-d_6, 100 MHz): δ_C 158.6 (C-3, 5), 145.1 (C-3′), 144.8 (C-4′), 143.6 (C-1), 132.7 (C-1′), 122.5 (C-6′), 115.5 (C-5′), 117.1 (C-2′), 106.3 (C-2, 6), 102.7 (C-1″), 100.2 (C-4), 77.1 (C-3″), 75.9 (C-5″), 73.4 (C-2″), 69.8 (C-4″), 60.7 (C-6″), 37.3 (C-α), 36.3 (C-α′).

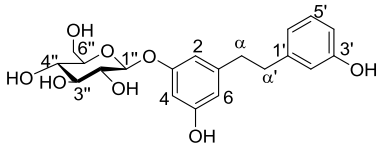

19
MW: 392.1471

3-*O*-*β*-D-glucosyl-3′,5-dihydroxybibenzyl (19): $C_{20}H_{24}O_8$, HR-ESI-MS: *m*/*z* 391.1394 [M–H]$^-$; ^{1}H NMR (DMSO-d_6, 400 MHz): δ_H 7.04 (t, *J* = 7.7 Hz, H-5′), 6.65–6.60 (m, overlapped, 2H, H-6′, 2′), 6.56 (ddd, *J* = 1.0, 2.5, 7.7 Hz, H-4′), 6.36 (t, *J* = 1.8 Hz, H-6), 6.27 (d, *J* = 1.8 Hz, 2H, H-2, 4), 4.73 (d, *J* = 7.6 Hz, H-1″), 3.68 (dd, *J* = 2.0, 11.8 Hz, H-6″a), 3.48 (dd, *J* = 5.4, 11.8 Hz, H-6″b), 3.25–3.15 (m, overlapped, 4H, H-2″–5″), 2.71 (m, overlapped, 4H, H-α, α′); ^{13}C NMR (DMSO-d_6, 100 MHz): δ_C 158.9 (C-3), 158.6 (C-5), 157.7 (C-3′), 144.0 (C-1), 143.5 (C-1′), 129.6 (C-5′), 119.4 (C-6′), 115.6 (C-2′), 113.2 (C-4′), 109.5 (C-2), 107.7 (C-6), 101.6 (C-4), 100.9 (C-1″), 77.5 (C-3″), 77.2 (C-5″), 73.7 (C-2″), 70.1 (C-4″), 61.0 (C-6″), 37.5 (C-α), 37.2 (C-α′).

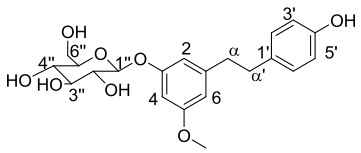

20
MW: 406.1628

3-*O*-*β*-D-glucosyl-5-methoxy-4′-hydroxybibenzyl (20): $C_{21}H_{26}O_8$, HR-ESI-MS: *m*/*z* 405.1552 [M–H]$^-$; ^{1}H NMR (DMSO-d_6, 400 MHz): δ_H 7.01 (*d*, *J* = 8.5 Hz, 2H, H-2′, 6′), 6.65 (d, *J* = 8.5 Hz, 2H, H-3′, 5′), 6.49 (dd, *J* = 2.1, 2.1 Hz, H-2), 6.43 (dd, *J* = 2.1, 2.1 Hz, H-4), 6.41 (dd, *J* = 2.1, 2.1 Hz, H-6), 4.79 (d, *J* = 7.6 Hz, H-1″), 3.70 (m, overlapped, H-6″a), 3.69 (s, 3H, 5-OMe), 3.45 (dd, *J* = 5.7, 11.7 Hz, H-6″b), 3.31–3.14 (m, overlapped, 4H, H-2″–5″), 2.73 (s, 4H, H-α, α′); ^{13}C NMR (DMSO-d_6, 100 MHz): δ_C 160.1 (C-5), 158.6 (C-3), 155.4 (C-4′), 144.1 (C-1), 131.6 (C-1′), 129.2

(C-2′, 6′), 115.0 (C-3′, 5′), 108.6 (C-2), 107.6 (C-6), 100.4 (C-1″), 99.6 (C-4), 77.2 (C-3″), 76.8 (C-5″), 73.3 (C-2″), 69.7 (C-4″), 60.6 (C-6″), 55.0 (5-OMe), 37.7 (C-α), 35.9 (C-α′).

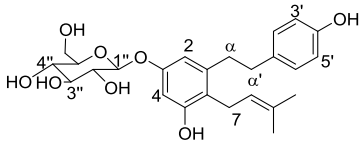

21
MW: 460.2097

3-*O*-*β*-D-glucosyl-6-isopentenyl-4′,5-dihydroxybibenzyl (21): $C_{25}H_{32}O_8$, HR-ESI-MS: *m*/*z* 459.2021 $[M–H]^-$; ^{1}H NMR (DMSO-d_6, 400 MHz): δ_H 9.22 (s, 5-OH), 9.14 (s, 4′-OH), 6.99 (d, *J* = 8.5 Hz, 2H, H-2′, 6′), 6.66 (d, *J* = 8.5 Hz, 2H, H-3′, 5′), 6.38 (d, *J* = 2.4 Hz, H-2), 6.37 (d, *J* = 2.4 Hz, H-4), 5.24 (d, *J* = 5.1 Hz, 2″-OH), 5.06 (d, *J* = 4.6 Hz, 3″-OH), 4.99 (m, overlapped, 2H, 4″-OH, H-8), 4.69 (d, *J* = 7.6 Hz, H-1″), 4.53 (t, *J* = 5.8 Hz, 6″-OH), 3.69 (dd, *J* = 1.8, 11.7 Hz, H-6″a), 3.49 (dd, *J* = 5.2, 11.7 Hz, H-6″b), 3.23–3.17 (m, overlapped, 4H, H-2″–5″), 2.65 (s, 4H, H-α, α′), 1.67 (s, 3H, H-10), 1.61 (s, 3H, H-11); ^{13}C NMR (DMSO-d_6, 100 MHz): δ_C 155.9 (C-3), 155.6 (C-5), 155.4 (C-4′), 141.5 (C-1), 131.9 (C-1′), 129.3 (C-9), 129.0 (C-2′, 6′), 124.3 (C-8), 119.4 (C-6), 115.0 (C-3′, 5′), 107.8 (C-2), 100.6 (C-4), 100.5 (C-1″), 77.0 (C-3″), 76.9 (C-5″), 73.5 (C-2″), 69.6 (C-4″), 60.7 (C-6″), 36.1 (C-α′), 35.1 (C-α), 25.5 (C-11), 24.2 (C-7), 17.8 (C-10).

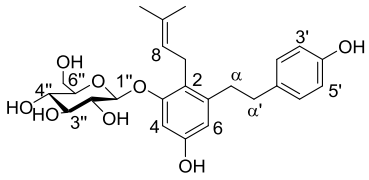

22
MW: 460.2097

2-Isopentenyl-3-*O*-*β*-D-glucosyl-4′,5-dihydroxybibenzyl (22): $C_{25}H_{32}O_8$, HR-ESI-MS: *m*/*z* 459.2020 $[M–H]^-$; ^{1}H NMR (DMSO-d_6, 400 MHz): δ_H 6.99 (d, *J* = 8.4 Hz, 2H, H-2′, 6′), 6.66 (d, *J* = 8.4 Hz, 2H, H-3′, 5′), 6.40 (d, *J* = 2.3 Hz, H-4), 6.28 (d, *J* = 2.3 Hz, H-6), 5.03 (t, *J* = 5.6 Hz, H-8), 4.68 (d, *J* = 7.2 Hz, H-1″), 3.70 (dd, *J* = 1.8, 11.7 Hz, H-6″a), 3.50 (dd, *J* = 5.0, 11.7 Hz, H-6″b), 3.24–3.17 (m, overlapped, 4H, H-2″–5″), 2.64 (m, overlapped, 4H, H-α, α′), 1.68 (s, 3H, H-10), 1.60 (s, 3H, H-11); ^{13}C NMR (DMSO-d_6, 100 MHz): δ_C 156.5 (C-3), 155.8 (C-5), 155.4 (C-4′), 141.3 (C-1), 131.9 (C-1′), 129.0 (C-2′, 6′), 128.8 (C-9), 124.7 (C-8), 118.9 (C-2),

115.0 (C-3′, 5′), 109.5 (C-6), 101.6 (C-1″), 100.8 (C-4), 77.0 (C-3″), 76.9 (C-5″), 73.5 (C-2″), 69.6 (C-4″), 60.7 (C-6″), 36.2 (C-α′), 35.1 (C-α), 25.5 (C-11), 23.9 (C-7), 17.8 (C-10).

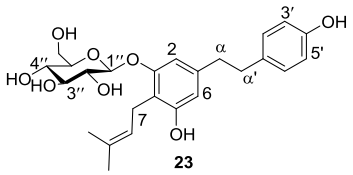

23
MW: 460.2097

3-*O*-*β*-D-glucosyl-4-isopentenyl-4′,5-dihydroxybibenzyl (23): $C_{25}H_{32}O_8$, HR-ESI-MS: *m*/*z* 459.2020 $[M–H]^–$; ^{1}H NMR (DMSO-d_6, 400 MHz): δ_H 7.11 (d, *J* = 8.7 Hz, 2H, H-2′, 6′), 6.94 (d, *J* = 8.7 Hz, 2H, H-3′, 5′), 6.15 (d, *J* = 2.4 Hz, H-2), 6.08 (d, *J* = 2.4 Hz, H-6), 5.03 (t, *J* = 5.6 Hz, H-8), 4.80 (d, *J* = 7.4 Hz, H-1″), 3.69 (dd, *J* = 1.8, 11.8 Hz, H-6″a), 3.50 (dd, *J* = 5.0, 11.8 Hz, H-6″b), 3.24–3.17 (m, overlapped, 4H, H-2″–5″), 2.64 (m, overlapped, 4H, H-α, α′), 1.67 (s, 3H, H-10), 1.60 (s, 3H, H-11); ^{13}C NMR (DMSO-d_6, 100 MHz): δ_C 155.7 (C-5, 3), 155.6 (C-4′), 141.3 (C-1), 135.2 (C-1′), 129.0 (C-2′, 6′), 128.9 (C-9), 124.8 (C-8), 116.3 (C-4), 116.1 (C-3′, 5′), 107.0 (C-6), 100.6 (C-1″), 100.4 (C-2), 76.6 (C-3″, 5″), 73.3 (C-2″), 69.7 (C-4″), 60.7 (C-6″), 36.2 (C-α′), 35.1 (C-α), 25.5 (C-11), 23.9 (C-7), 17.8 (C-10).

Supplementary spectra

Supplementary MS spectra of products (1–34)

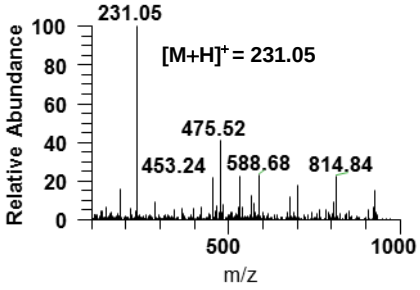

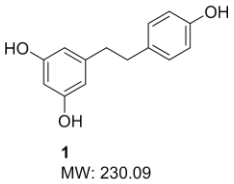

Spectrum S1. The ESI-MS spectrum of **1**.

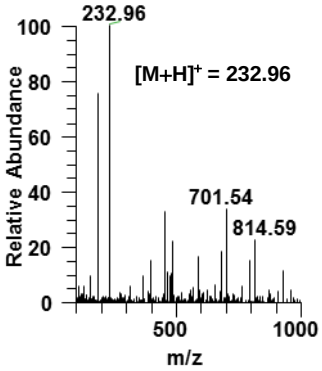

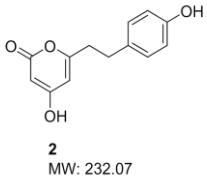

Spectrum S2. The ESI-MS spectrum of **2**.

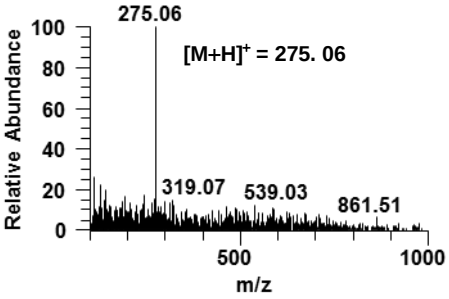

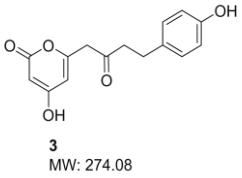

Spectrum S3. The ESI-MS spectrum of **3**.

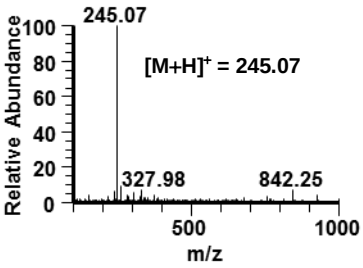

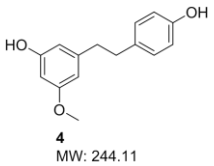

Spectrum S4. The ESI-MS spectrum of **4**.

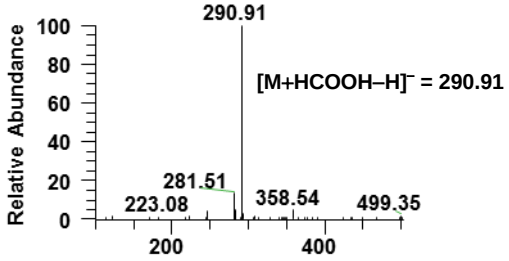

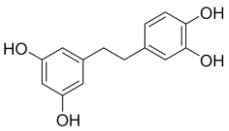

5
MW: 246.09

Spectrum S5. The ESI-MS spectrum of **5**.

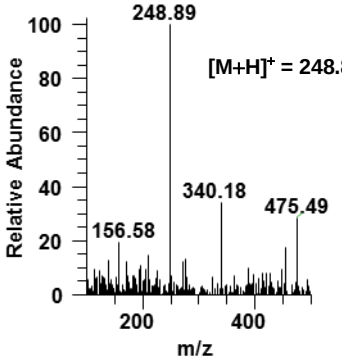

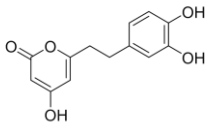

6
MW: 248.07

Spectrum S6. The ESI-MS spectrum of **6**.

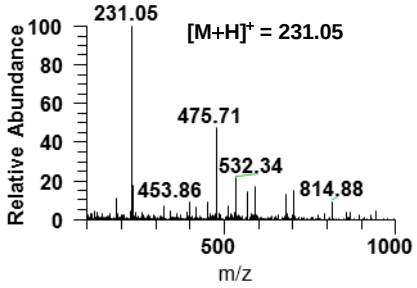

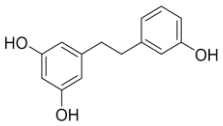

7
MW: 230.09

Spectrum S7. The ESI-MS spectrum of **7**.

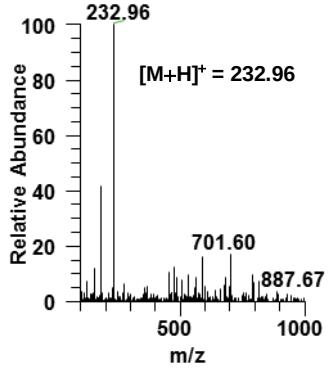

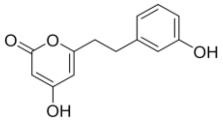

8
MW: 232.07

Spectrum S8. The ESI-MS spectrum of **8**.

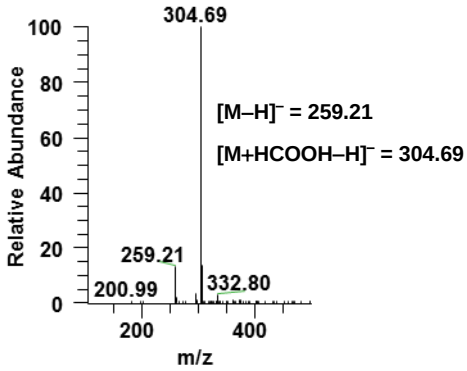

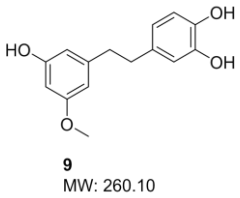

Spectrum S9. The ESI-MS spectrum of **9**.

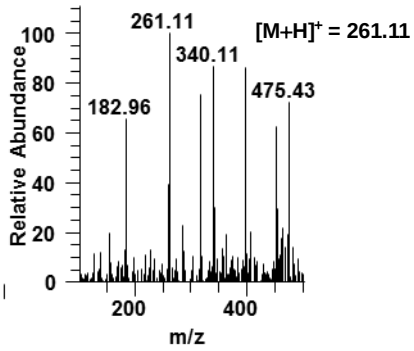

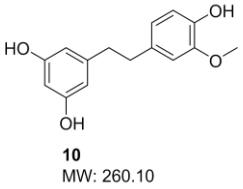

Spectrum S10. The ESI-MS spectrum of **10**.

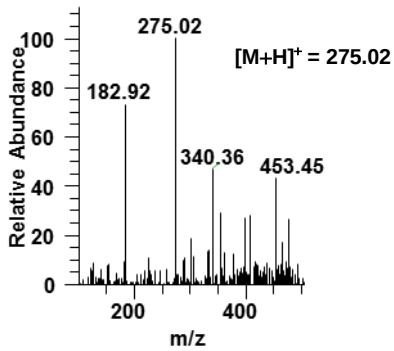

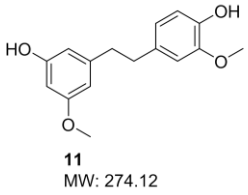

Spectrum S11. The ESI-MS spectrum of **11**.

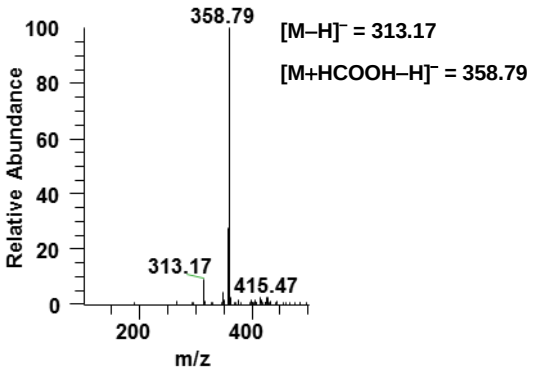

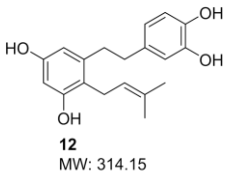

12
MW: 314.15

Spectrum S12. The ESI-MS spectrum of **12**.

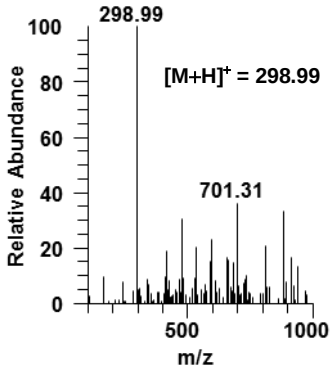

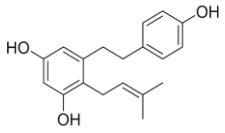

13
MW: 298.16

Spectrum S13. The ESI-MS spectrum of **13**.

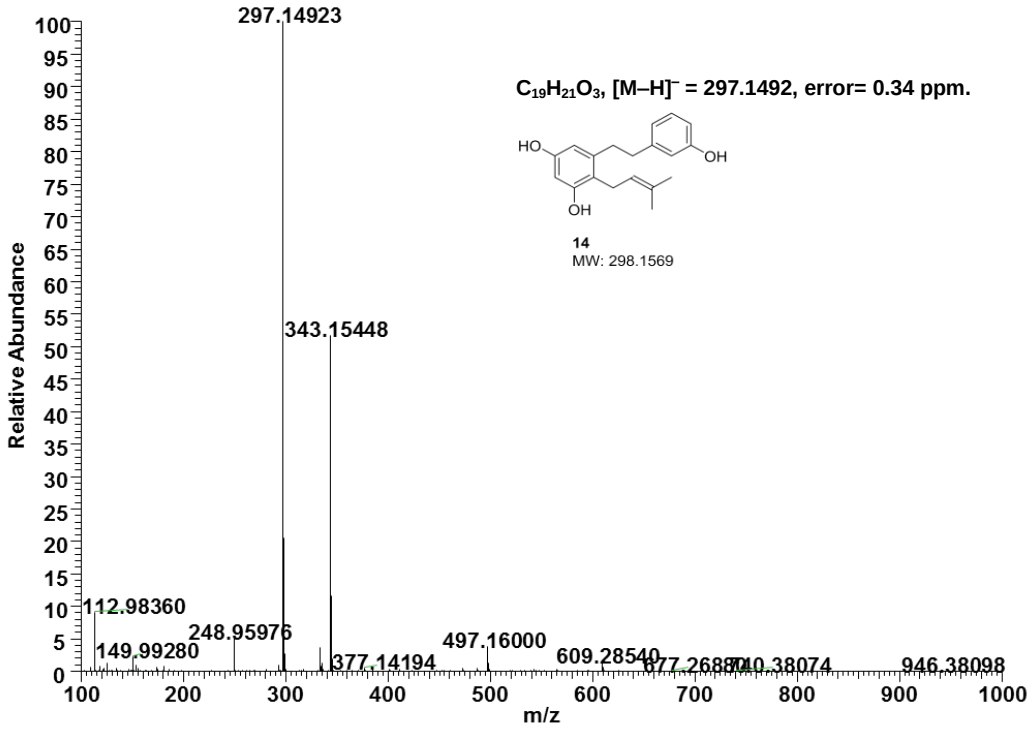

Spectrum S14. The HR-ESI-MS spectrum of **14**.

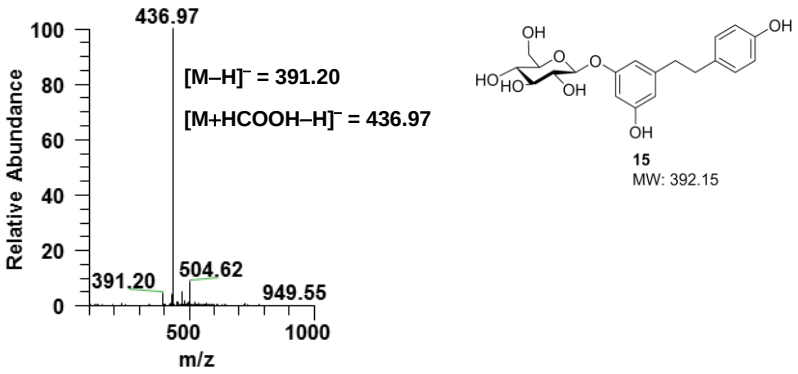

Spectrum S15. The ESI-MS spectrum of **15**.

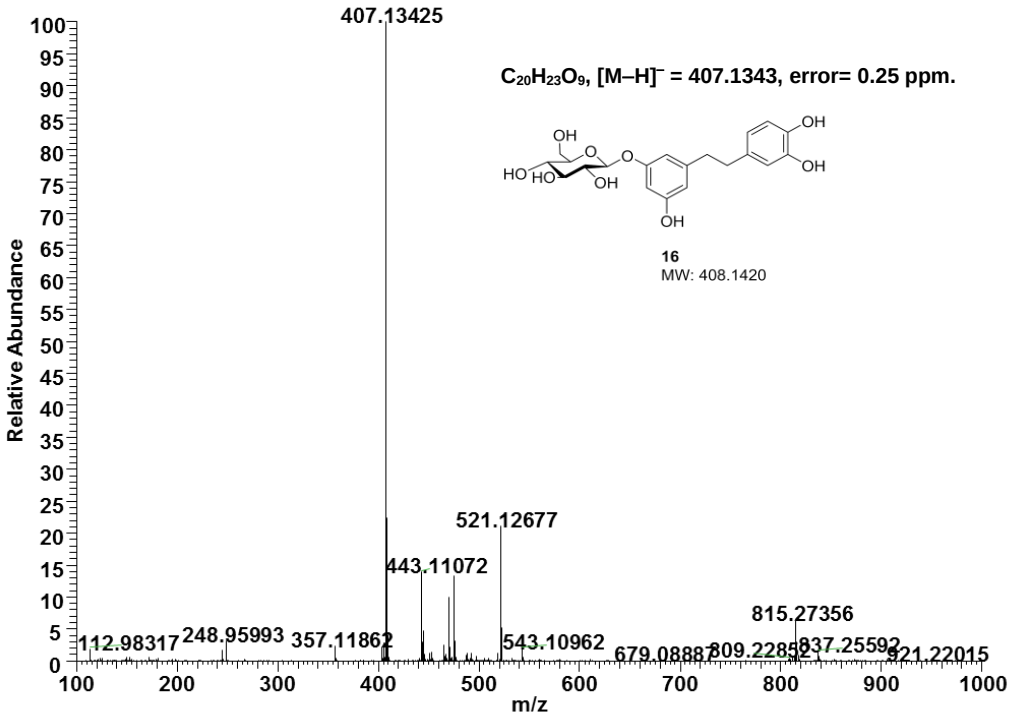

Spectrum S16. The HR-ESI-MS spectrum of **16**.

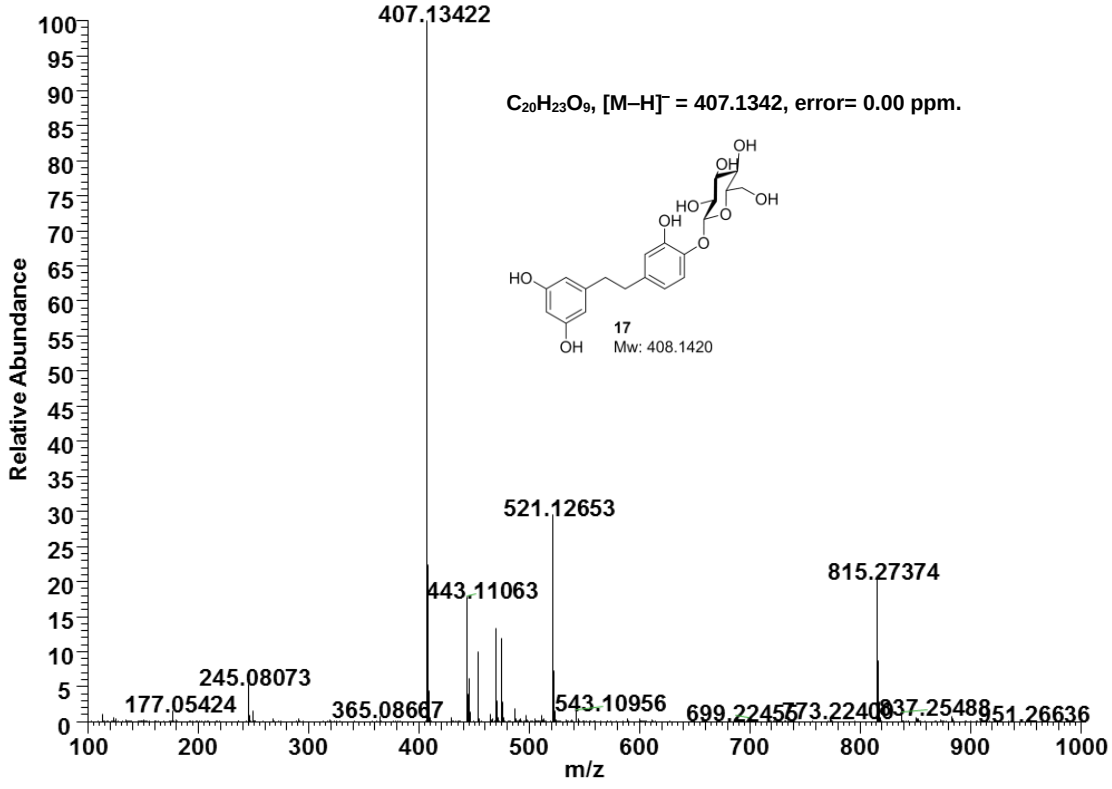

Spectrum S17. The HR-ESI-MS spectrum of **17**.

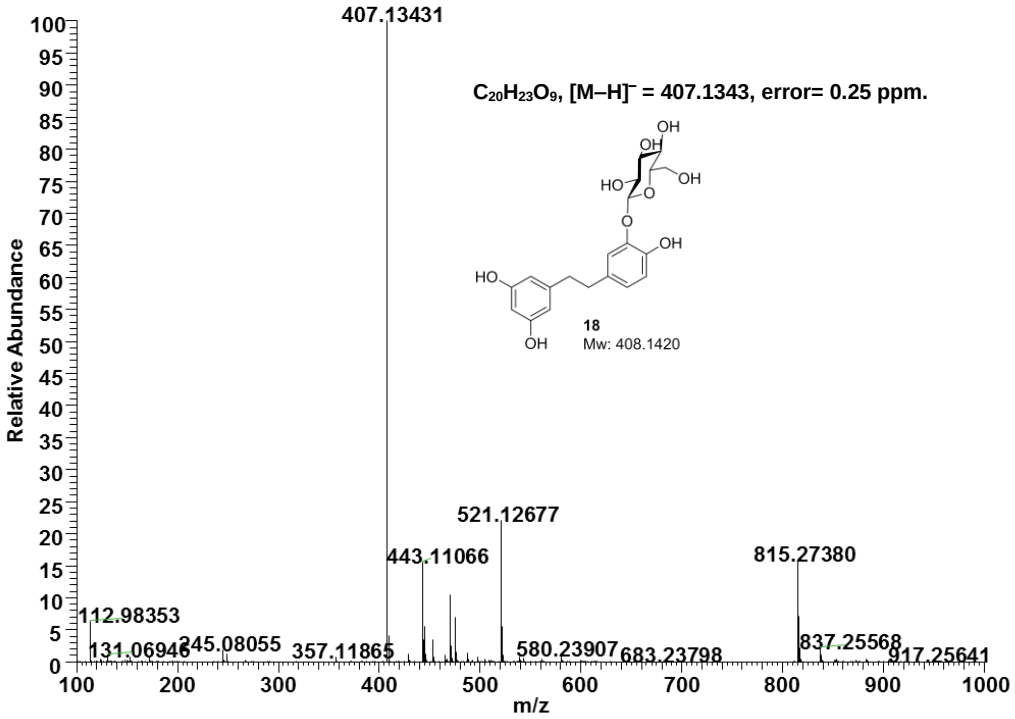

Spectrum S18. The HR-ESI-MS spectrum of **18**.

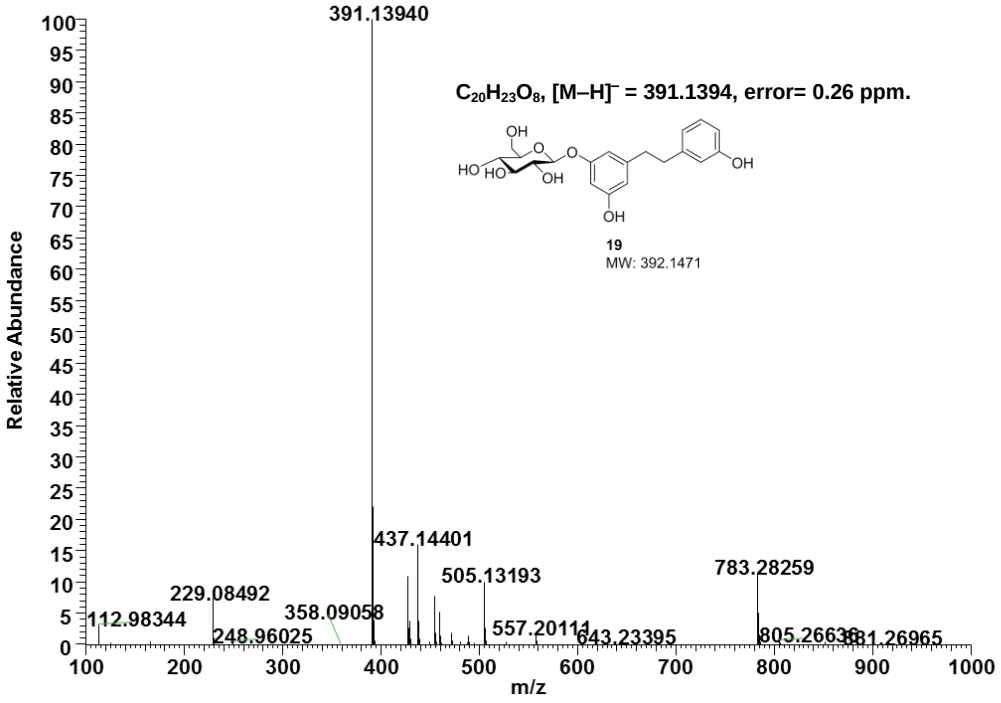

Spectrum S19. The HR-ESI-MS spectrum of **19**.

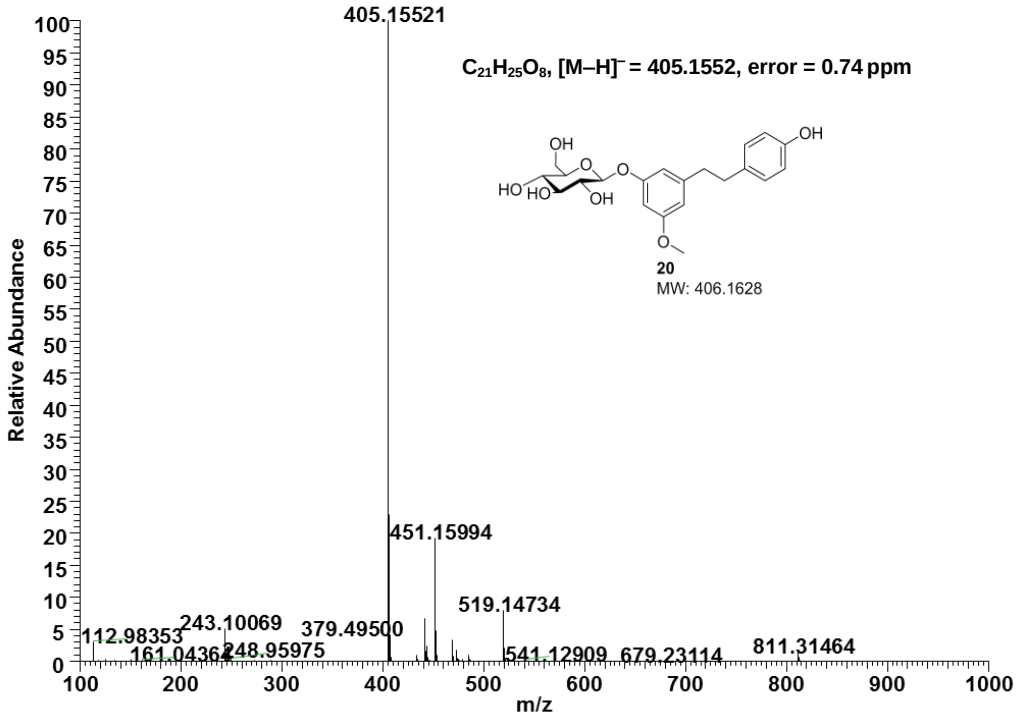

Spectrum S20. The HR-ESI-MS spectrum of **20**.

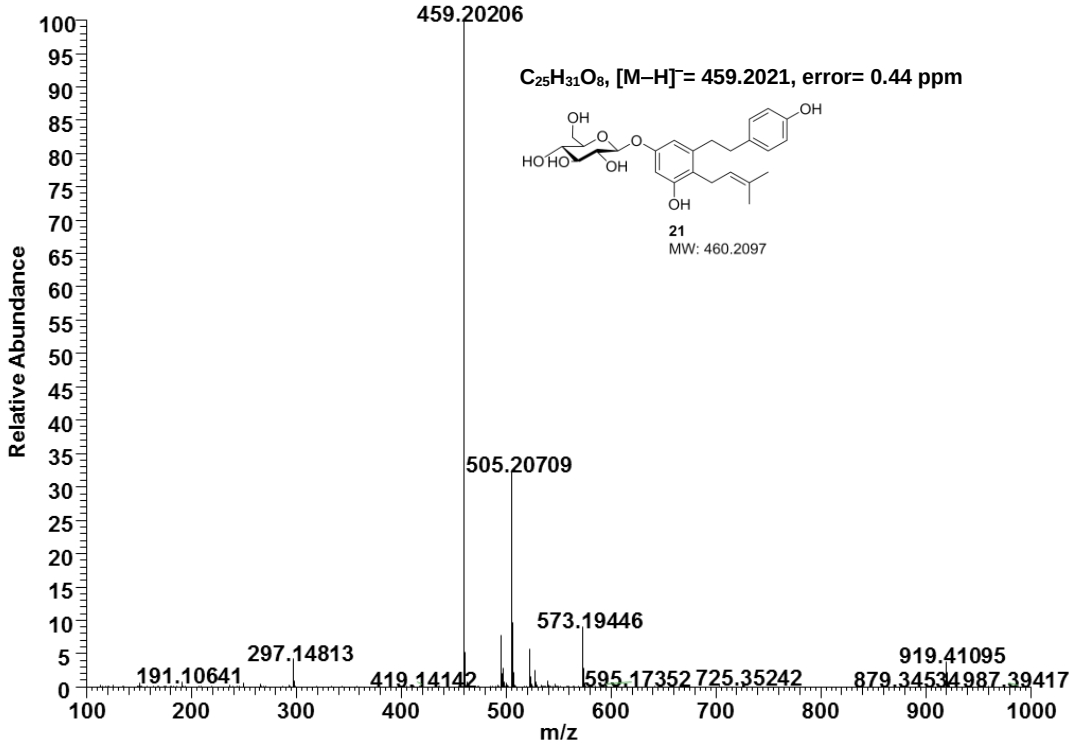

Spectrum S21. The HR-ESI-MS spectrum of **21**.

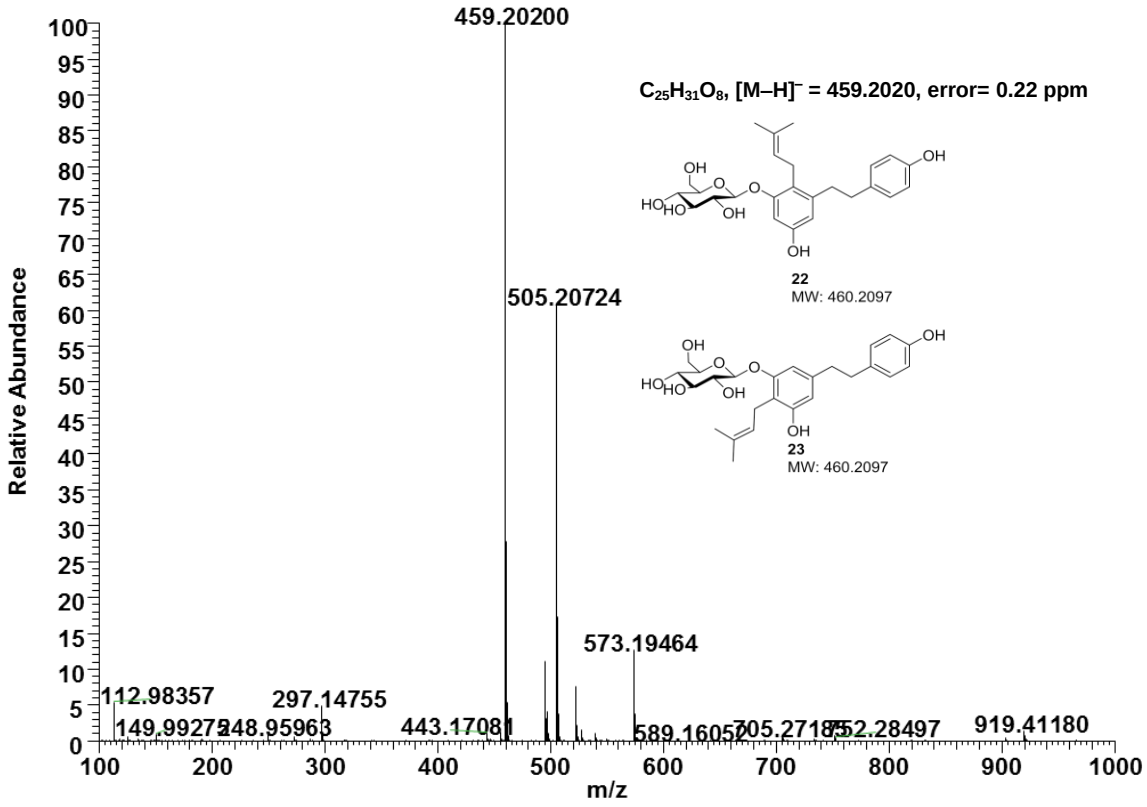

Spectrum S22. The HR-ESI-MS spectrum of **22** and **23**.

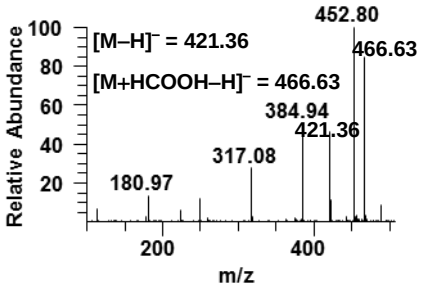

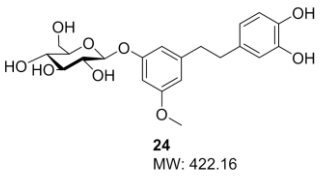

Spectrum S23. The ESI-MS spectrum of **24**.

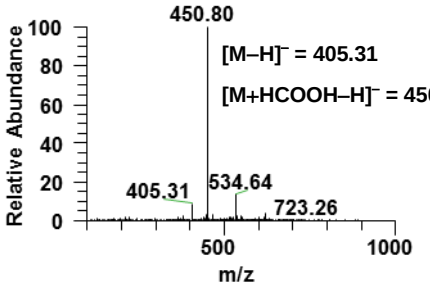

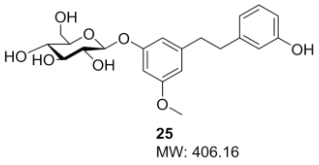

Spectrum S24. The ESI-MS spectrum of **25**.

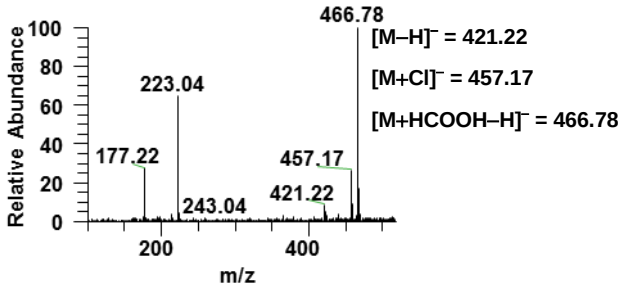

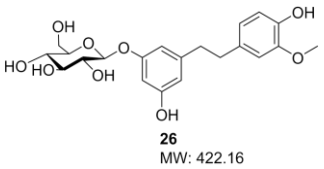

Spectrum S25. The ESI-MS spectrum of **26**.

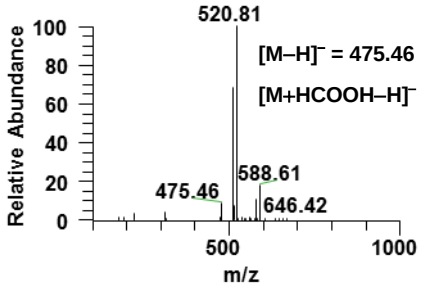

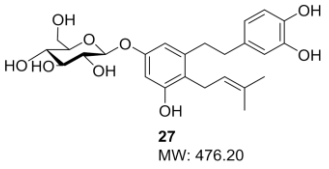

Spectrum S26. The ESI-MS spectrum of **27**.

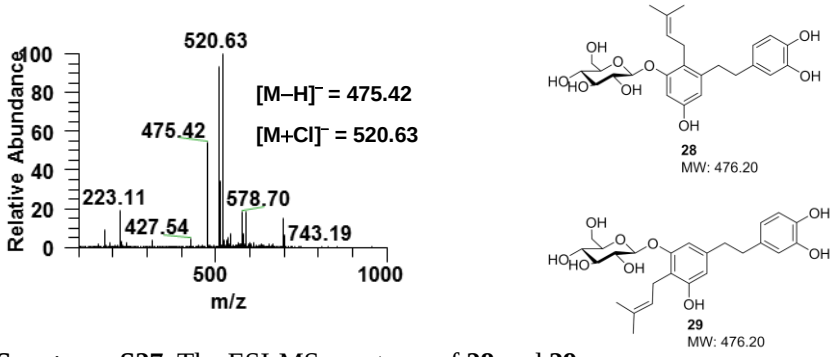

Spectrum S27. The ESI-MS spectrum of **28** and **29**.

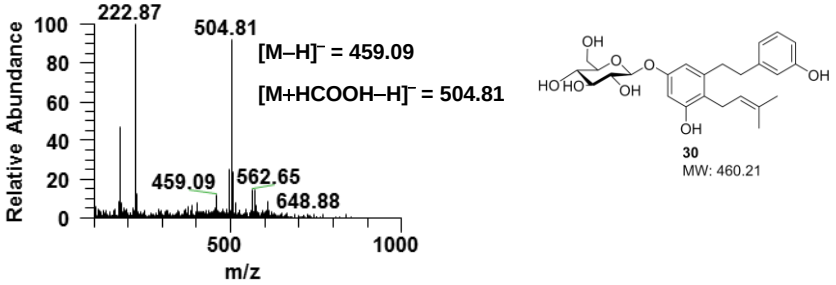

Spectrum S28. The ESI-MS spectrum of **30**.

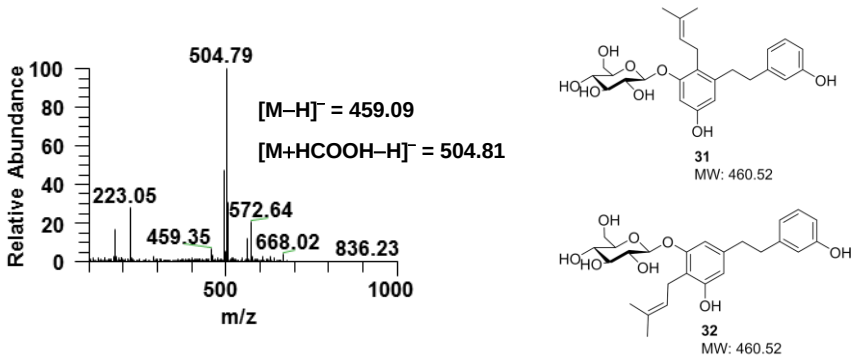

Spectrum S29. The ESI-MS spectrum of **31** and **32**.

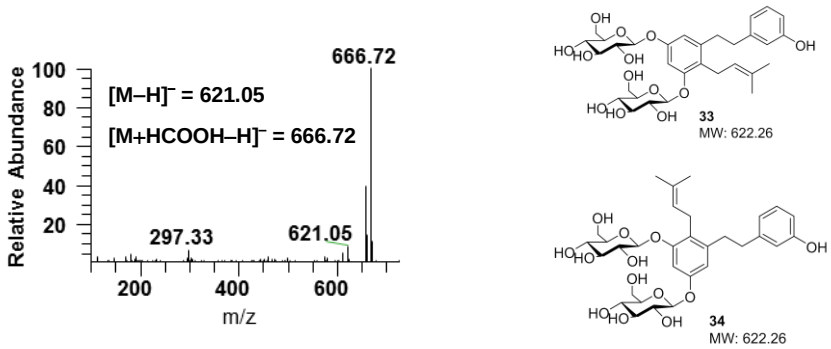

Spectrum S30. The ESI-MS spectrum of **33** and **34**.

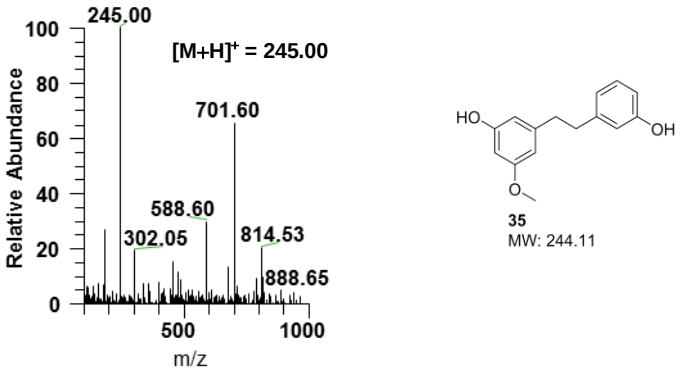

Spectrum S31. The ESI-MS spectrum of **35**.

Supplementary NMR spectra of bibenzyl derivatives (1–23)

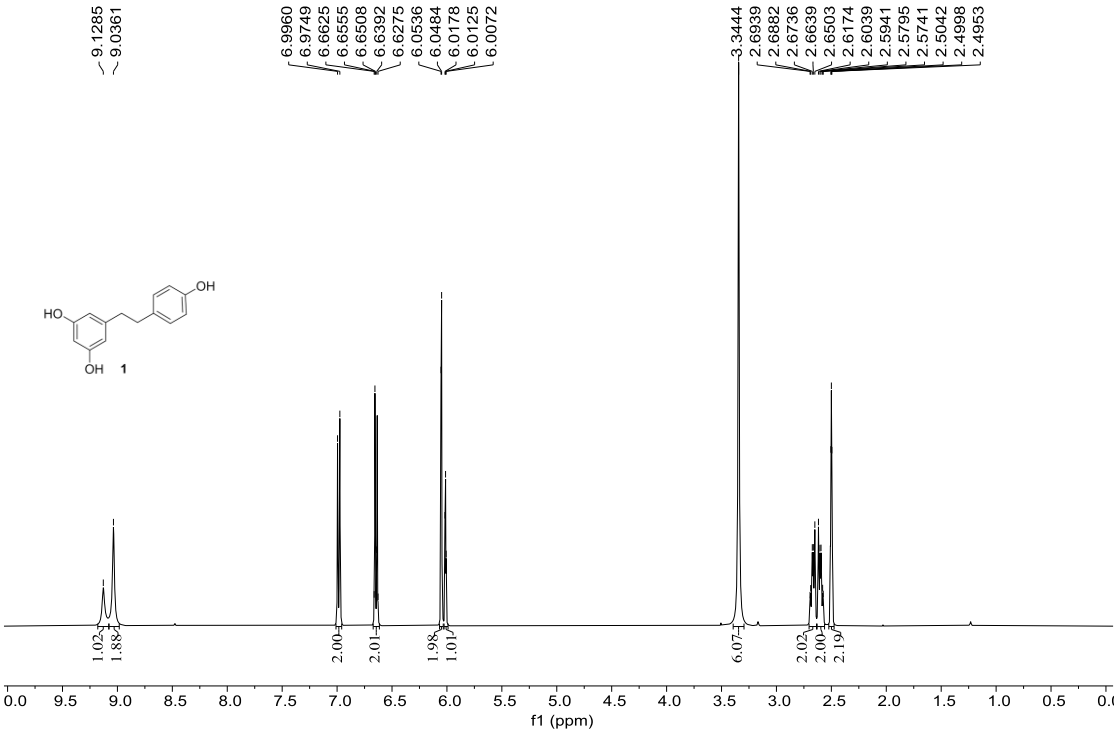

Spectrum S32. ^{1}H NMR spectrum of **1** in DMSO-d_6 at 400 MHz.

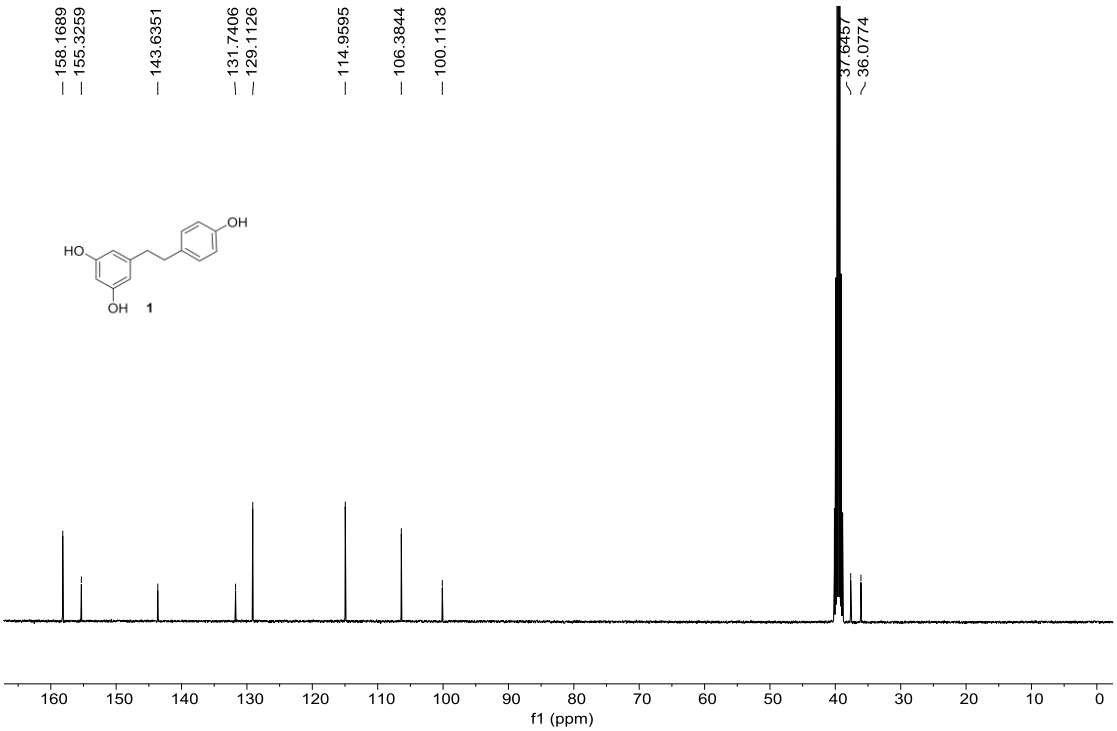

Spectrum S33. ^{13}C NMR spectrum of **1** in DMSO-d_6 at 100 MHz.

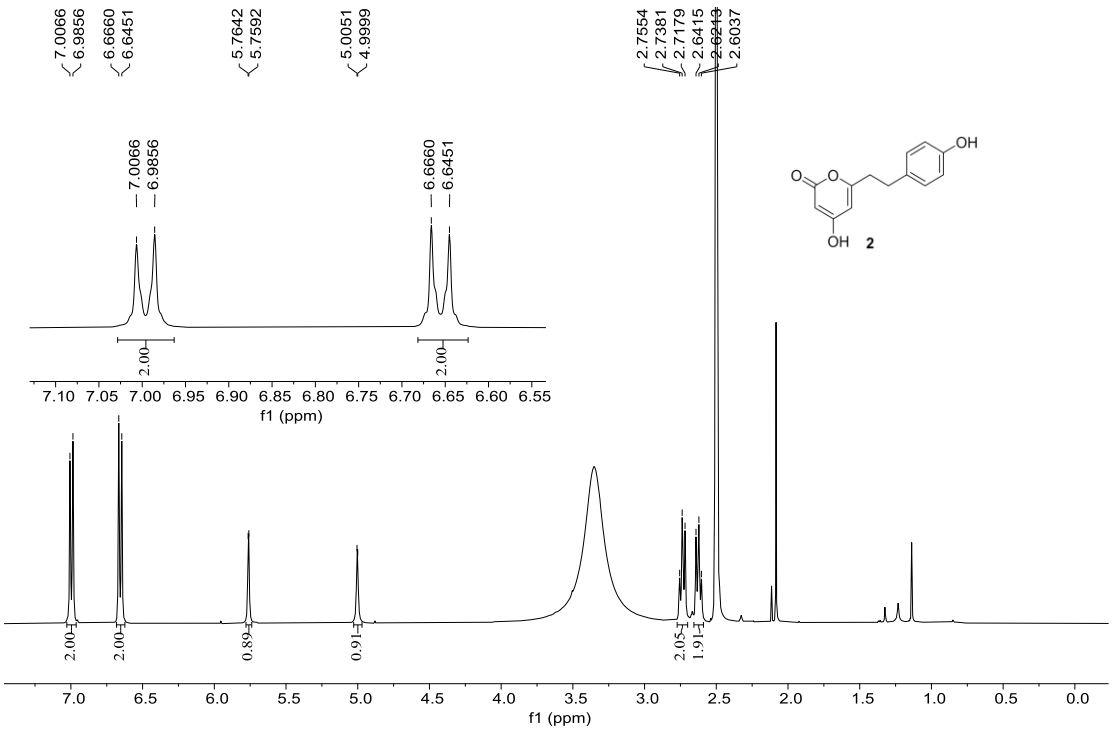

Spectrum S34. ^{1}H NMR spectrum of **2** in DMSO-d_6 at 400 MHz.

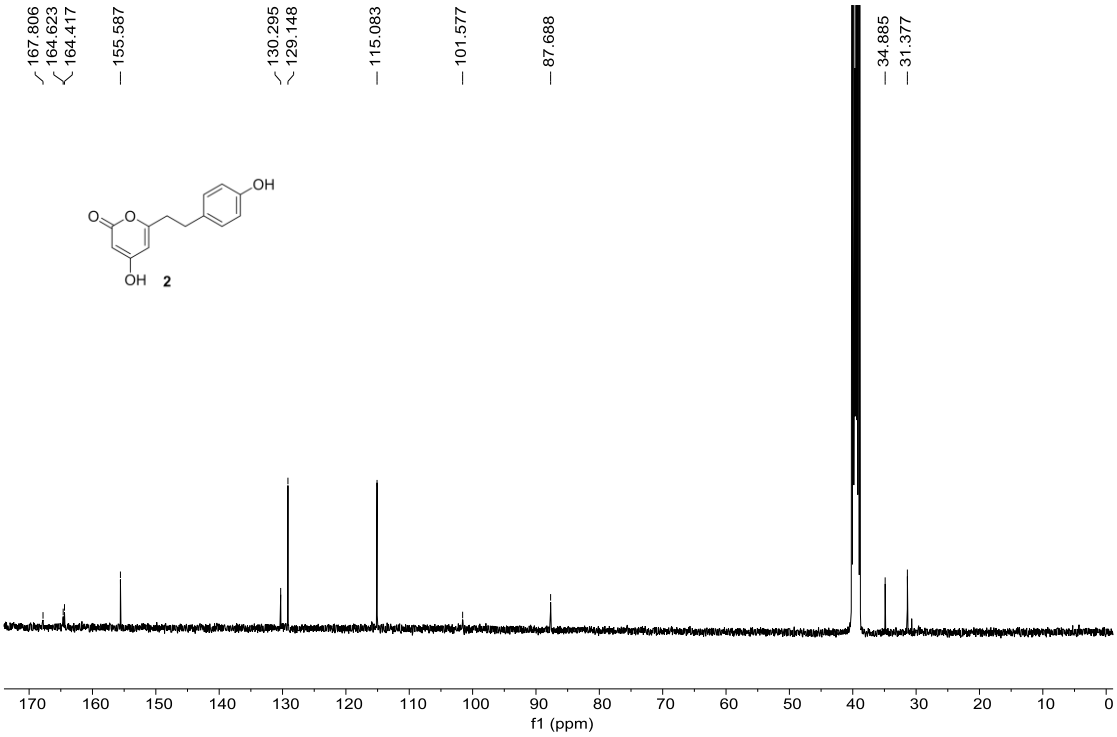

Spectrum S35. ^{13}C NMR spectrum of **2** in DMSO-d_6 at 100 MHz.

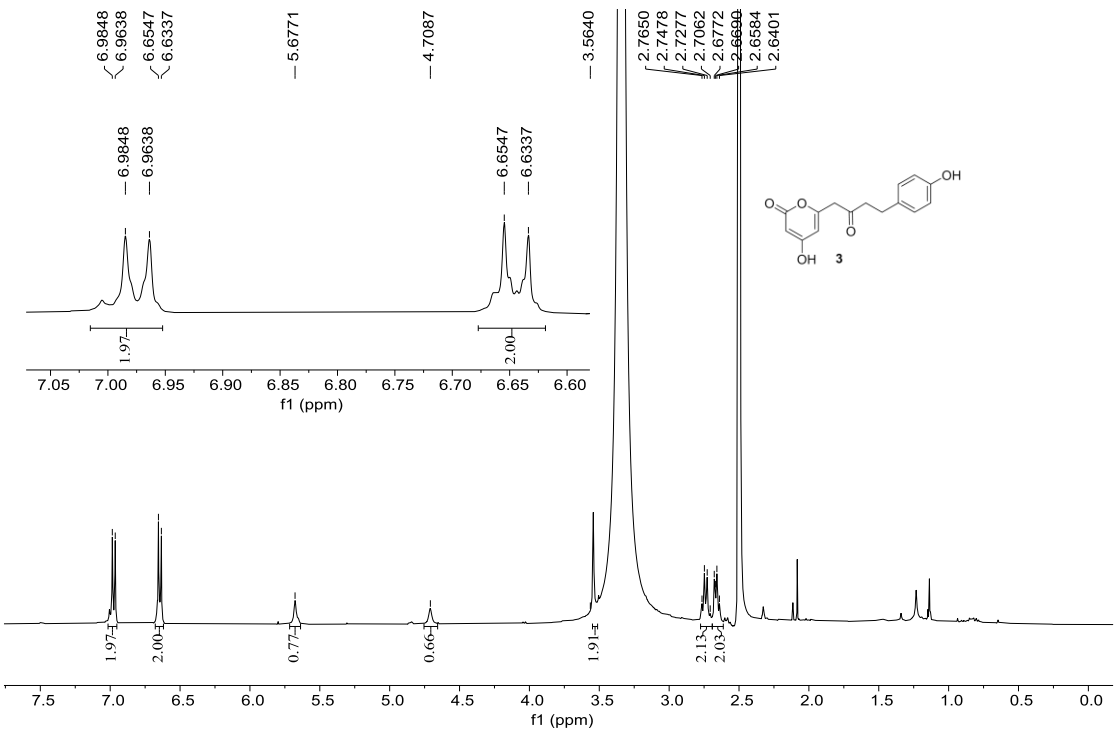

Spectrum S36. ^{1}H NMR spectrum of **3** in DMSO-d_6 at 400 MHz.

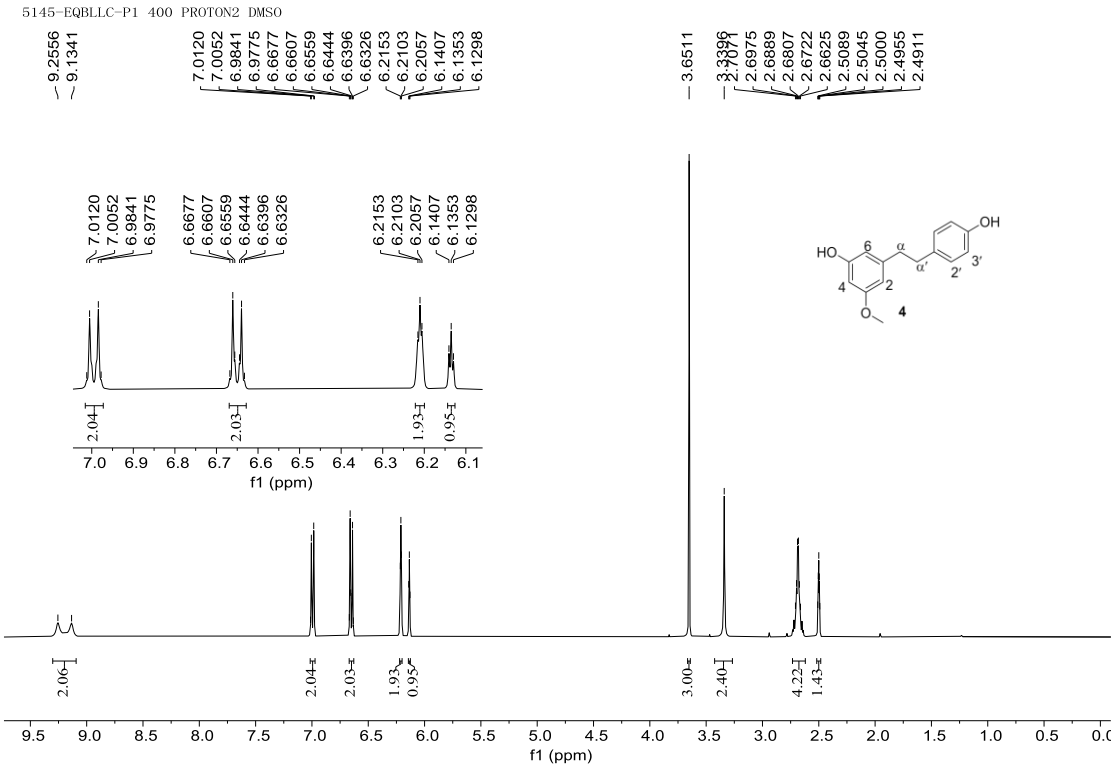

Spectrum S37. ^{1}H NMR spectrum of **4** in DMSO-d_6 at 400 MHz.

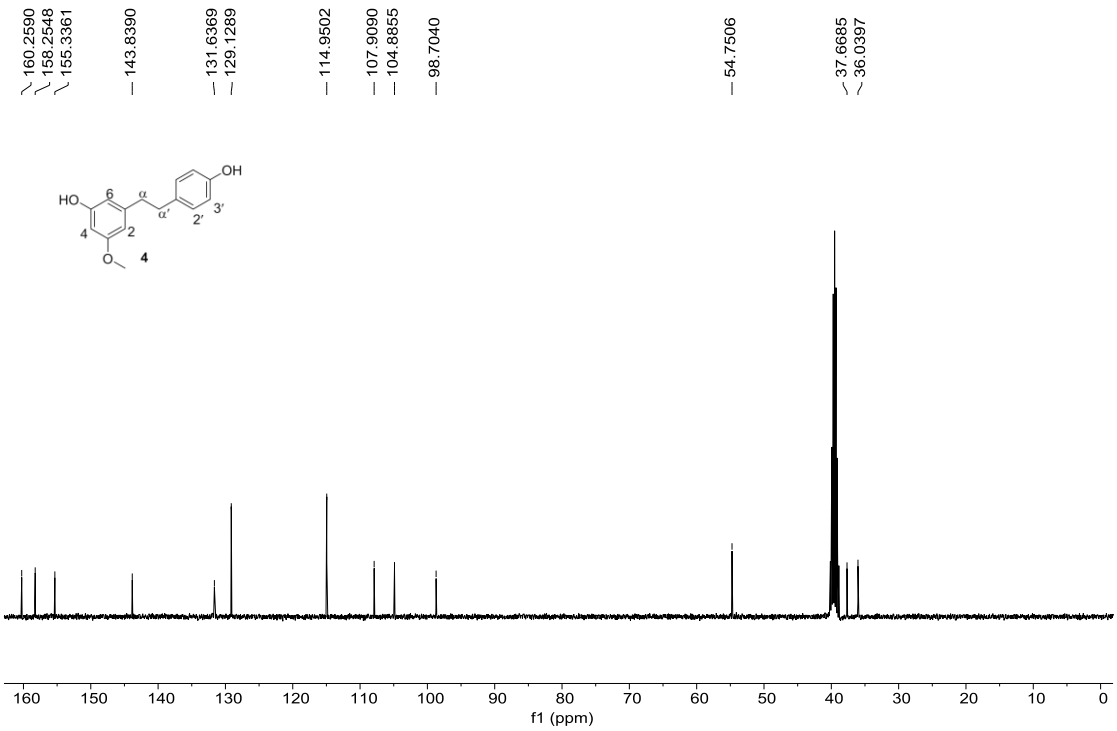

Spectrum S38. ^{13}C NMR spectrum of **4** in DMSO-d_6 at 100 MHz.

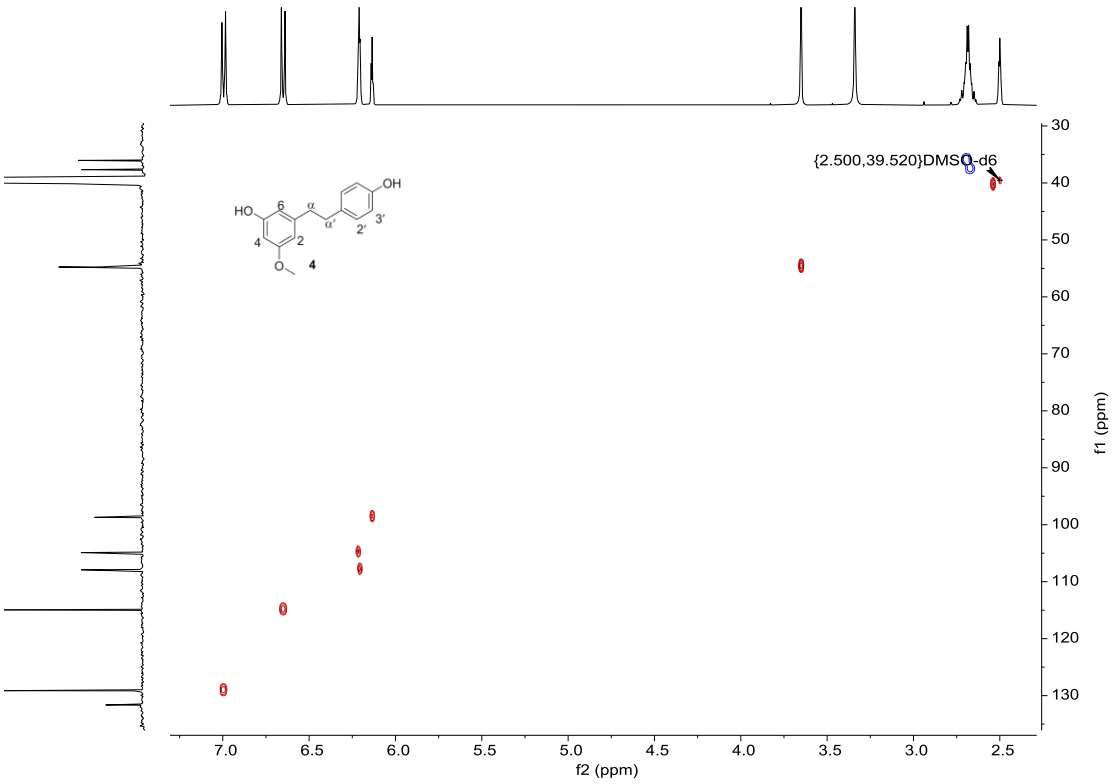

Spectrum S39. HSQC spectrum of **4** in DMSO-d_6.

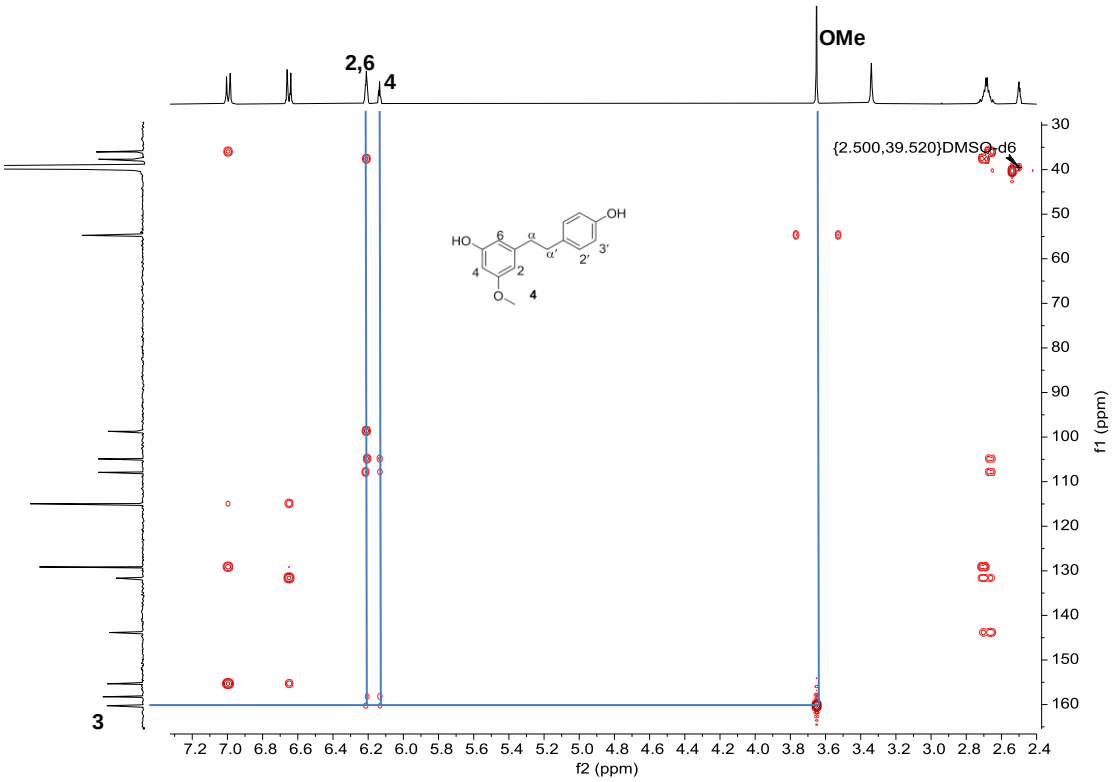

Spectrum S40. HMBC spectrum of **4** in DMSO-d_6.

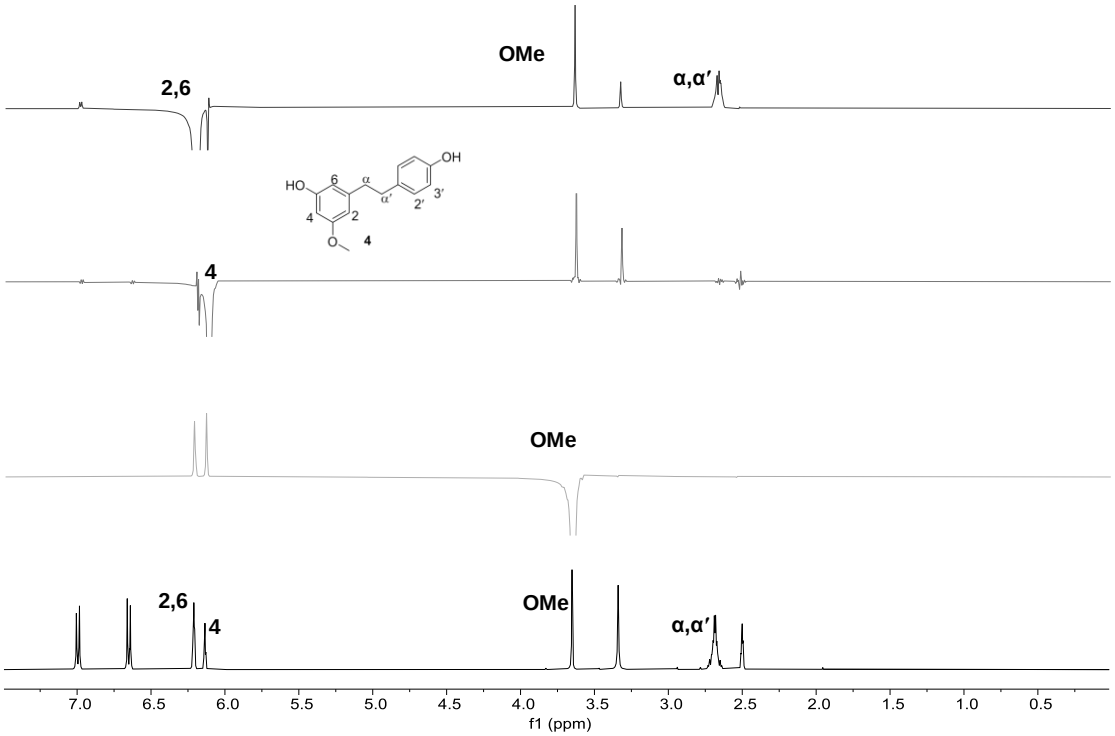

Spectrum S41. NOESY spectrum of **4** in DMSO-d_6.

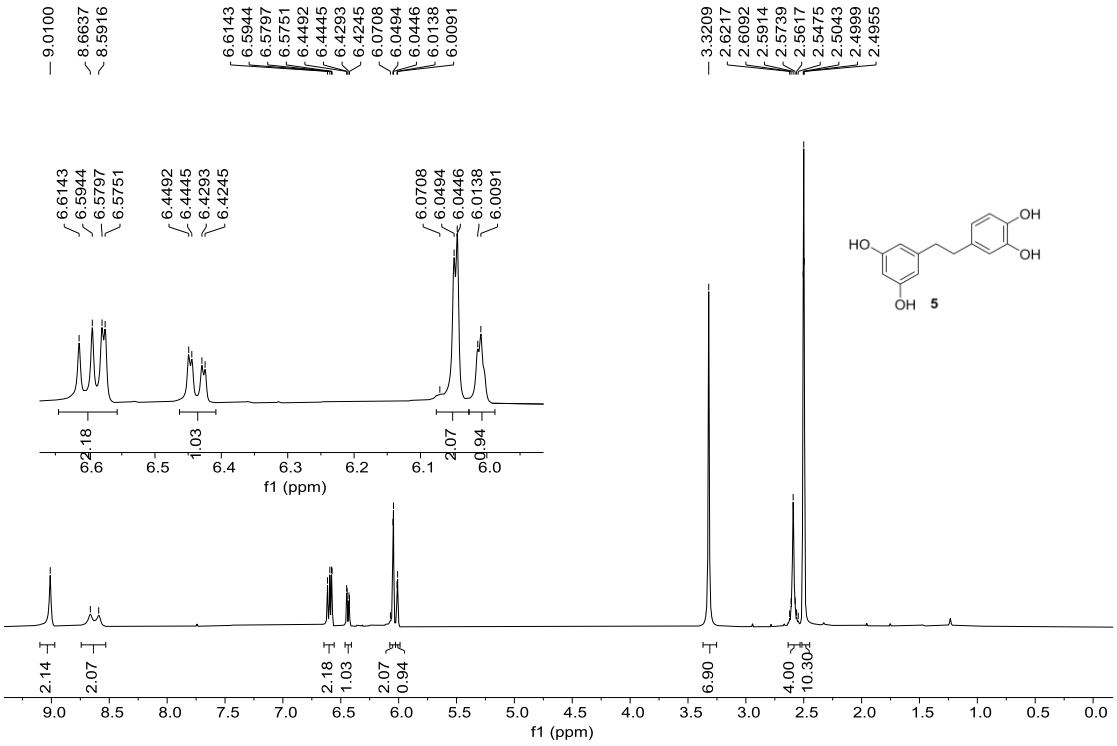

Spectrum S42. ^{1}H NMR spectrum of **5** in DMSO-d_6 at 400 MHz.

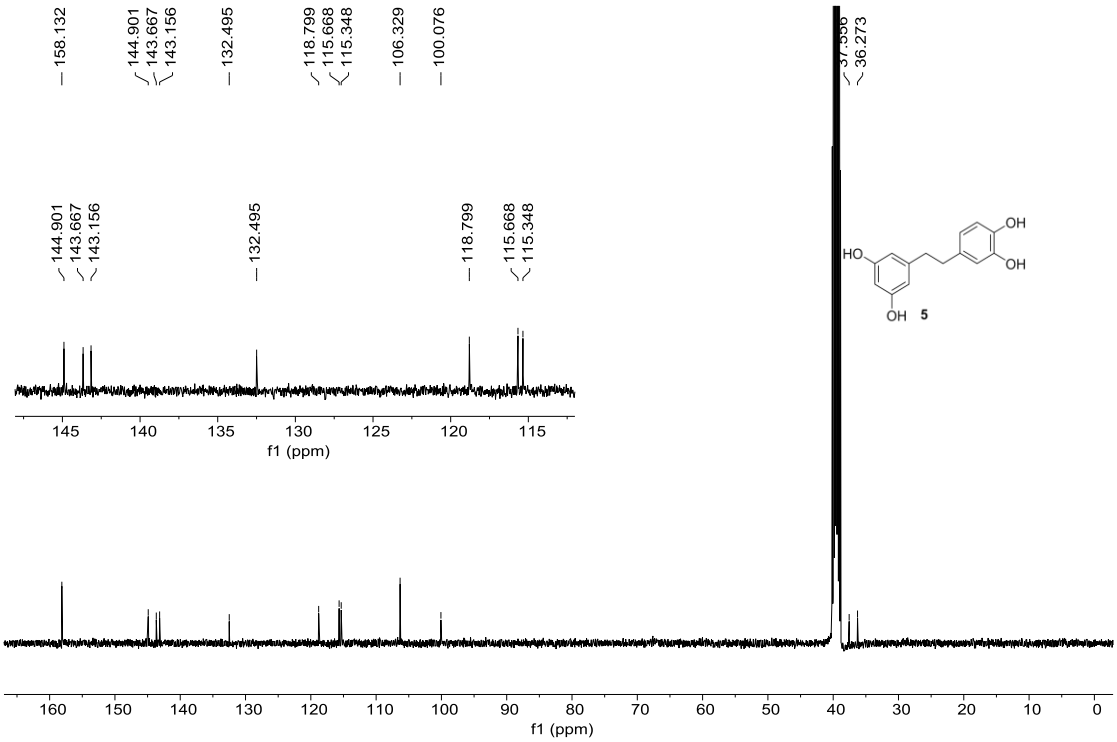

Spectrum S43. ^{13}C NMR spectrum of **5** in DMSO-d_6 at 100 MHz.

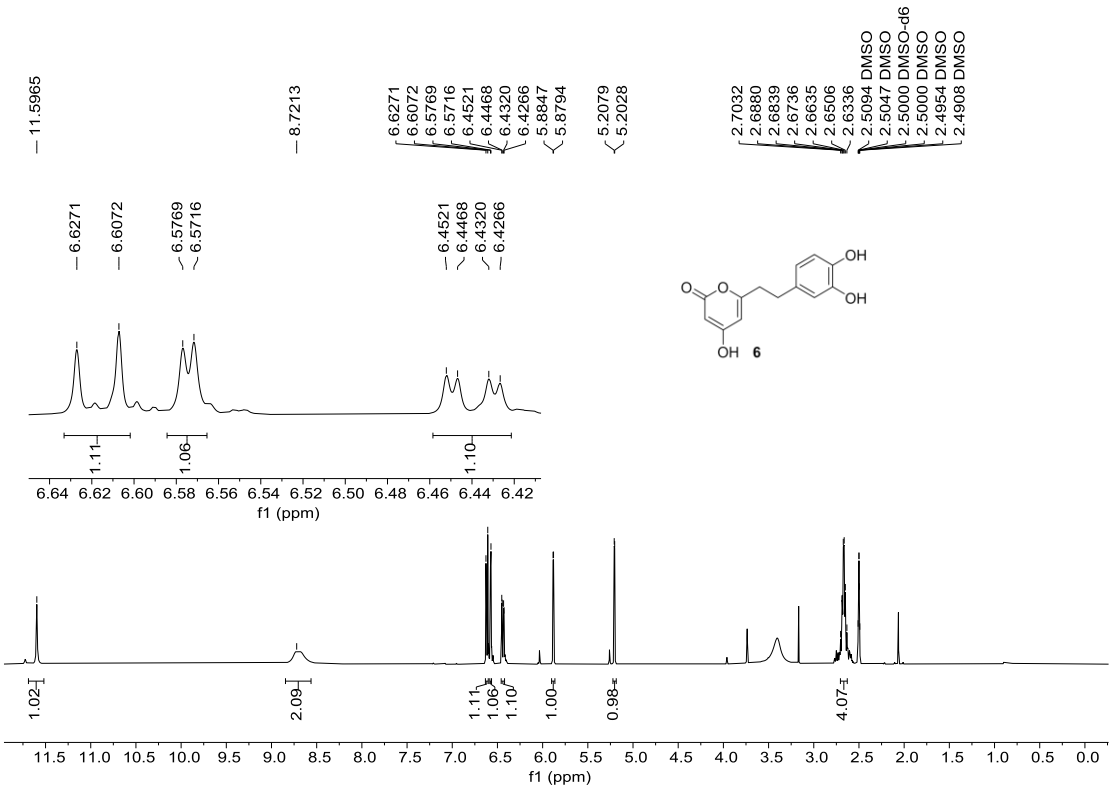

Spectrum S44. ^{1}H NMR spectrum of **6** in DMSO-d_6 at 400 MHz.

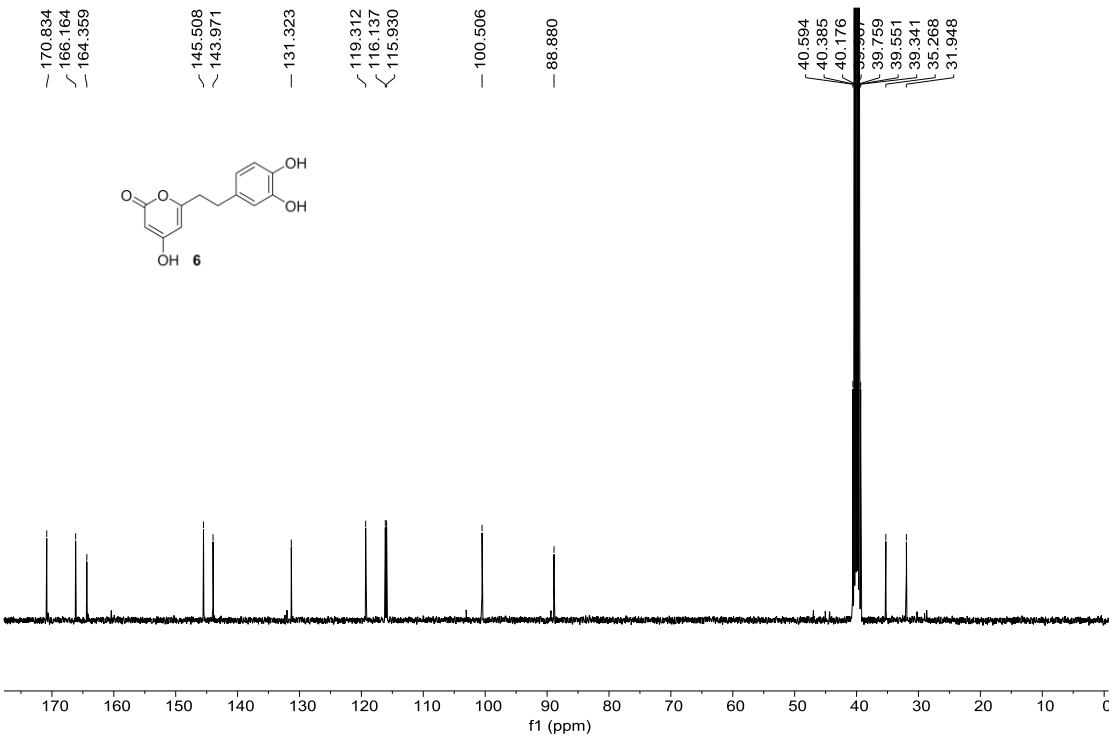

Spectrum S45. ^{13}C NMR spectrum of **6** in DMSO-d_6 at 100 MHz.

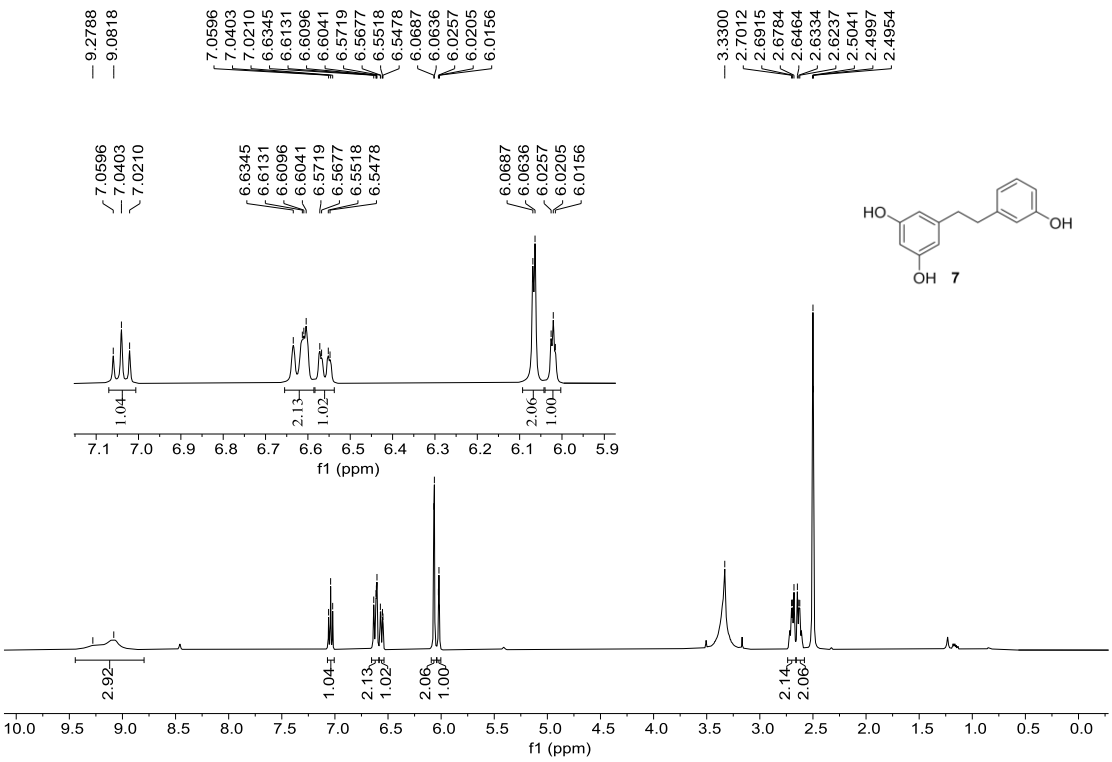

Spectrum S46. ^{1}H NMR spectrum of **7** in DMSO-d_6 at 400 MHz.

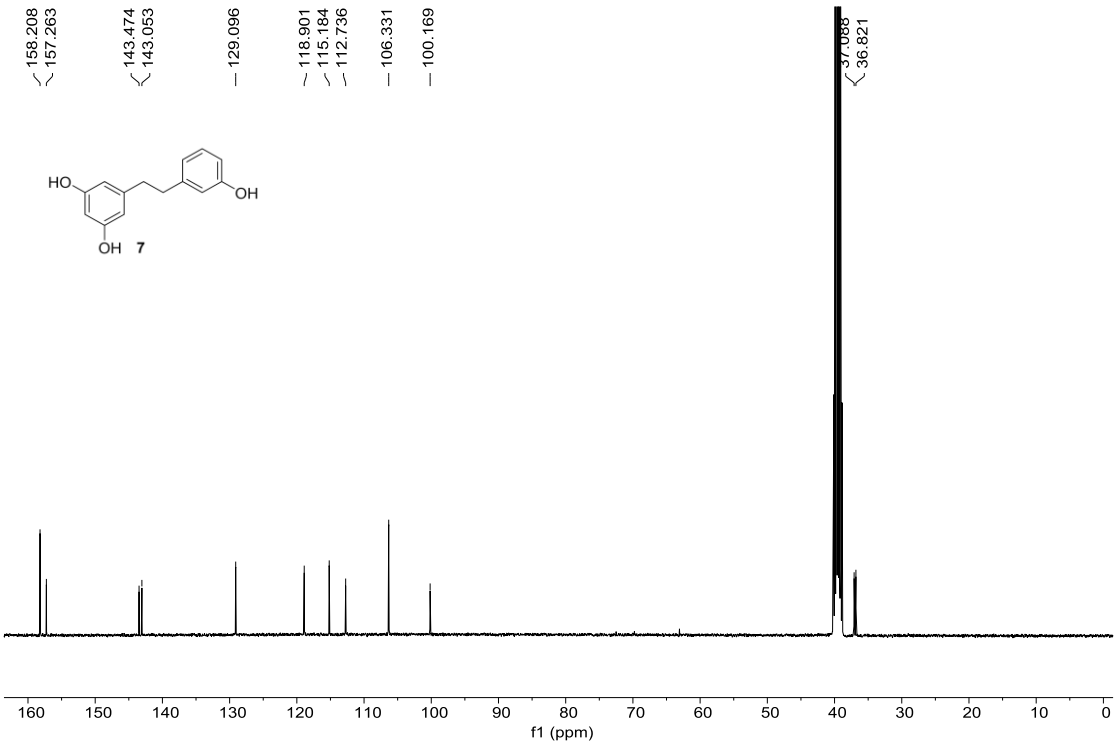

Spectrum S47. ^{13}C NMR spectrum of **7** in DMSO-d_6 at 100 MHz.

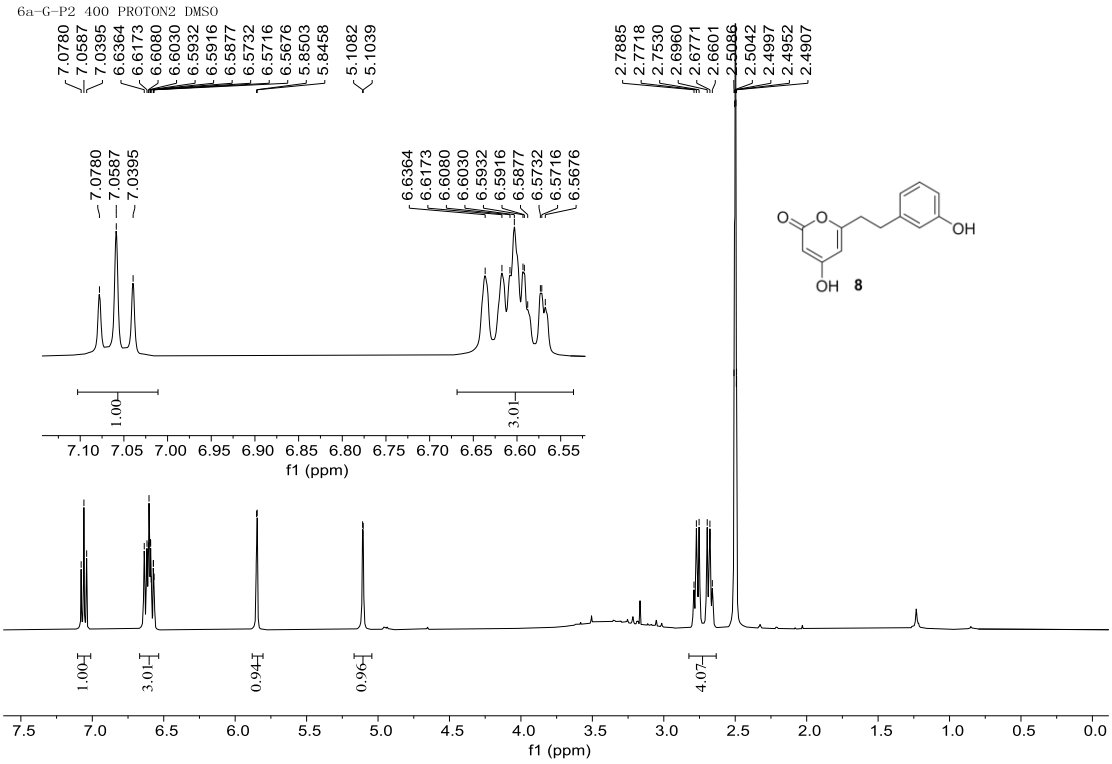

Spectrum S48. ^{1}H NMR spectrum of **8** in DMSO-d_6 at 400 MHz.

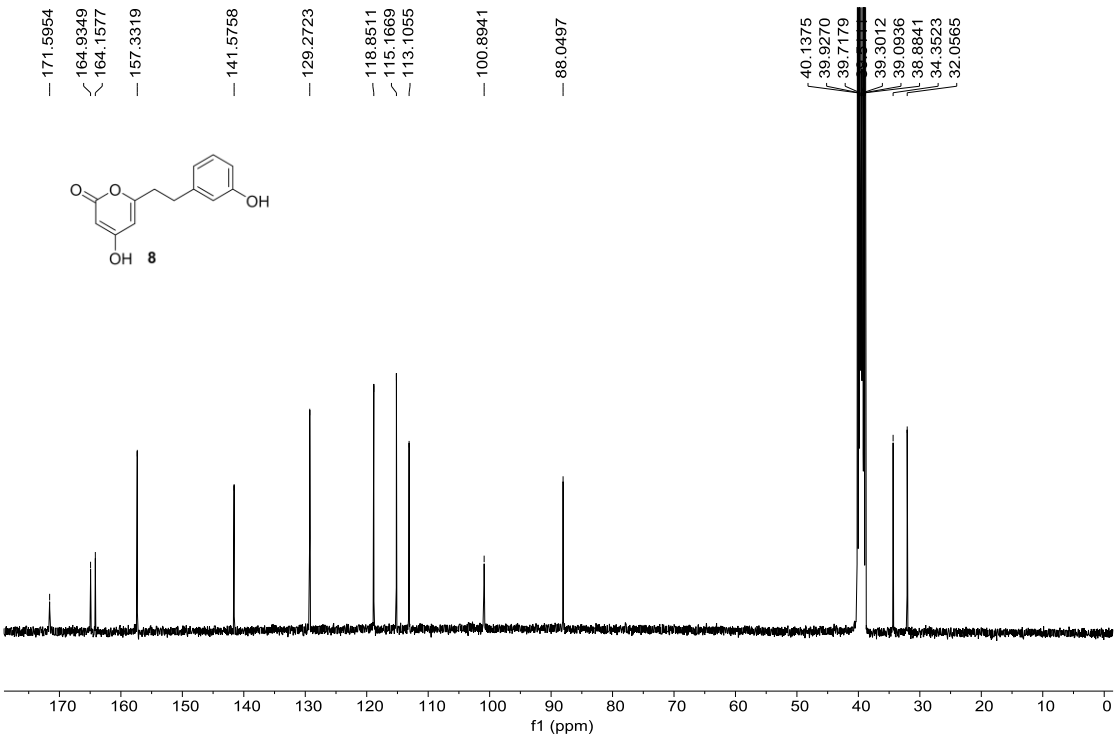

Spectrum S49. ^{13}C NMR spectrum of **8** in DMSO-d_6 at 100 MHz.

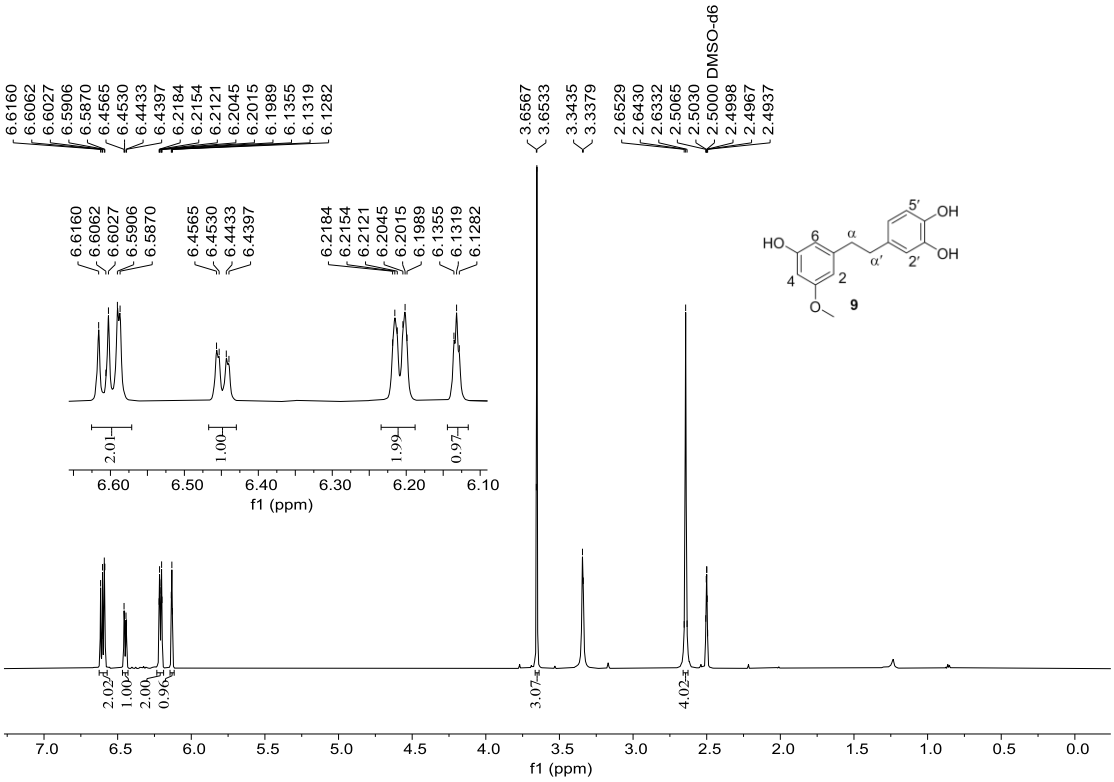

Spectrum S50. ^{1}H NMR spectrum of **9** in DMSO-d_6 at 600 MHz.

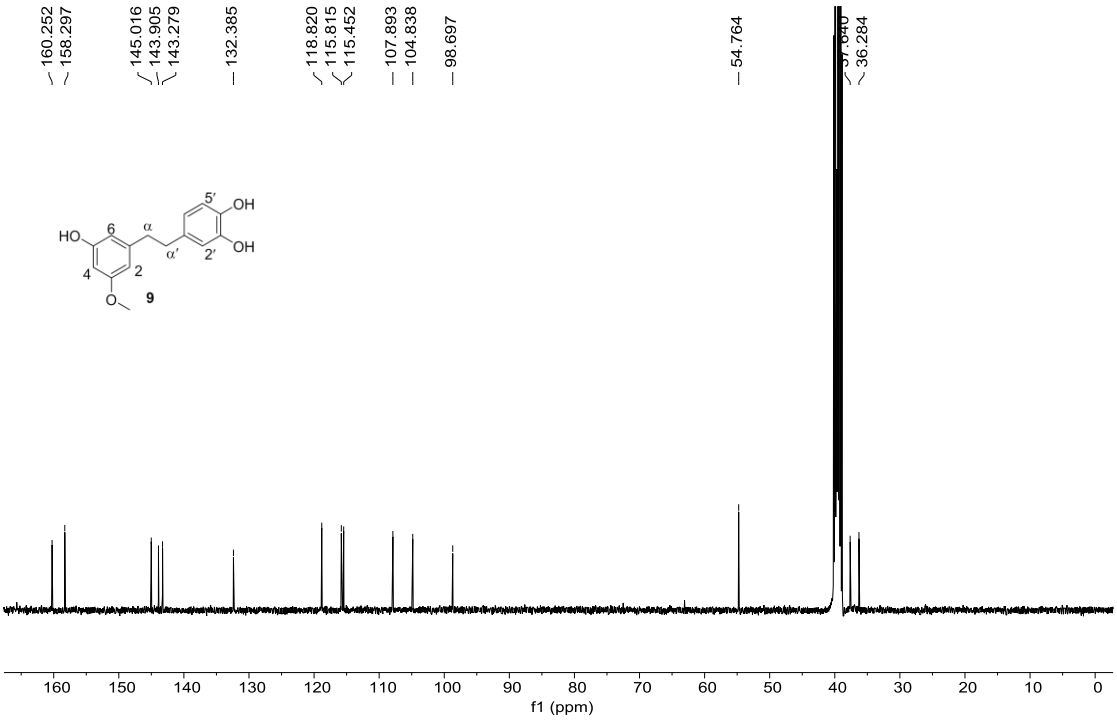

Spectrum S51. ^{13}C NMR spectrum of **9** in DMSO-d_6 at 100 MHz.

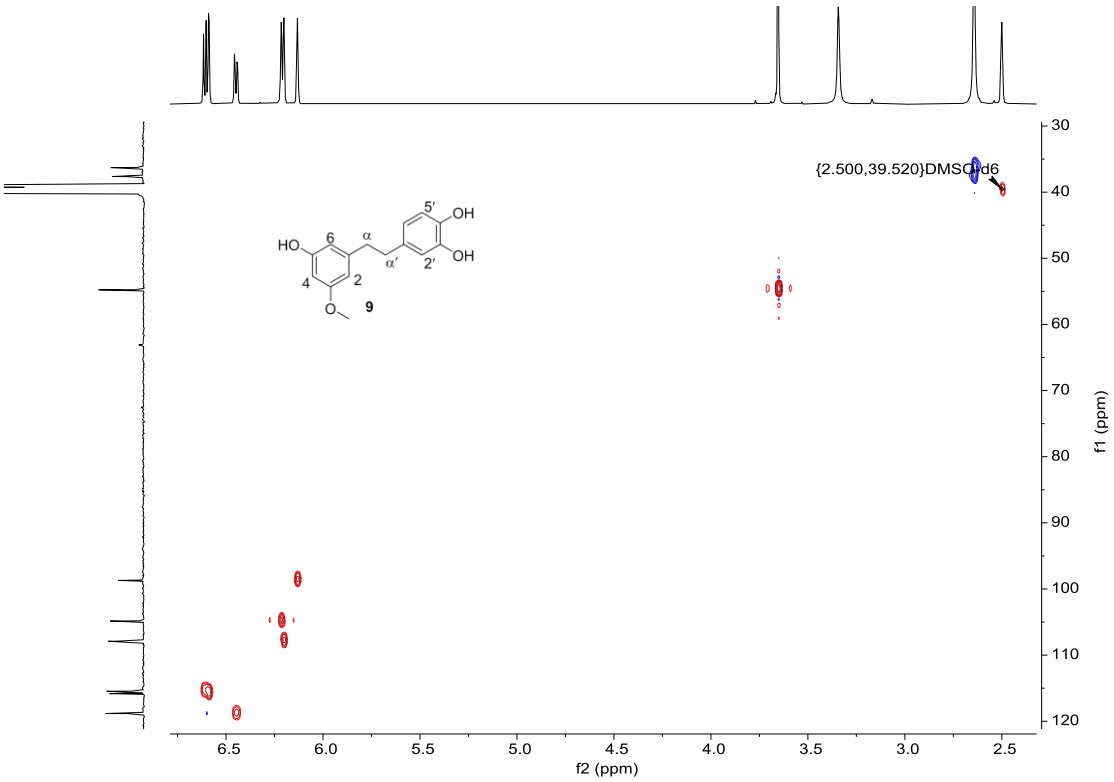

Spectrum S52. HSQC spectrum of **9** in DMSO-d_6.

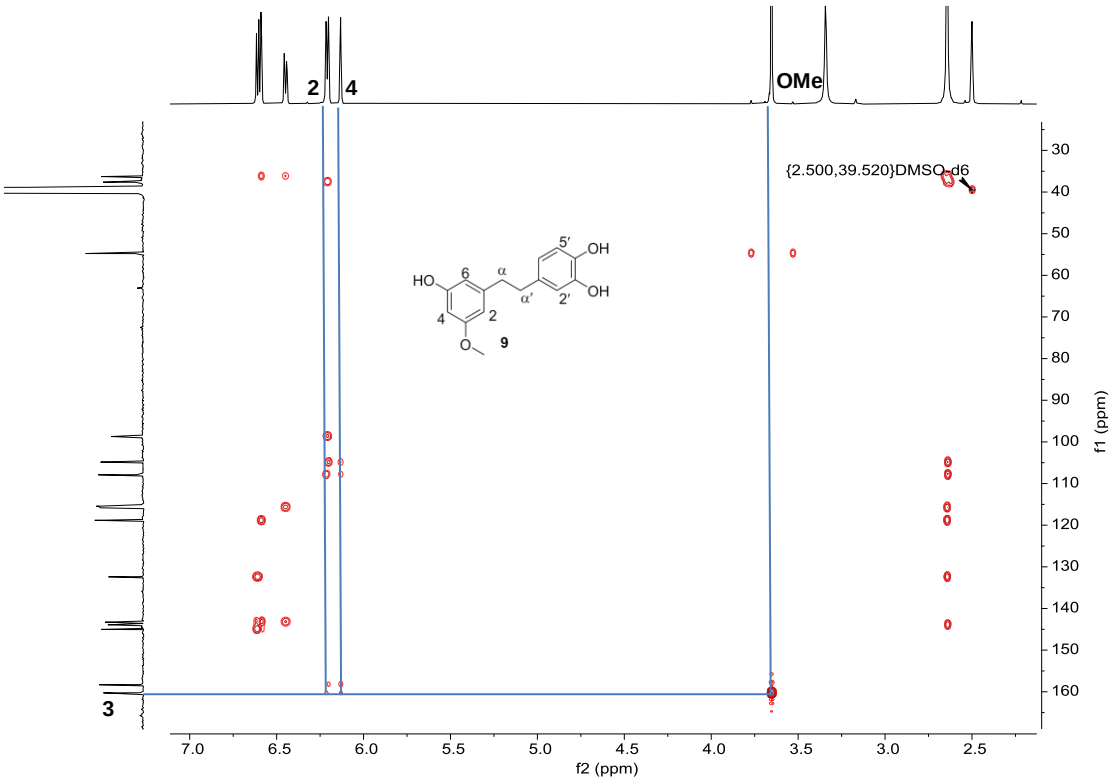

Spectrum S53. HMBC spectrum of **9** in DMSO-d_6.

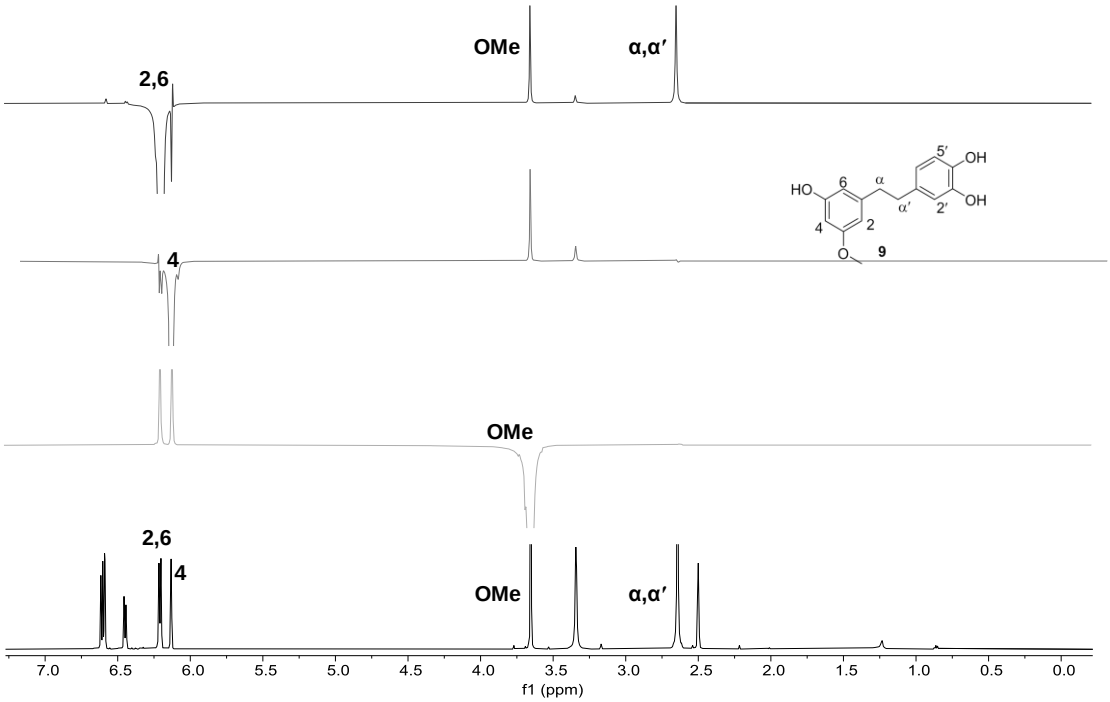

Spectrum S54. NOESY spectrum of **9** in DMSO-d_6.

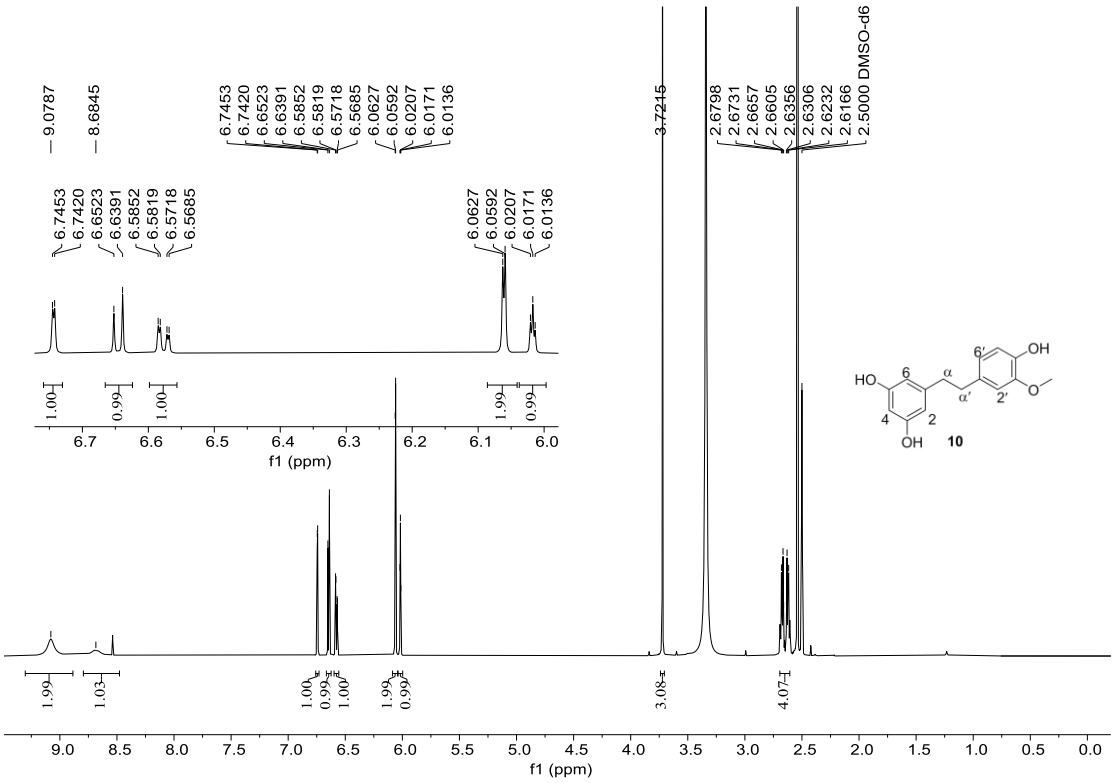

Spectrum S55. ^{1}H NMR spectrum of **10** in DMSO-d_6 at 600 MHz.

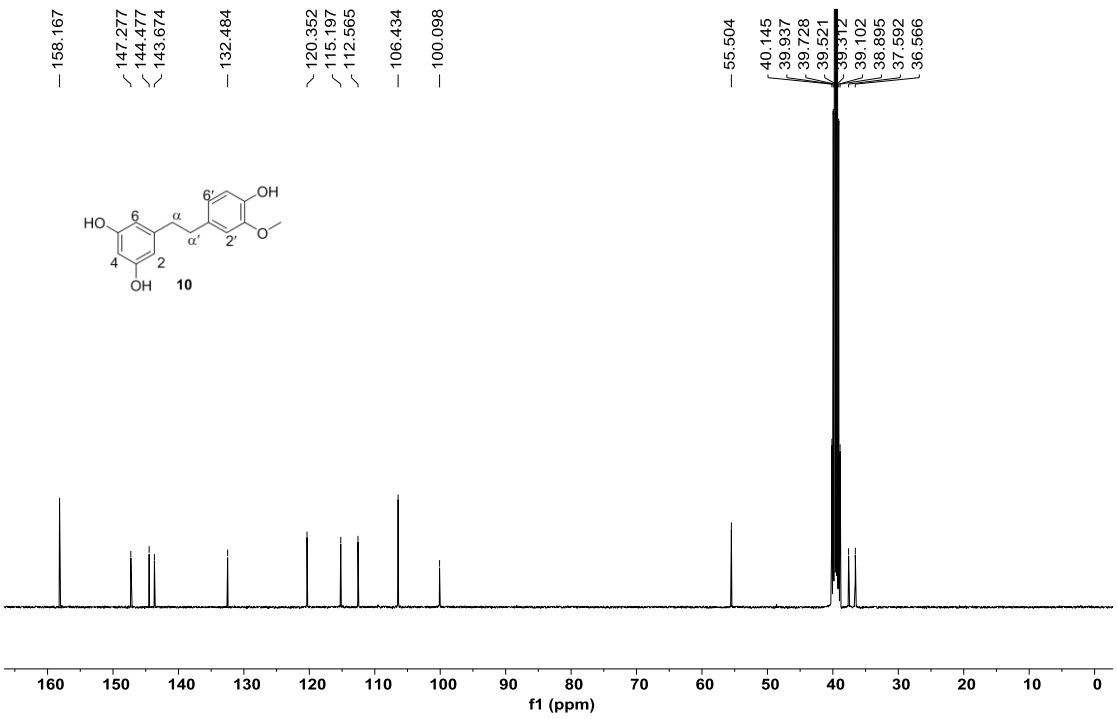

Spectrum S56. ^{13}C NMR spectrum of **10** in DMSO-d_6 at 100 MHz.

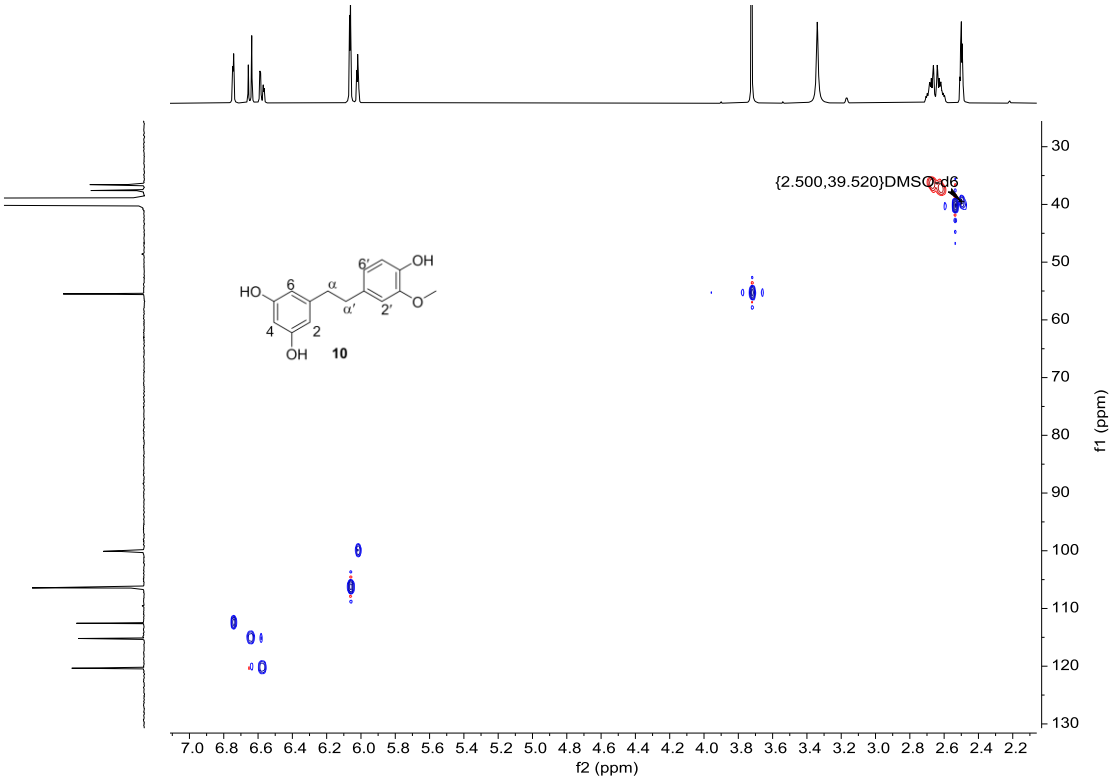

Spectrum S57. HSQC spectrum of **10** in DMSO-d_6.

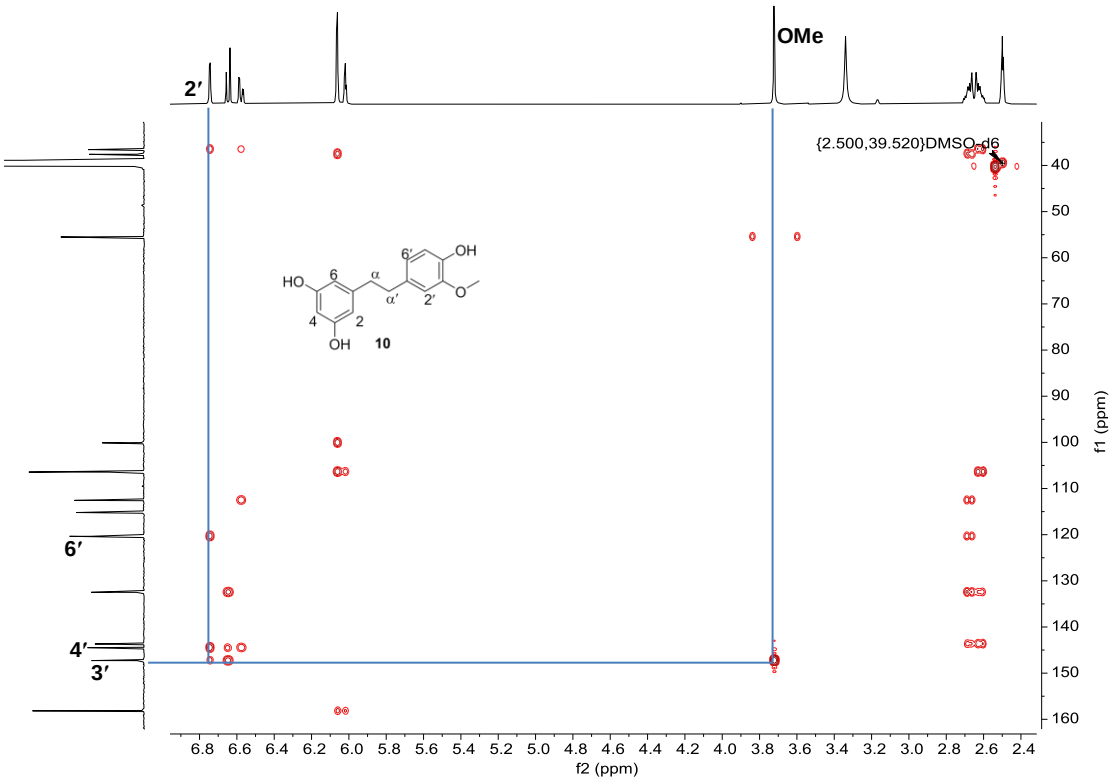

Spectrum S58. HMBC spectrum of **10** in DMSO-d_6.

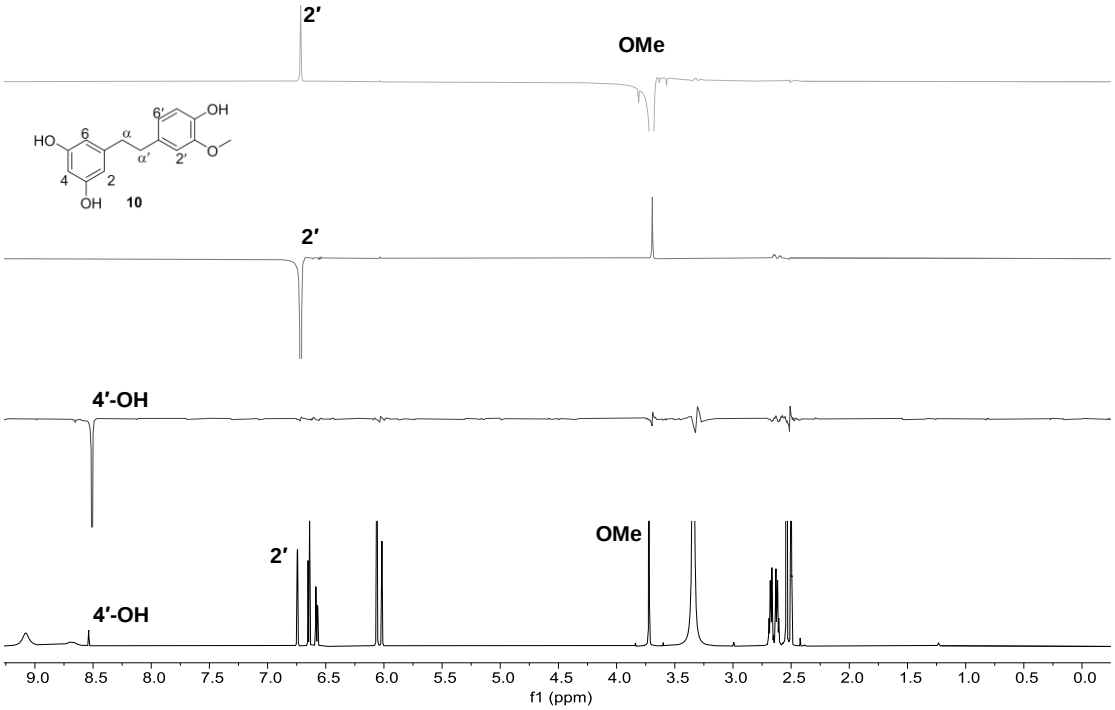

Spectrum S59. NOESY spectrum of **10** in DMSO-d_6.

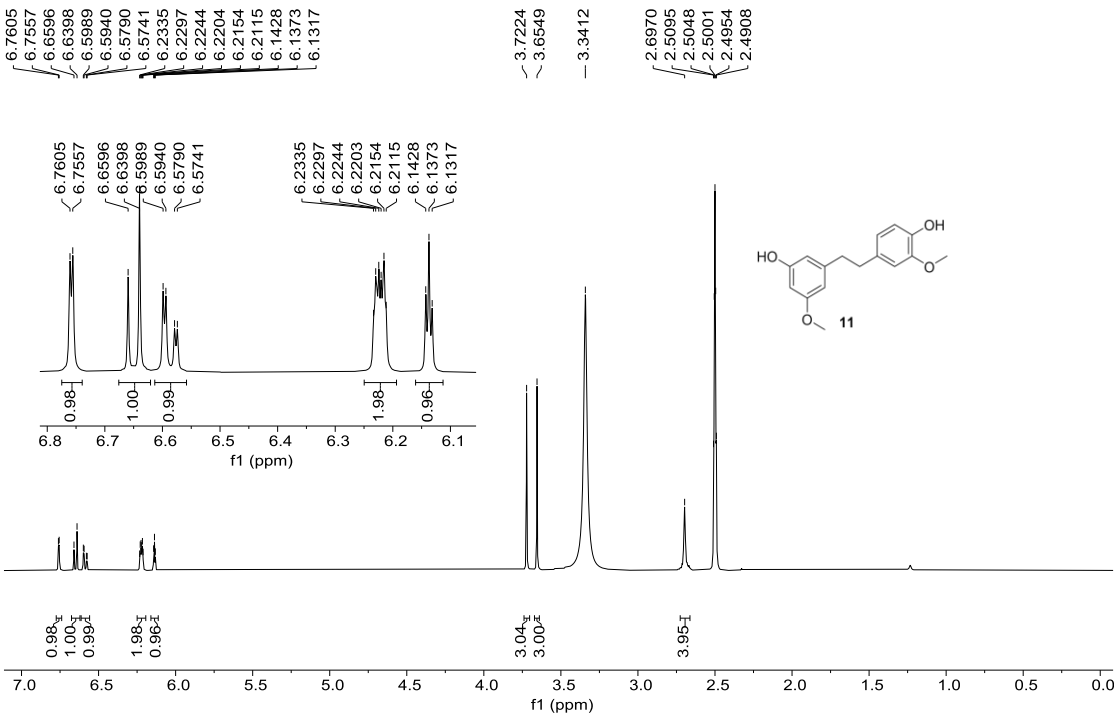

Spectrum S60. ^{1}H NMR spectrum of **11** in DMSO-d_6 at 400 MHz.

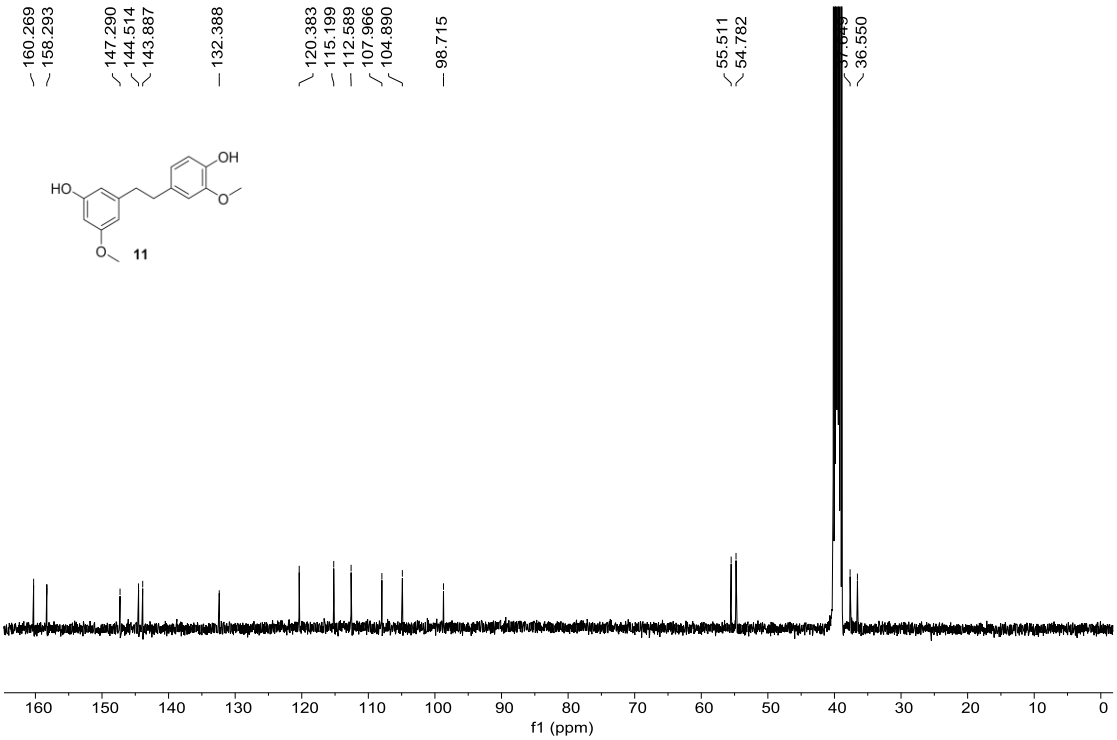

Spectrum S61. ^{13}C NMR spectrum of **11** in DMSO-d_6 at 100 MHz.

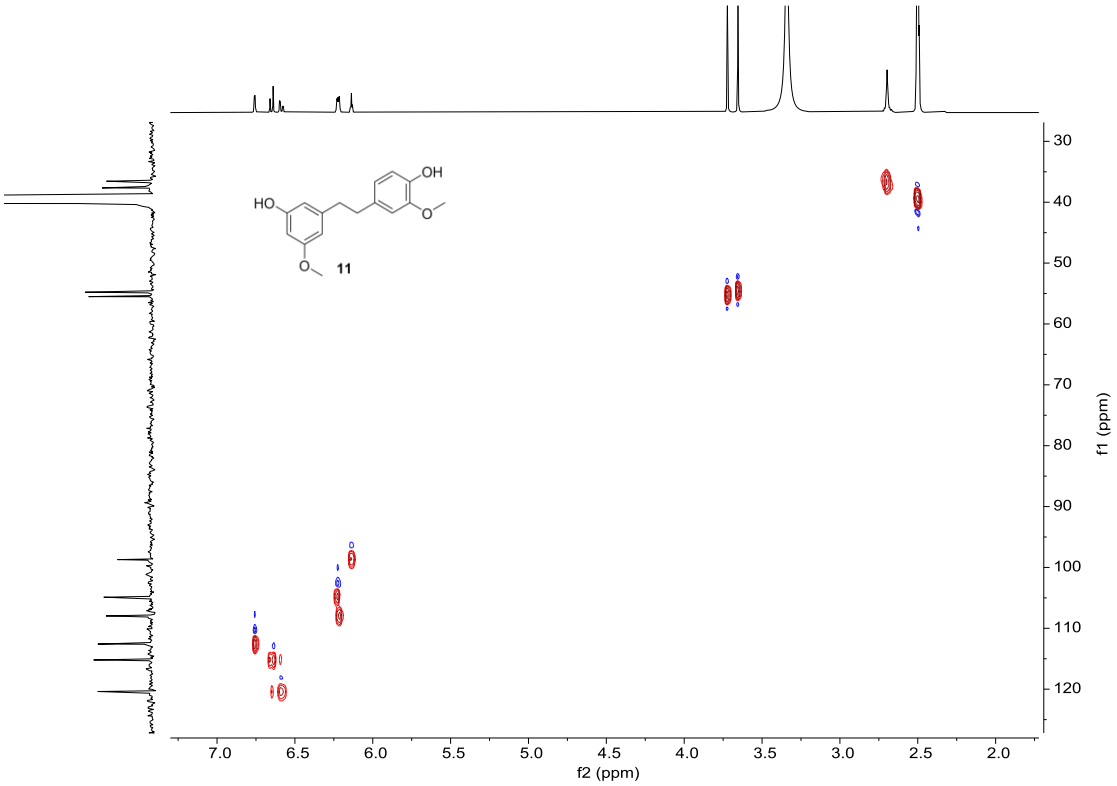

Spectrum S62. HSQC spectrum of **11** in DMSO-d_6.

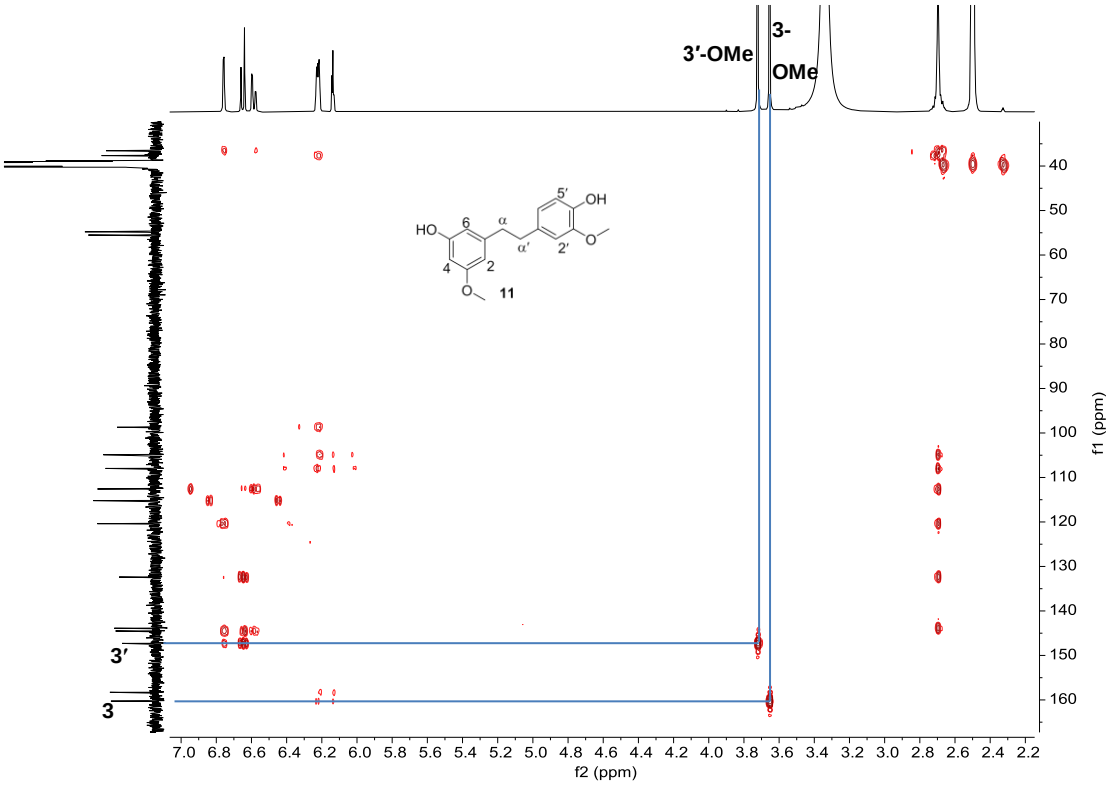

Spectrum S63. HMBC spectrum of **11** in DMSO-d_6.

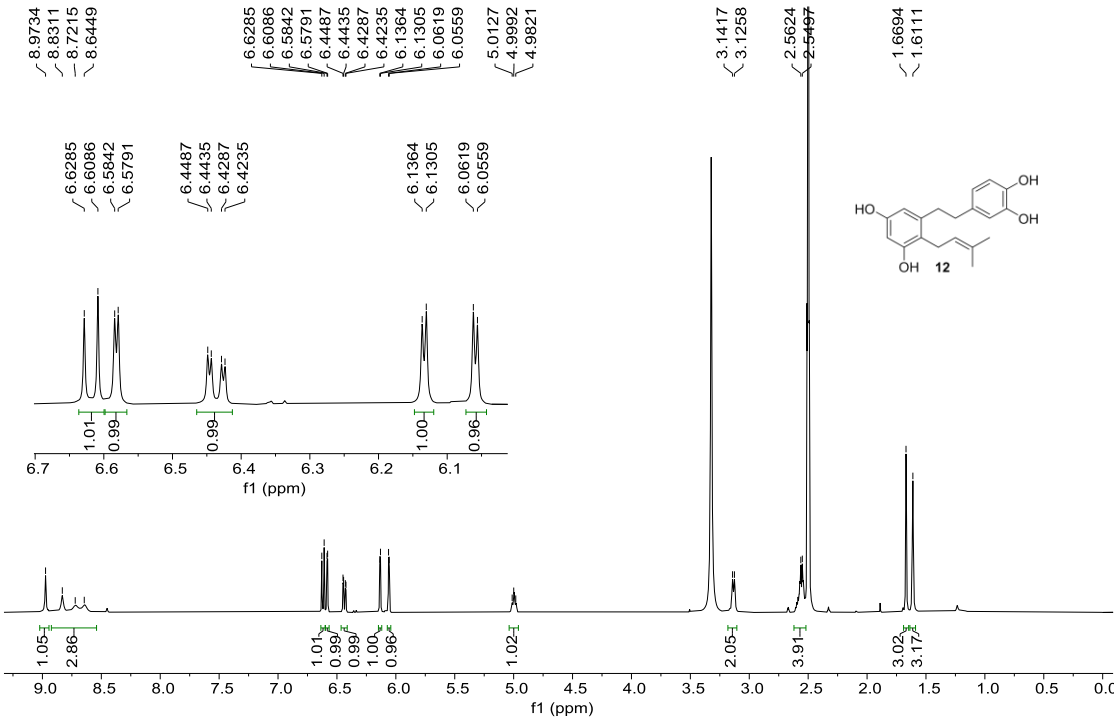

Spectrum S64. ^{1}H NMR spectrum of **12** in DMSO-d_6 at 400 MHz.

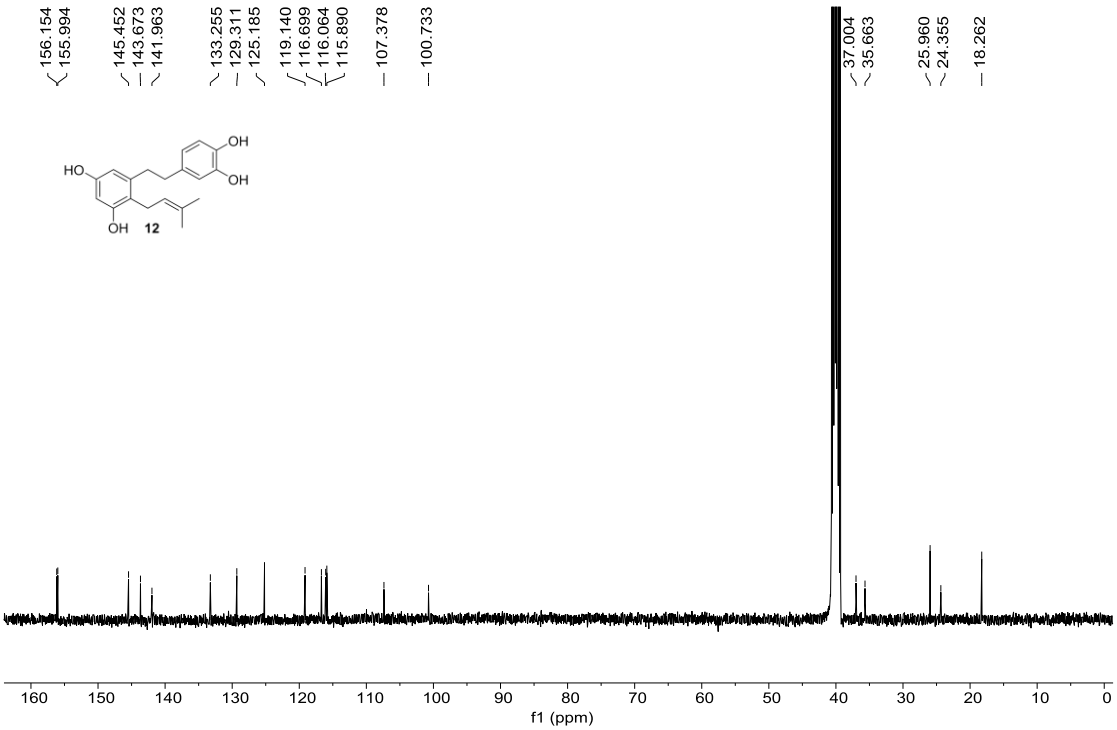

Spectrum S65. ^{13}C NMR spectrum of **12** in DMSO-d_6 at 100 MHz.

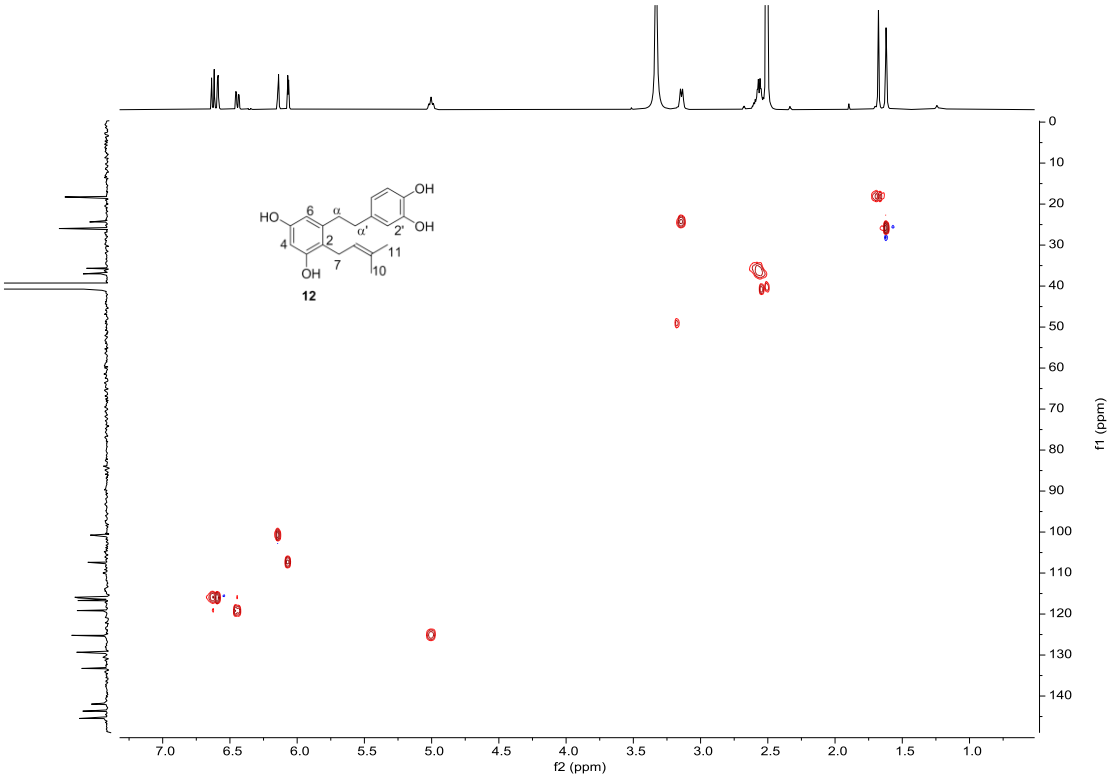

Spectrum S66. HSQC spectrum of **12** in DMSO-d_6.

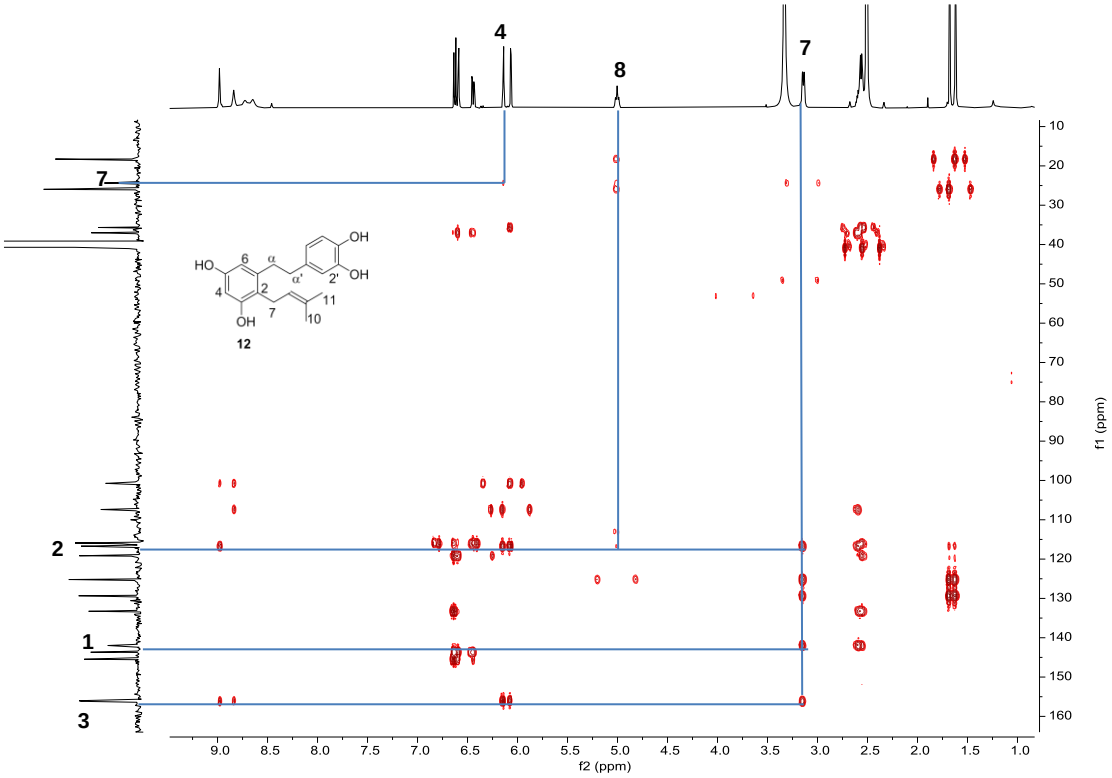

Spectrum S67. HMBC spectrum of **12** in DMSO-d_6.

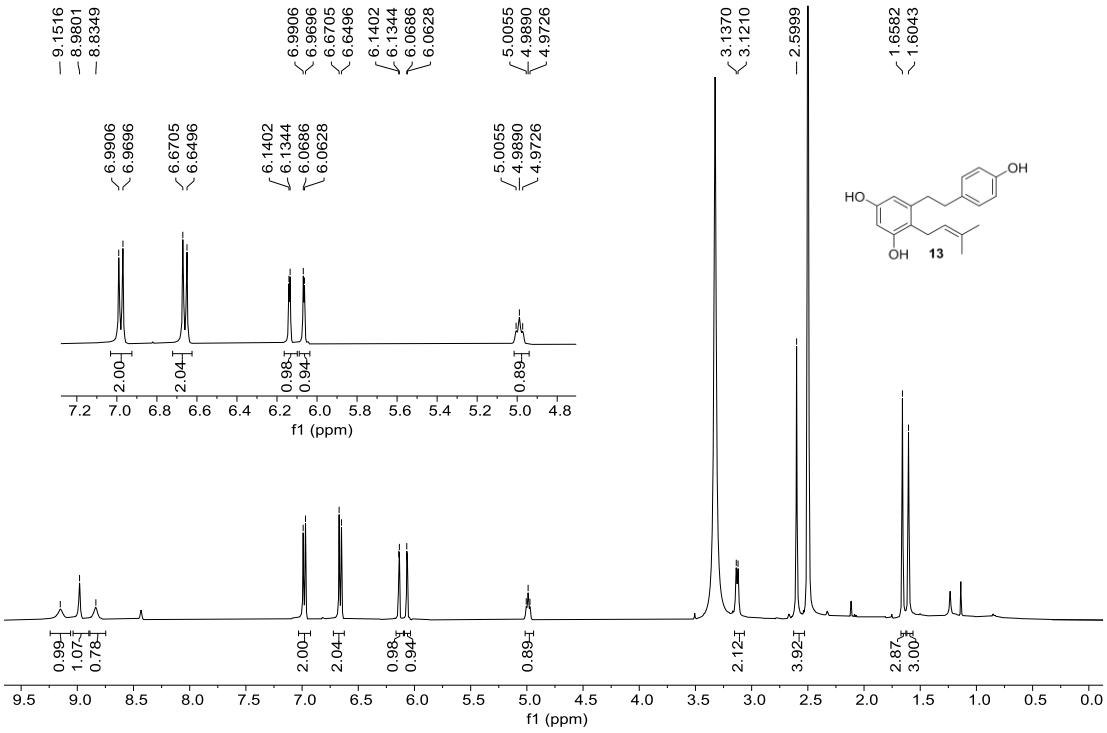

Spectrum S68. ^{1}H NMR spectrum of **13** in DMSO-d_6 at 400 MHz.

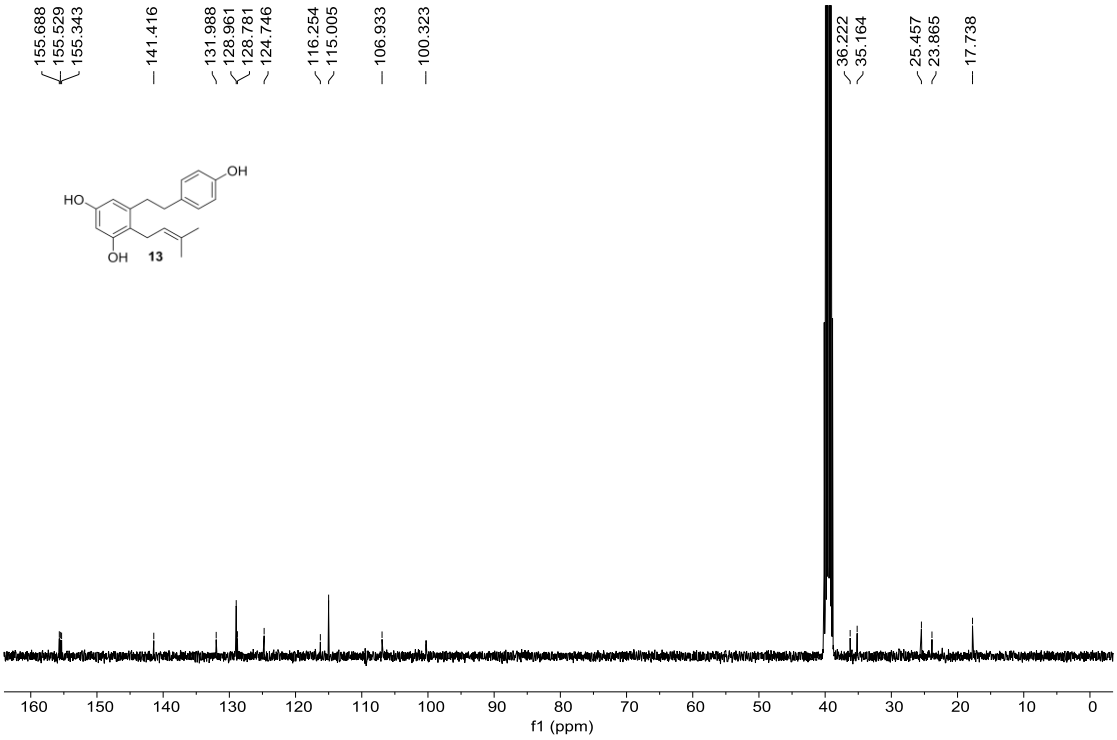

Spectrum S69. ^{13}C NMR spectrum of **13** in DMSO-d_6 at 100 MHz.

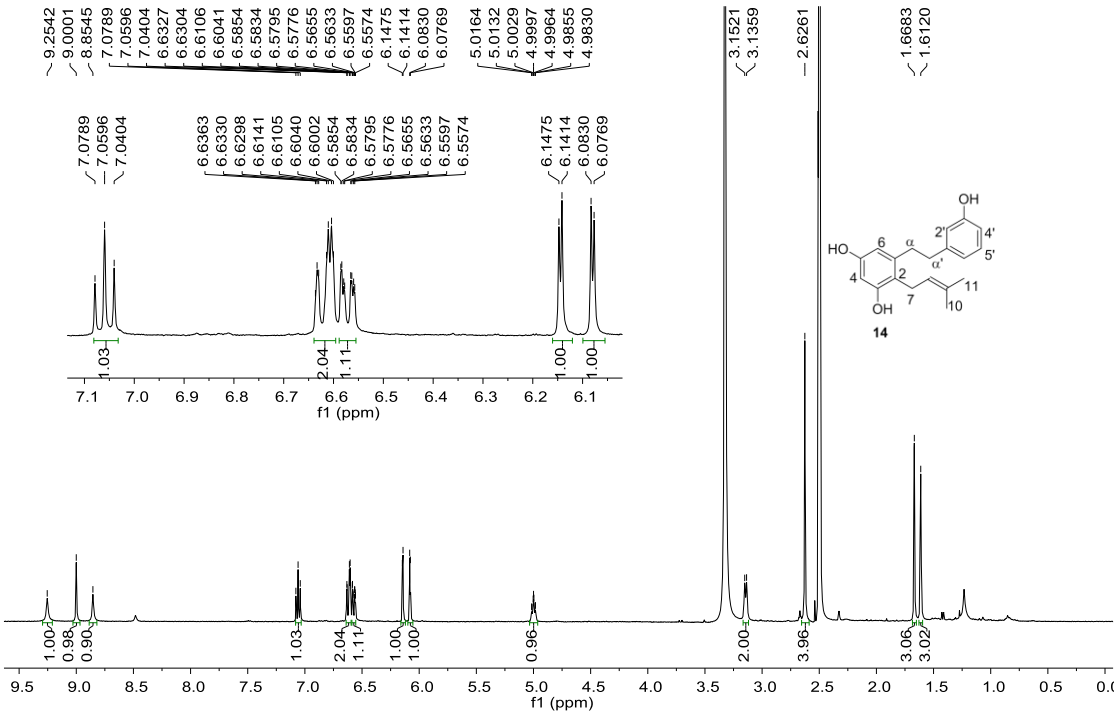

Spectrum S70. ^{1}H NMR spectrum of **14** in DMSO-d_6 at 400 MHz.

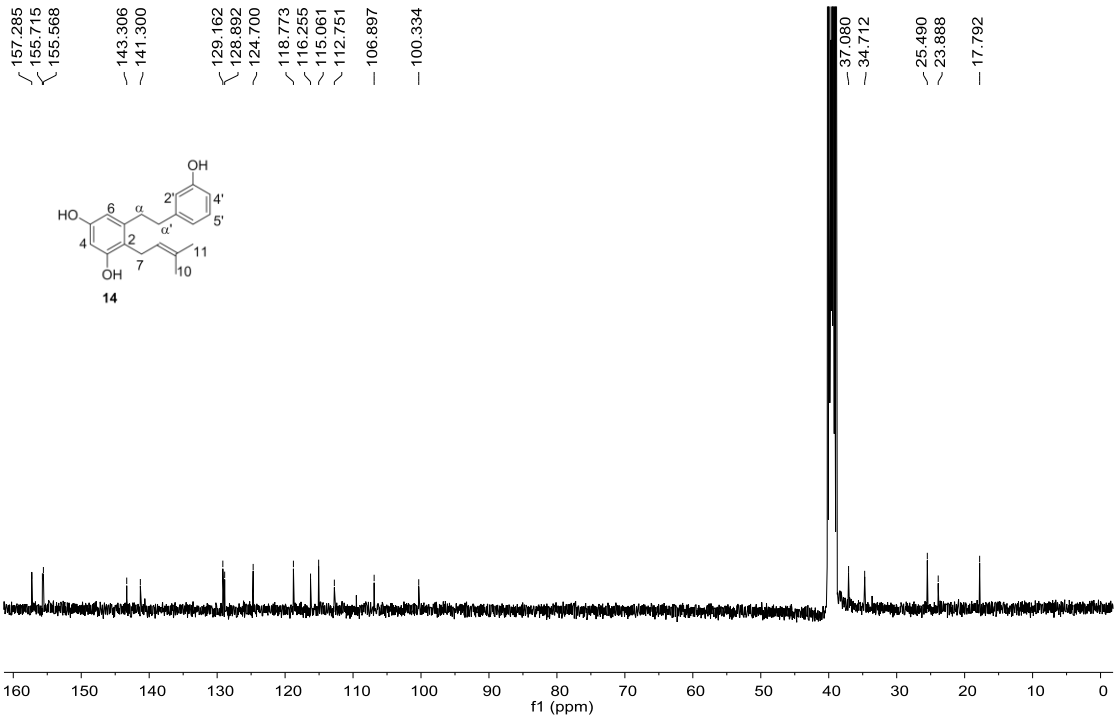

Spectrum S71. ^{13}C NMR spectrum of **14** in DMSO-d_6 at 100 MHz.

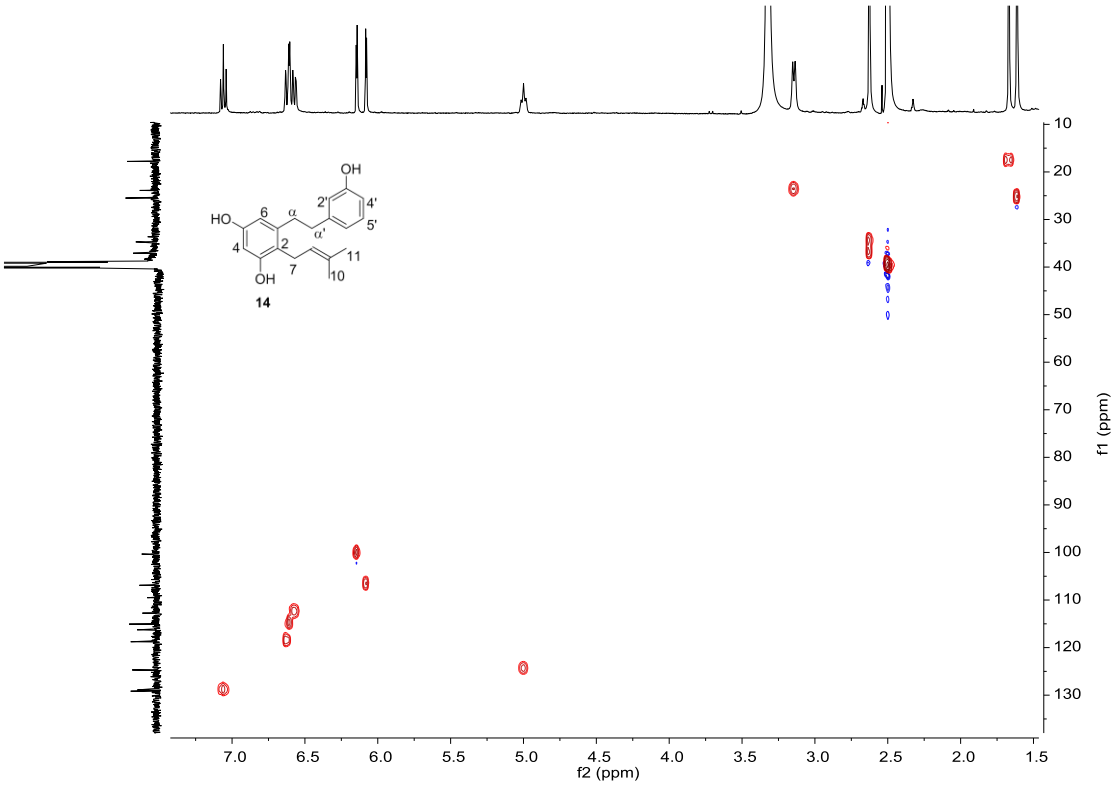

Spectrum S72. HSQC spectrum of **14** in DMSO-d_6.

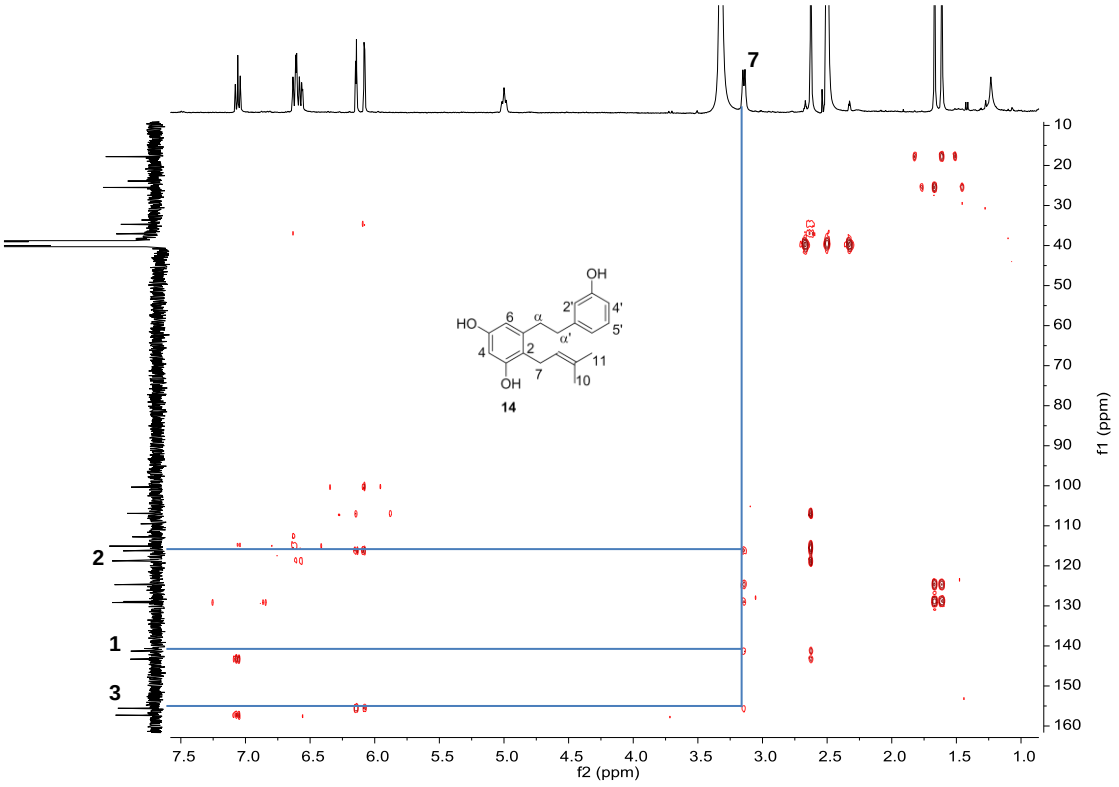

Spectrum S73. HMBC spectrum of **14** in DMSO-d_6.

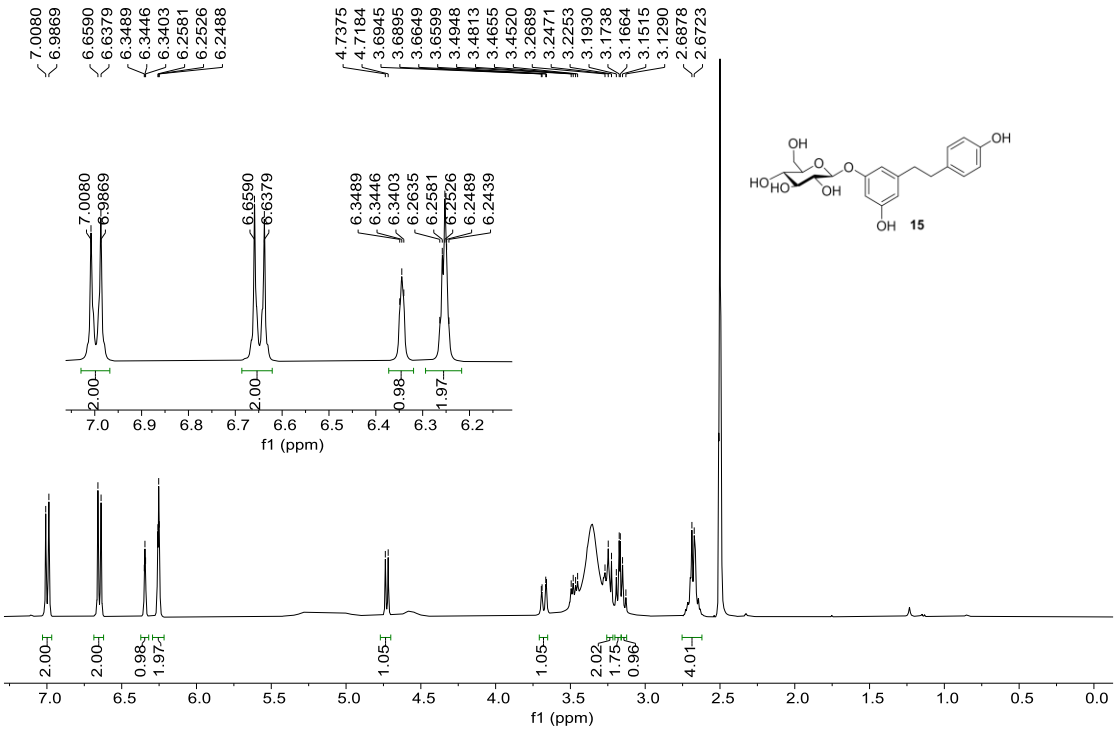

Spectrum S74. ^{1}H NMR spectrum of **15** in DMSO-d_6 at 400 MHz.

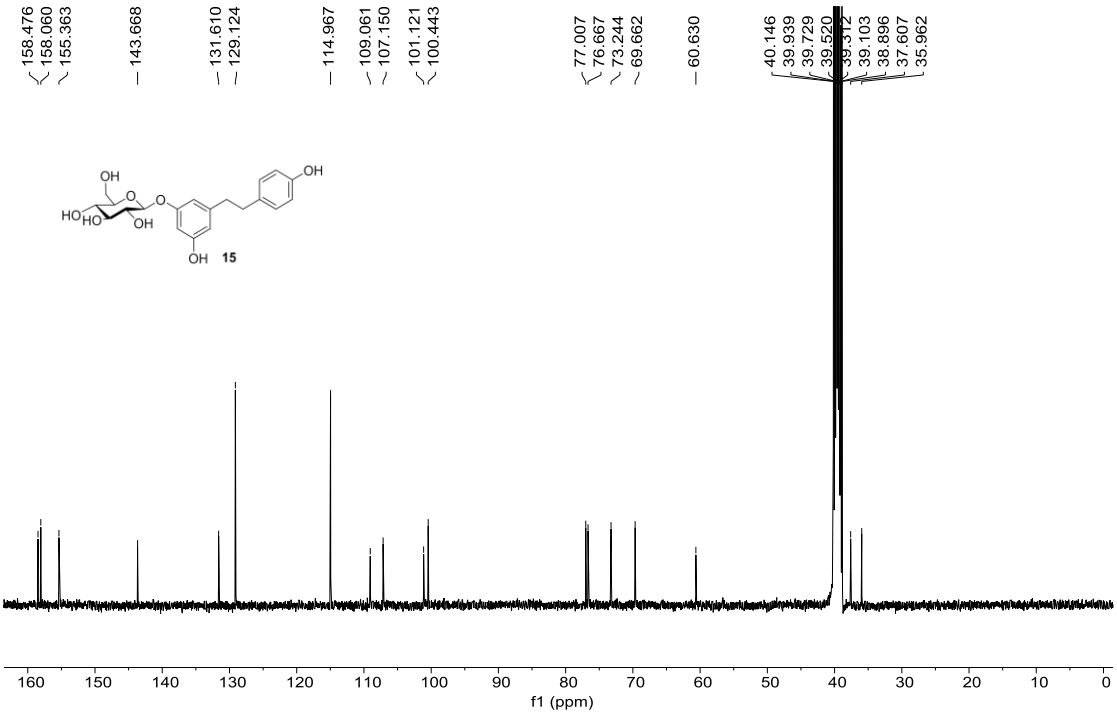

Spectrum S75. ^{13}C NMR spectrum of **15** in DMSO-d_6 at 100 MHz.

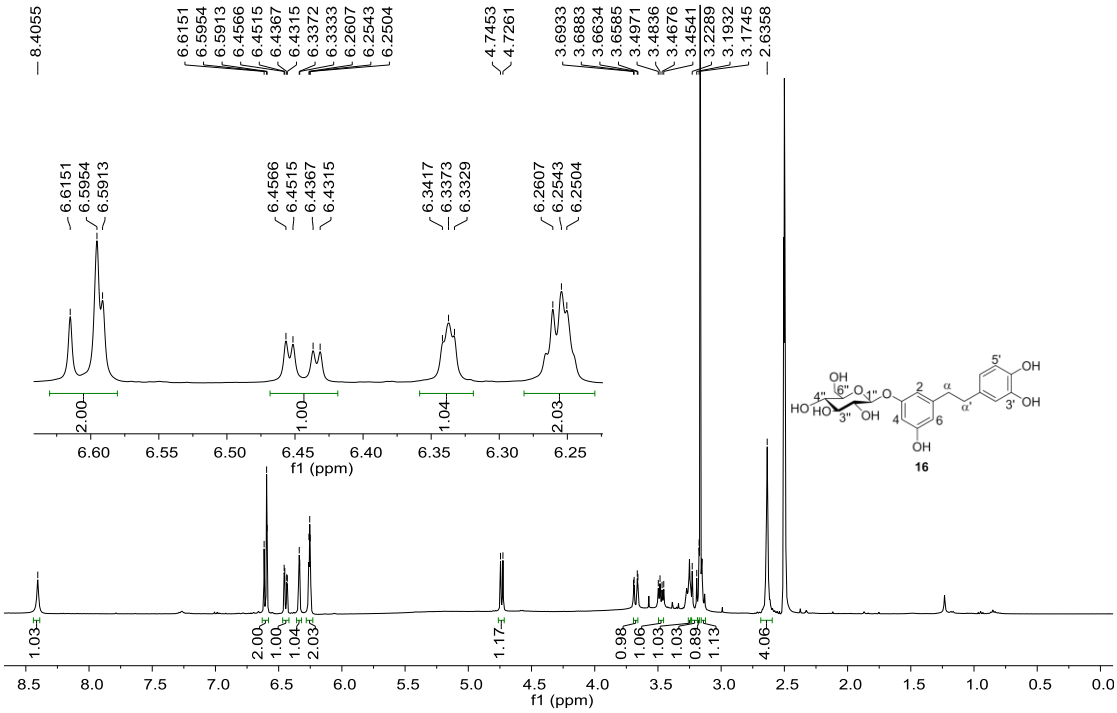

Spectrum S76. ^{1}H NMR spectrum of **16** in DMSO-d_6 at 400 MHz.

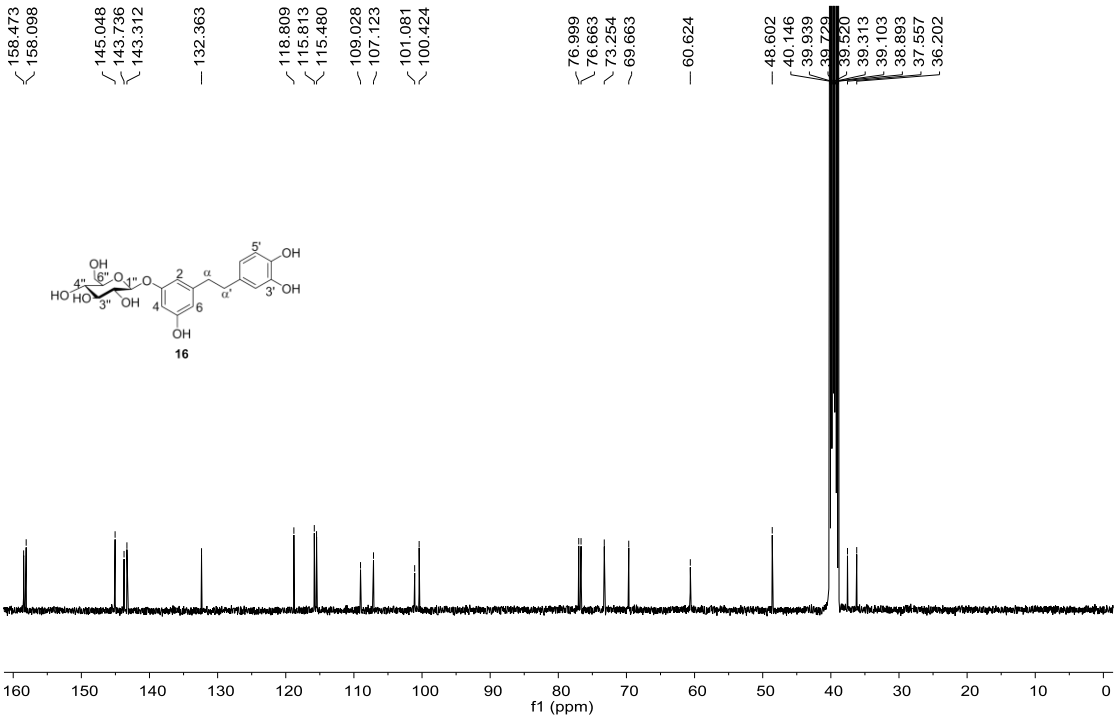

Spectrum S77. ^{13}C NMR spectrum of **16** in DMSO-d_6 at 100 MHz.

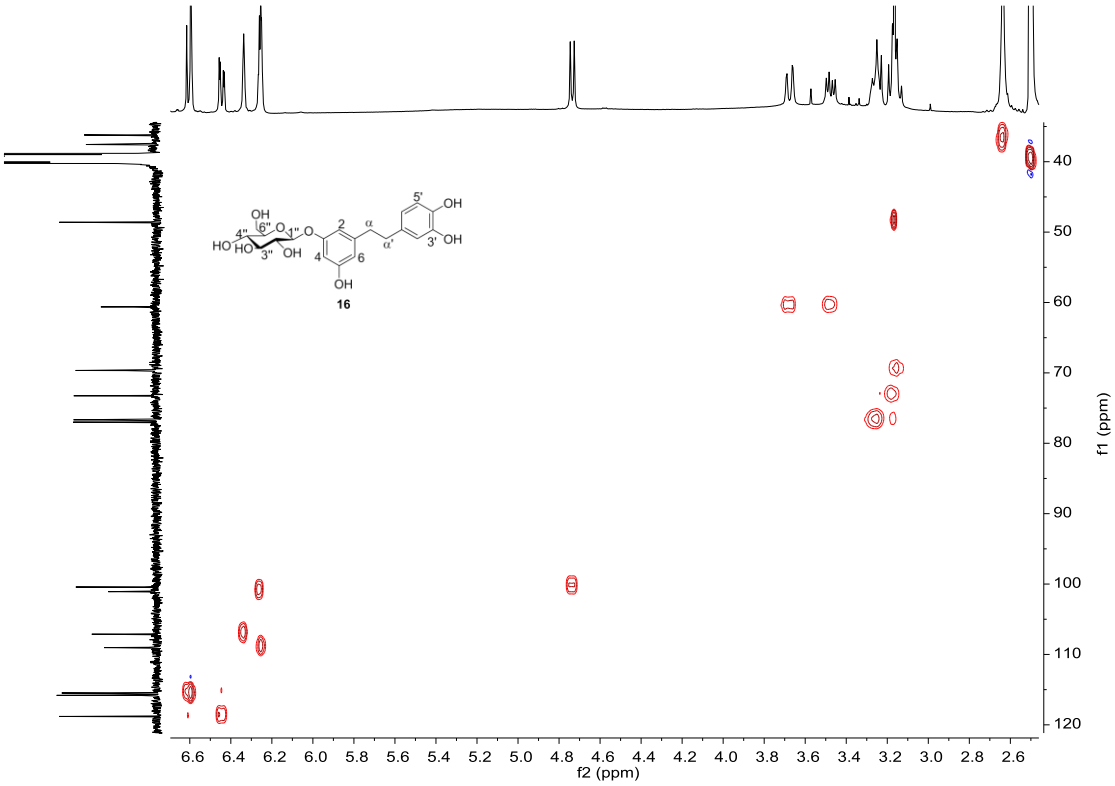

Spectrum S78. HSQC spectrum of **16** in DMSO-d_6.

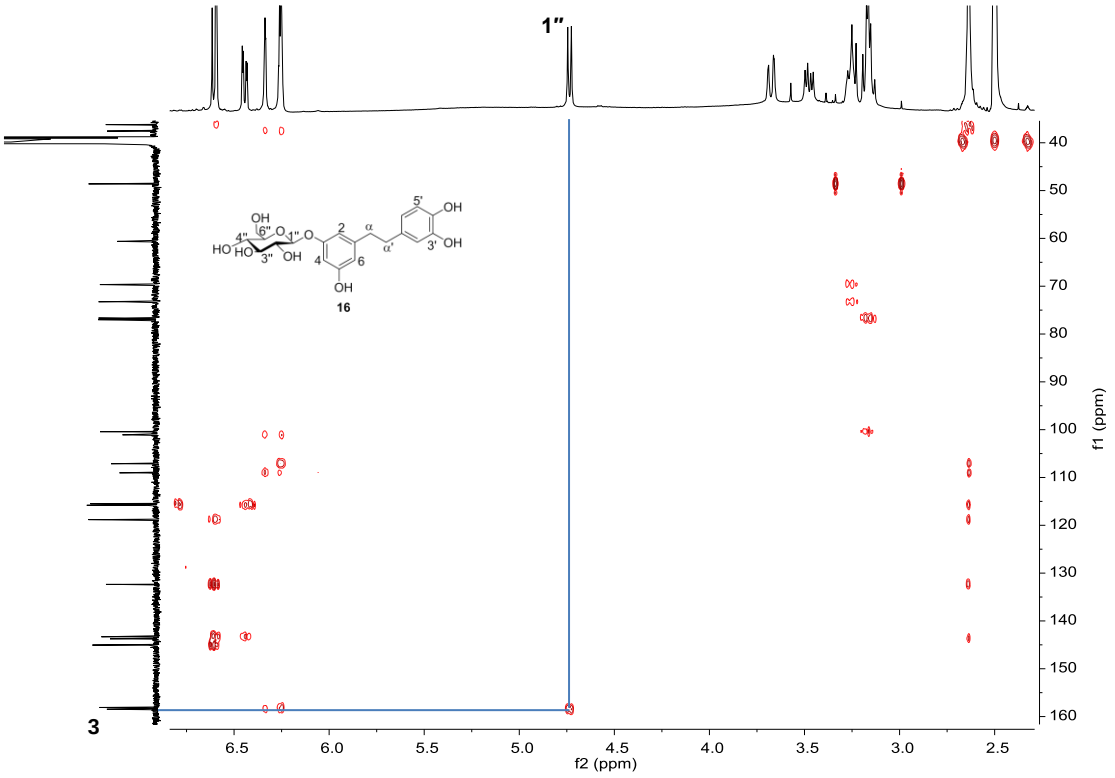

Spectrum S79. HMBC spectrum of **16** in DMSO-d_6.

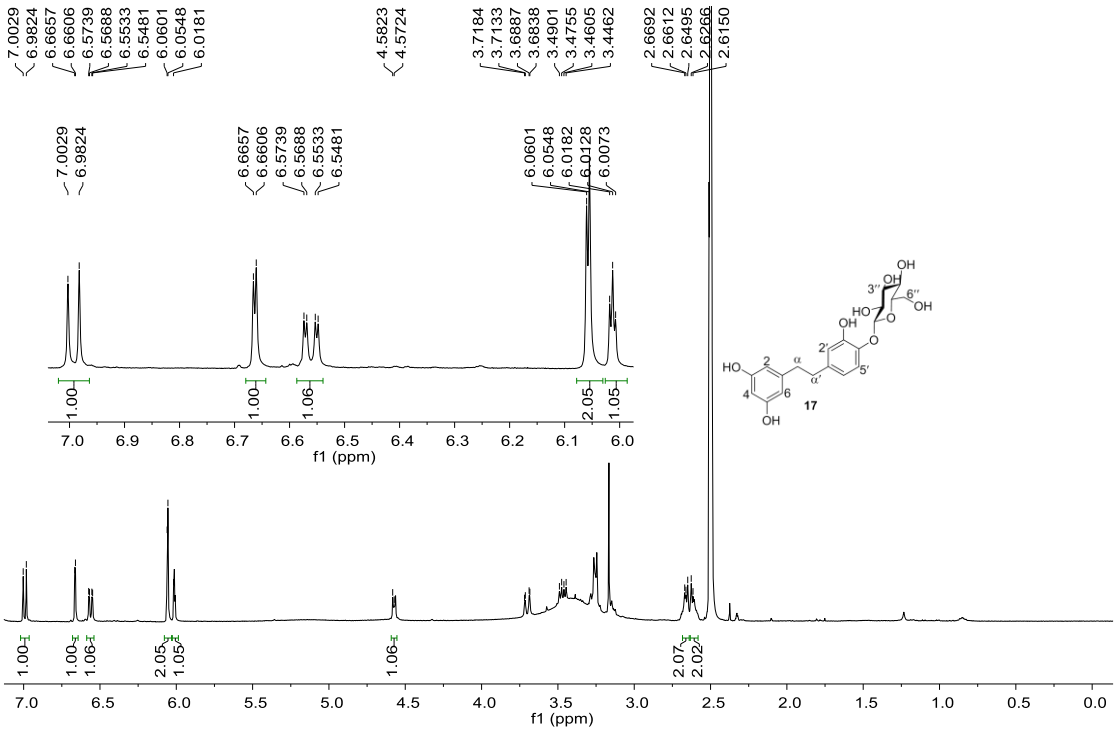

Spectrum S80. ^{1}H NMR spectrum of **17** in DMSO-d_6 at 400 MHz.

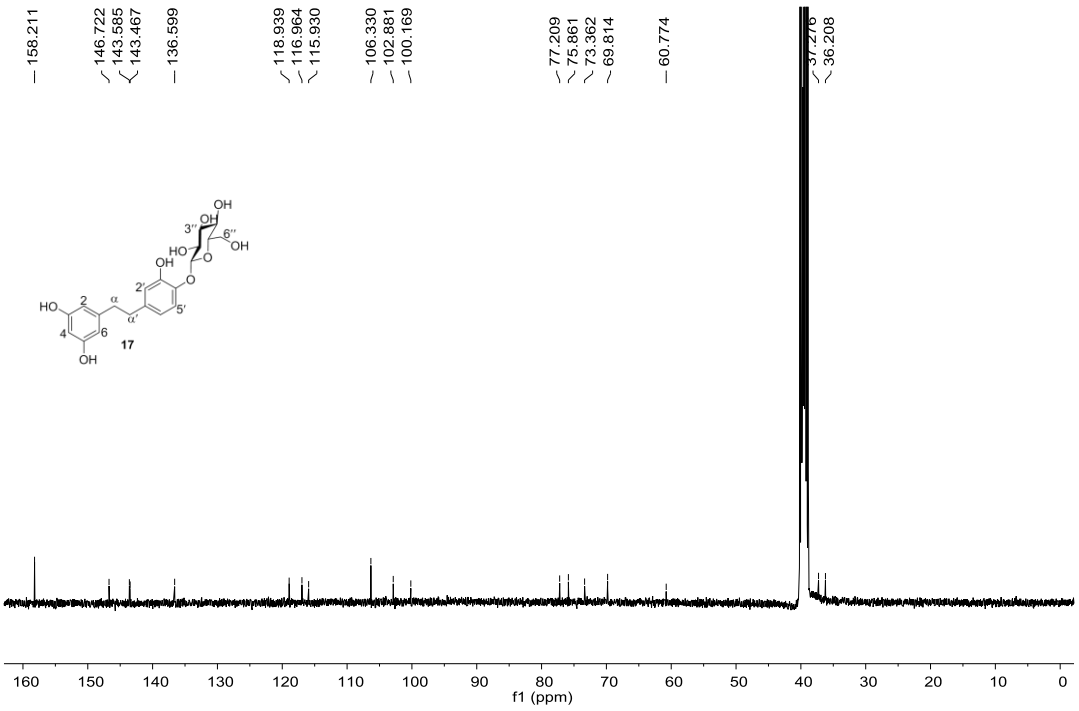

Spectrum S81. ^{13}C NMR spectrum of **17** in DMSO-d_6 at 100 MHz.

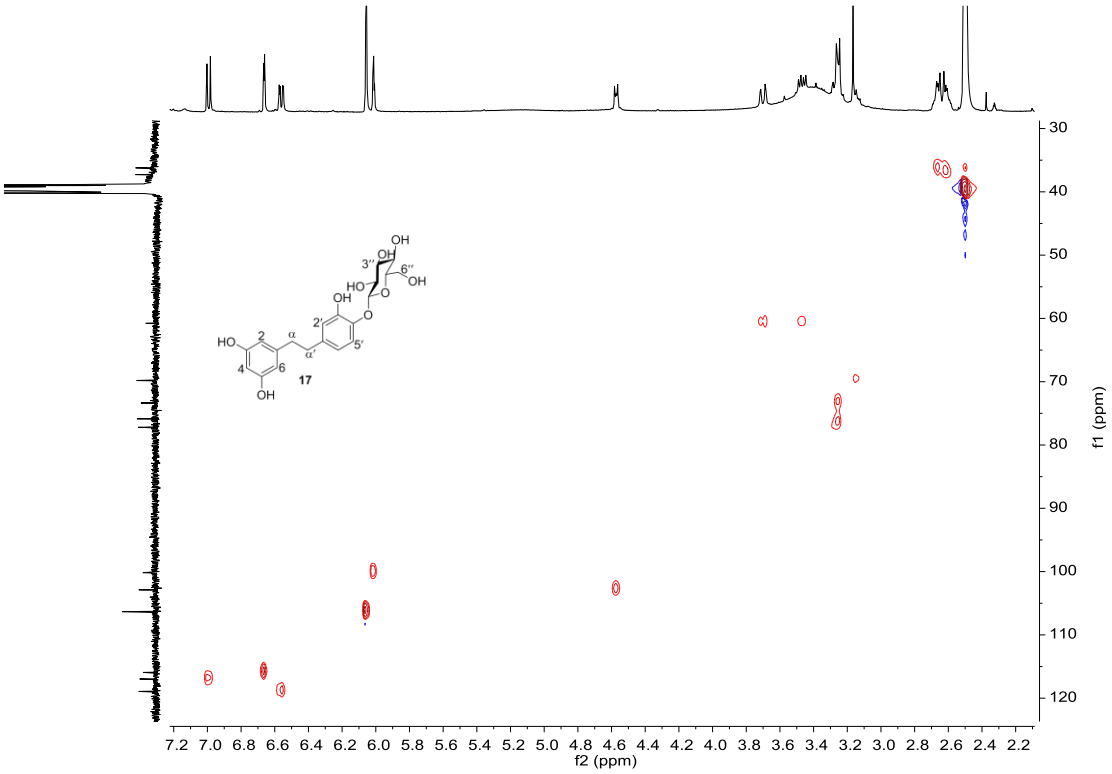

Spectrum S82. HSQC spectrum of **17** in DMSO-d_6.

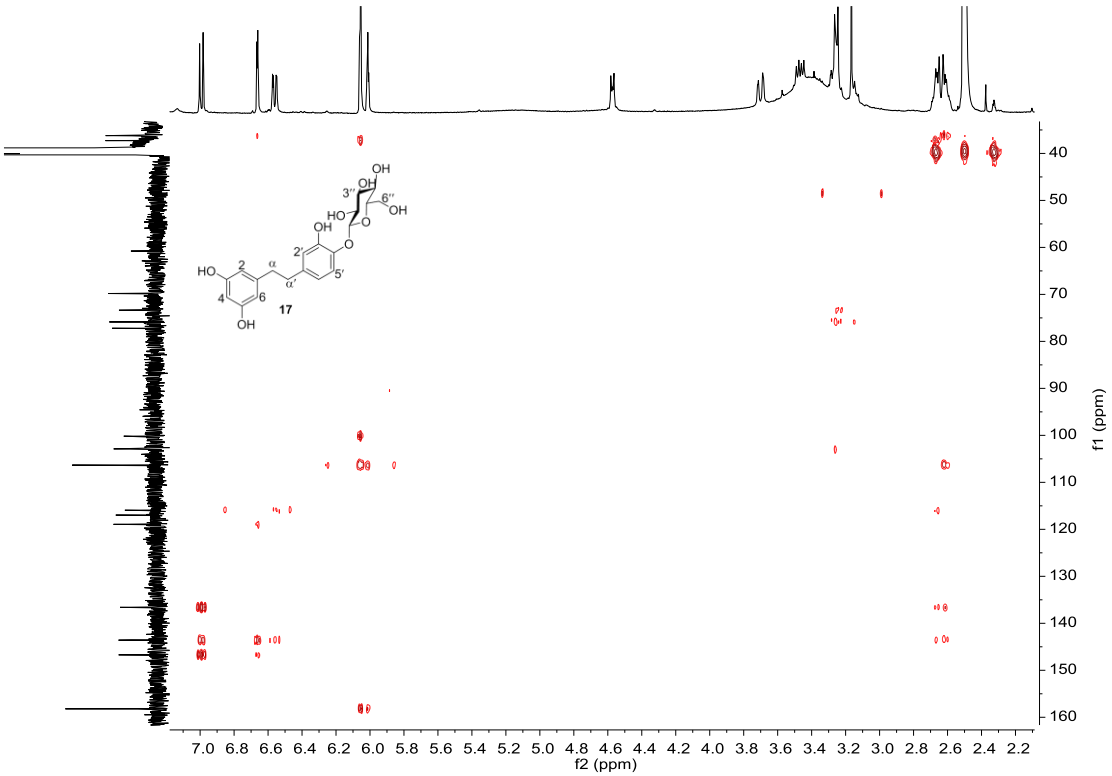

Spectrum S83. HMBC spectrum of **17** in DMSO-d_6.

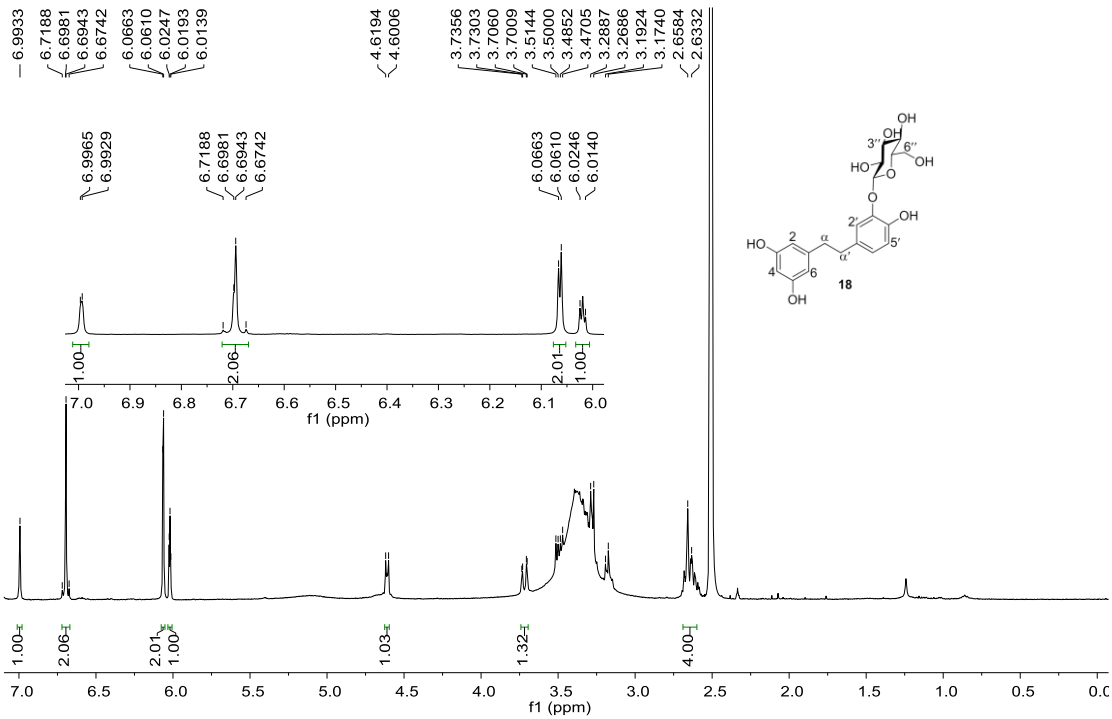

Spectrum S84. ^{1}H NMR spectrum of **18** in DMSO-d_6 at 400 MHz.

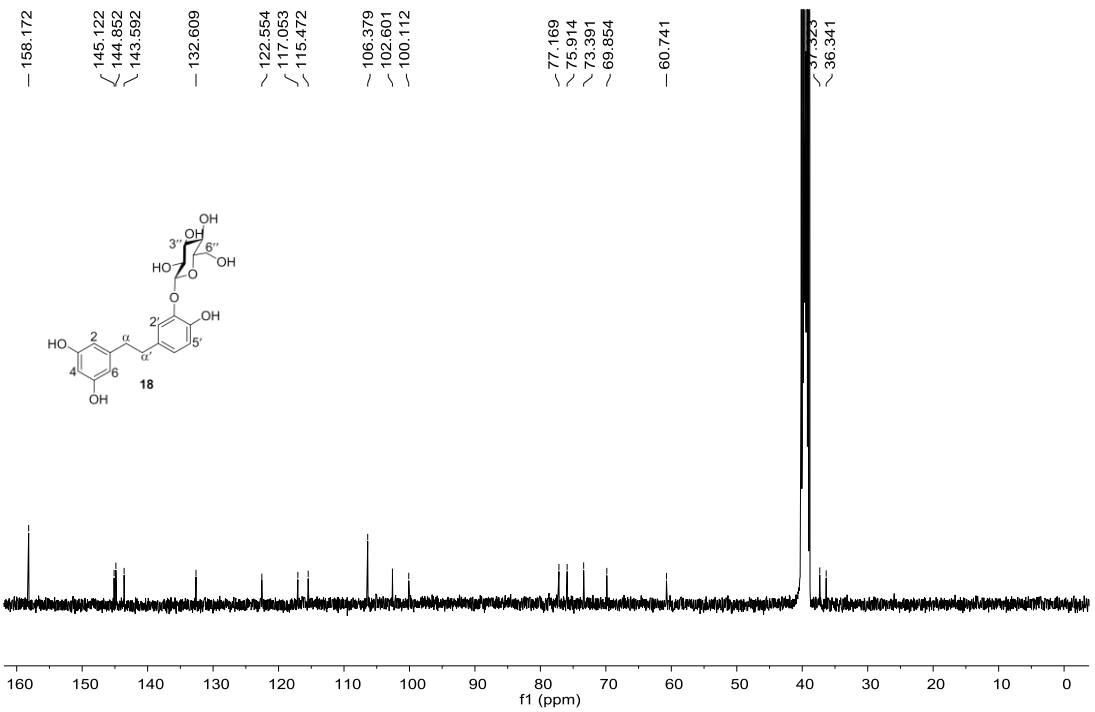

Spectrum S85. ^{13}C NMR spectrum of **18** in DMSO-d_6 at 100 MHz.

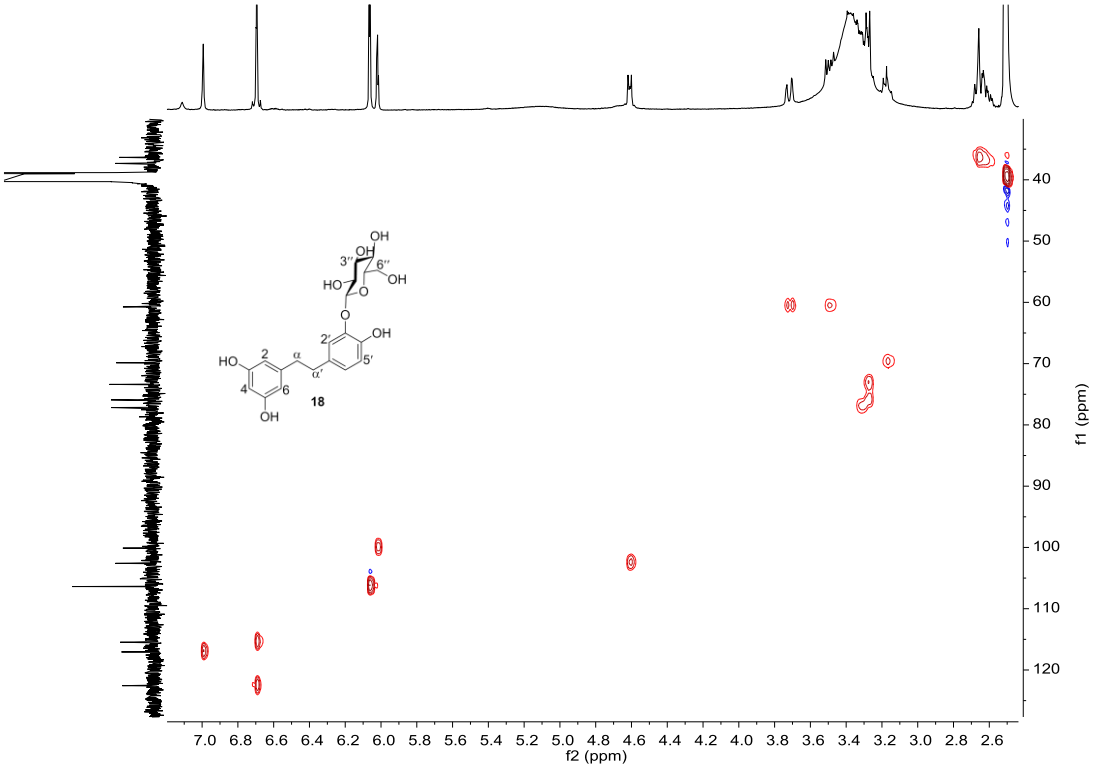

Spectrum S86. HSQC spectrum of **18** in DMSO-d_6.

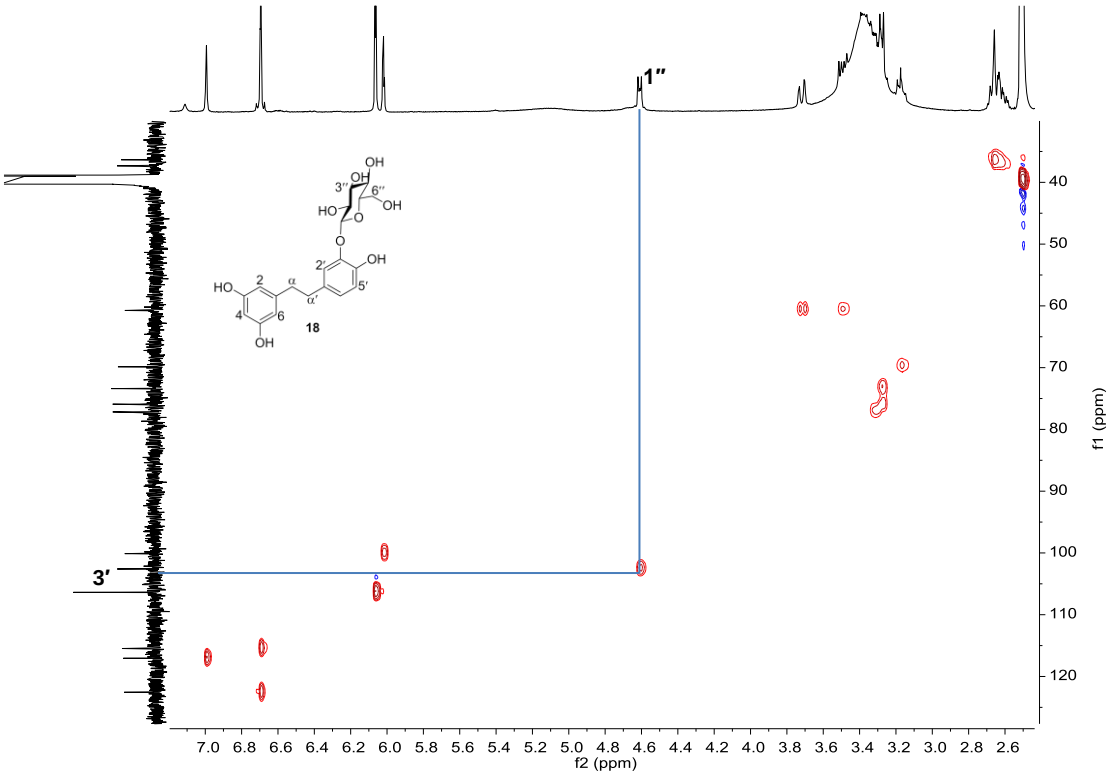

Spectrum S87. HMBC spectrum of **18** in DMSO-d_6.

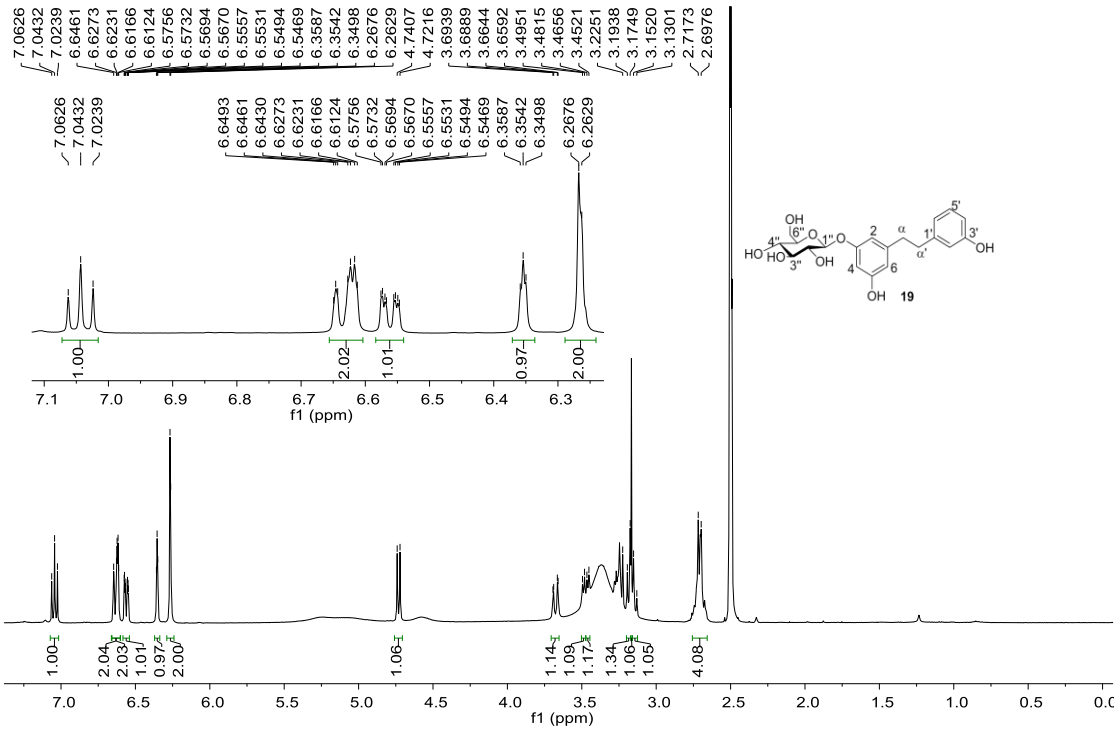

Spectrum S88. ^{1}H NMR spectrum of **19** in DMSO-d_6 at 400 MHz.

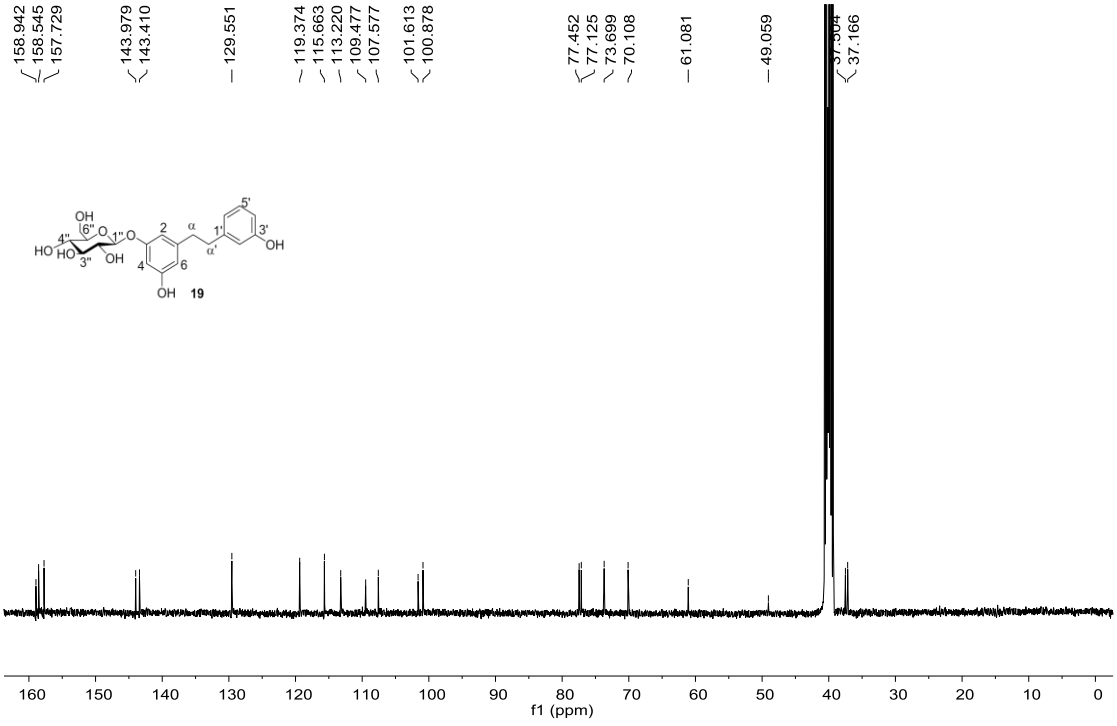

Spectrum S89. ^{13}C NMR spectrum of **19** in DMSO-d_6 at 100 MHz.

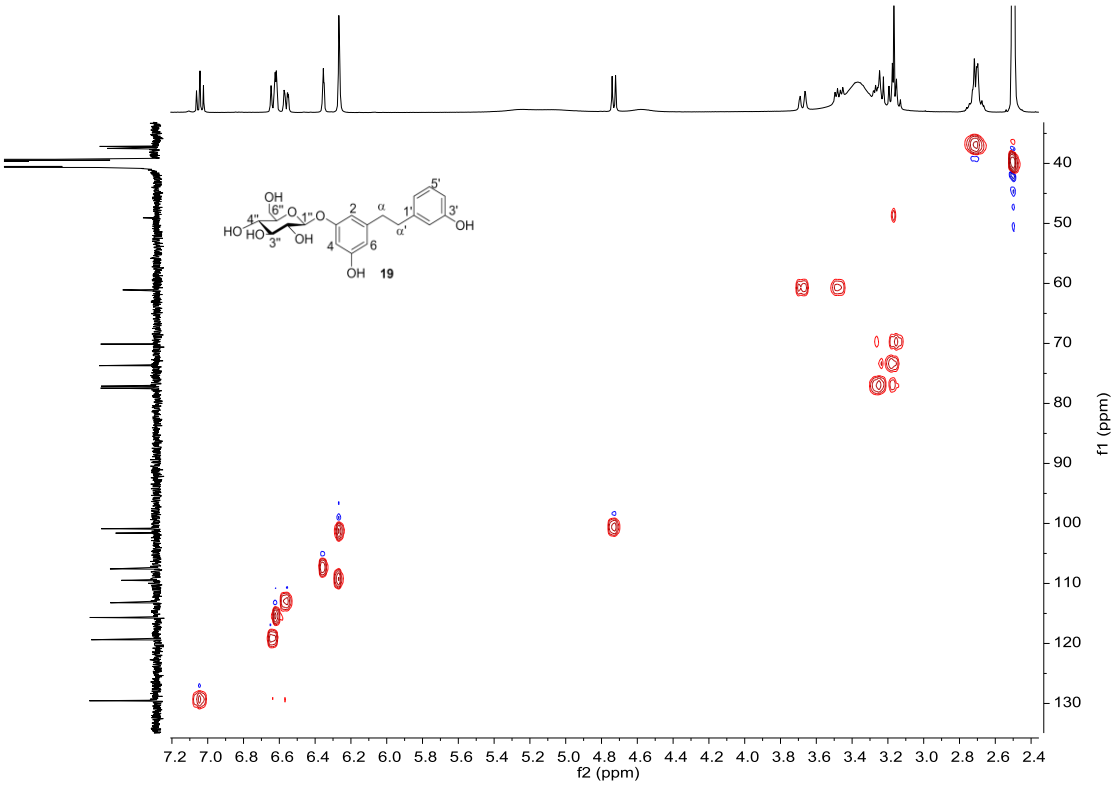

Spectrum S90. HSQC spectrum of **19** in DMSO-d_6.

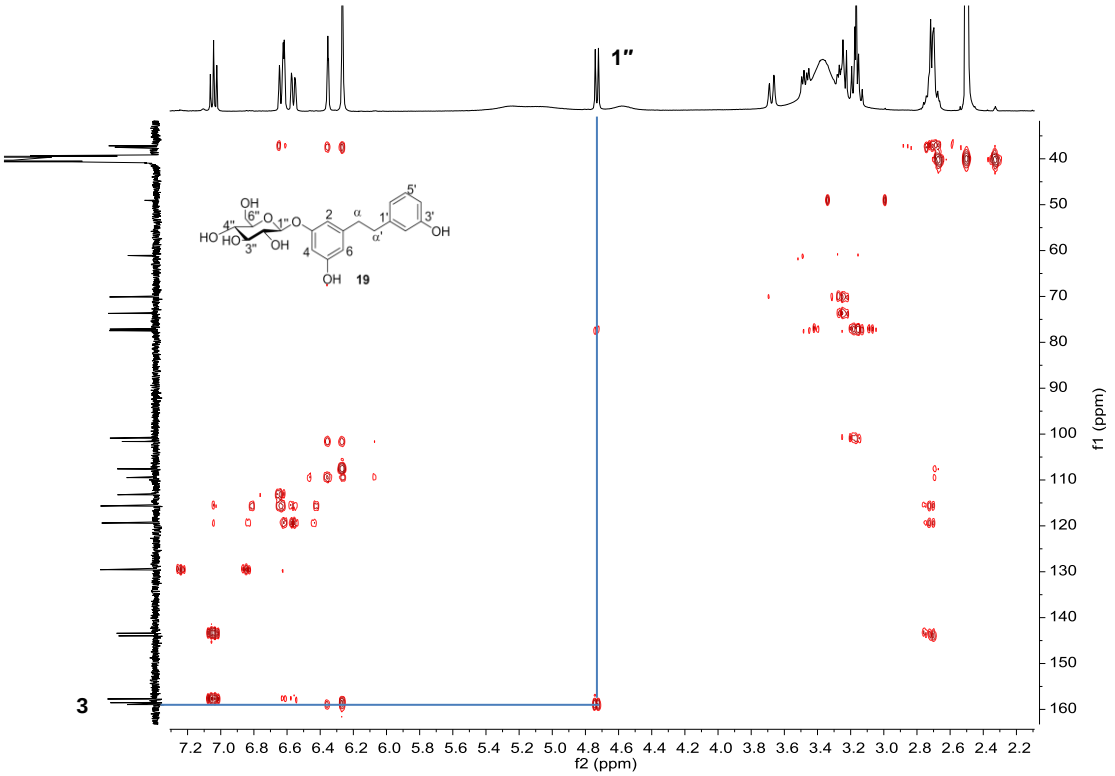

Spectrum S91. HMBC spectrum of **19** in DMSO-d_6.

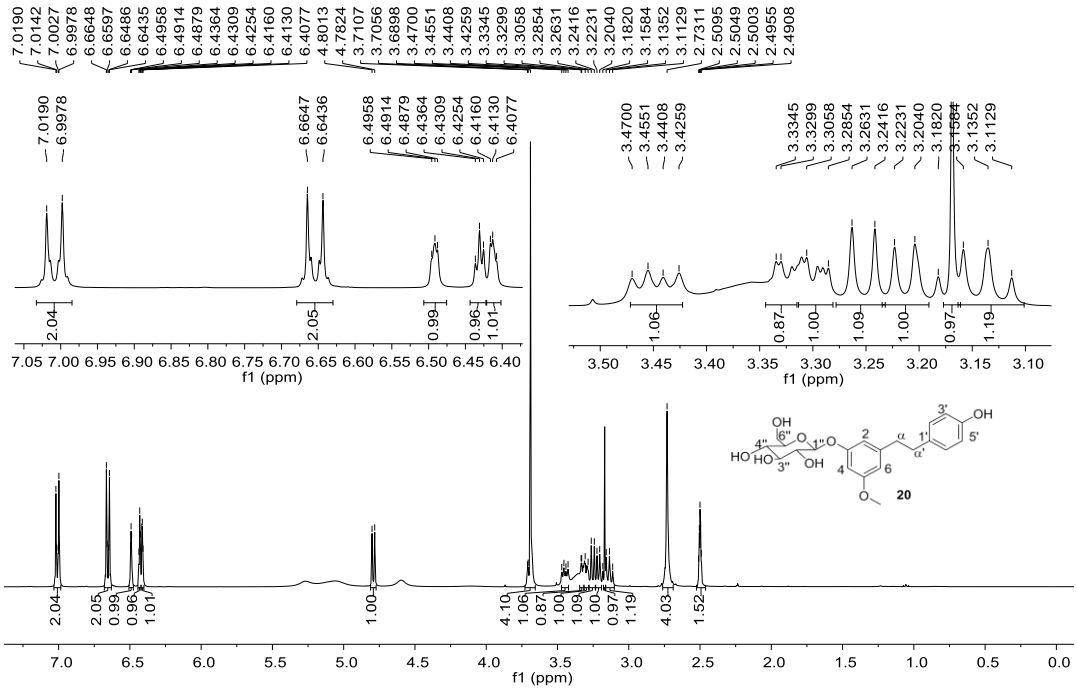

Spectrum S92. ^{1}H NMR spectrum of **20** in DMSO-d_6 at 400 MHz.

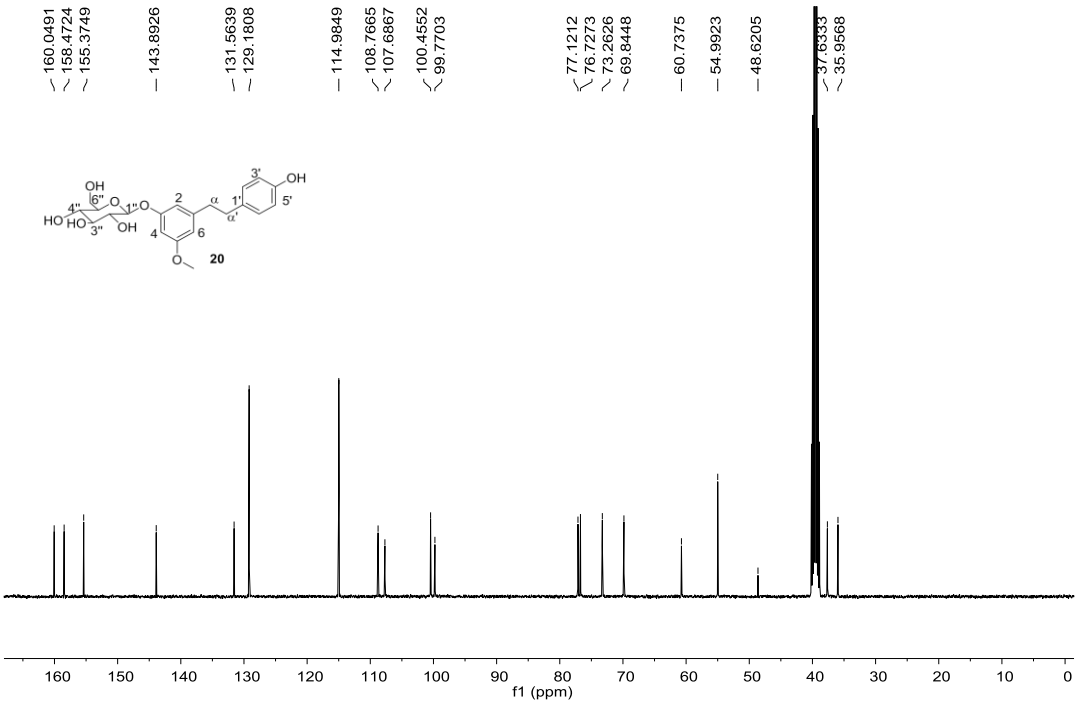

Spectrum S93. ^{13}C NMR spectrum of **20** in DMSO-d_6 at 100 MHz.

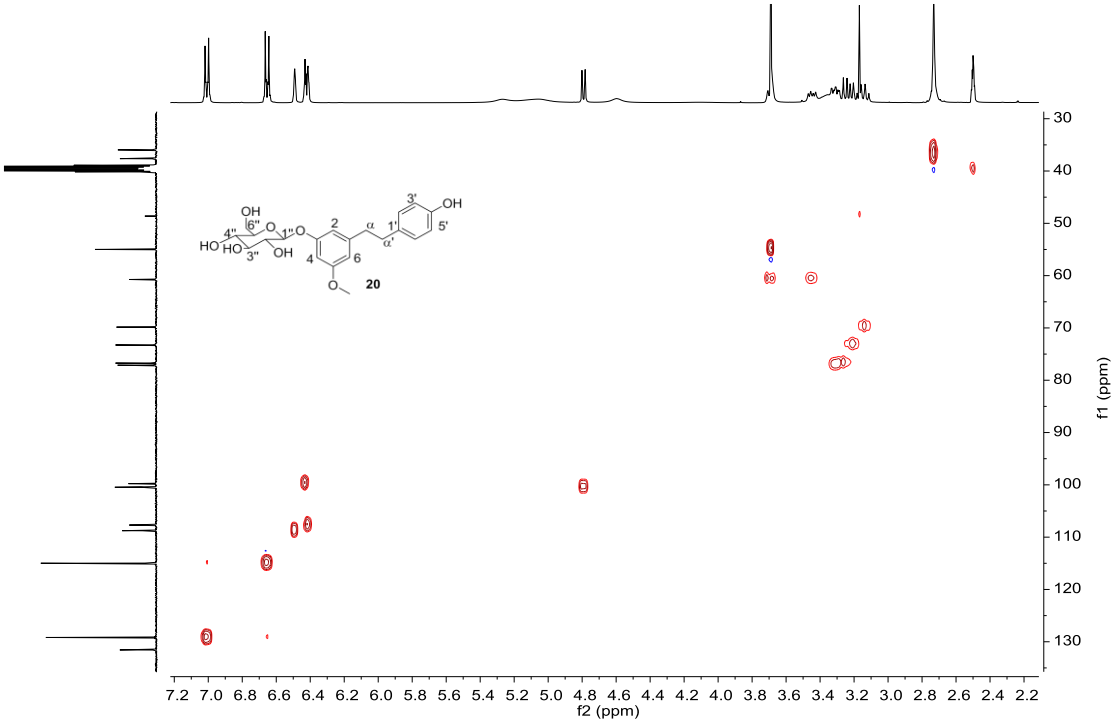

Spectrum S94. HSQC spectrum of **20** in DMSO-d_6.

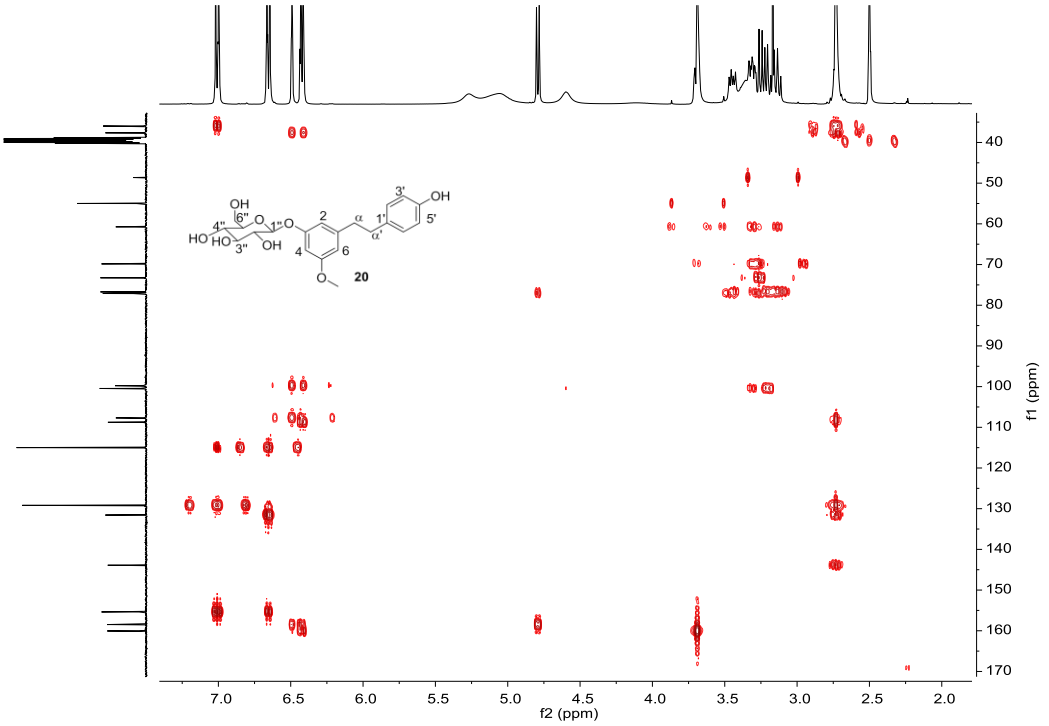

Spectrum S95. HMBC spectrum of **20** in DMSO-d_6.

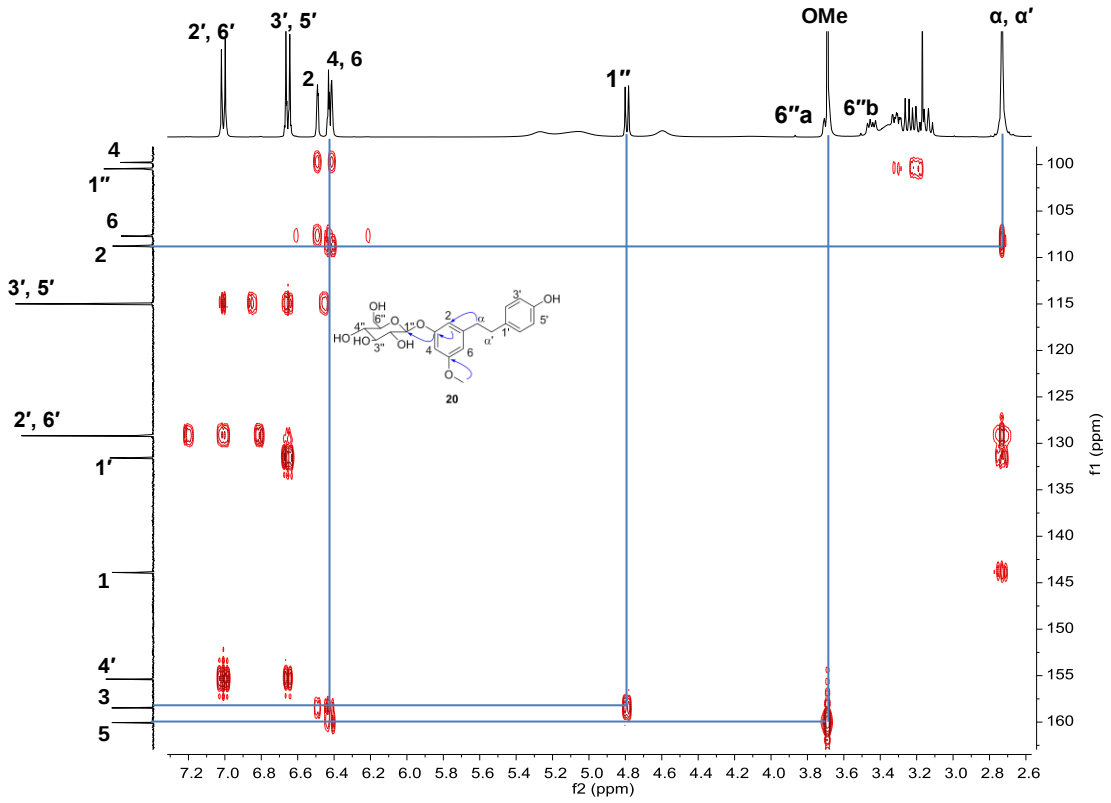

Spectrum S96. The partial enlarged view of HMBC spectrum of **20** in DMSO-d_6.

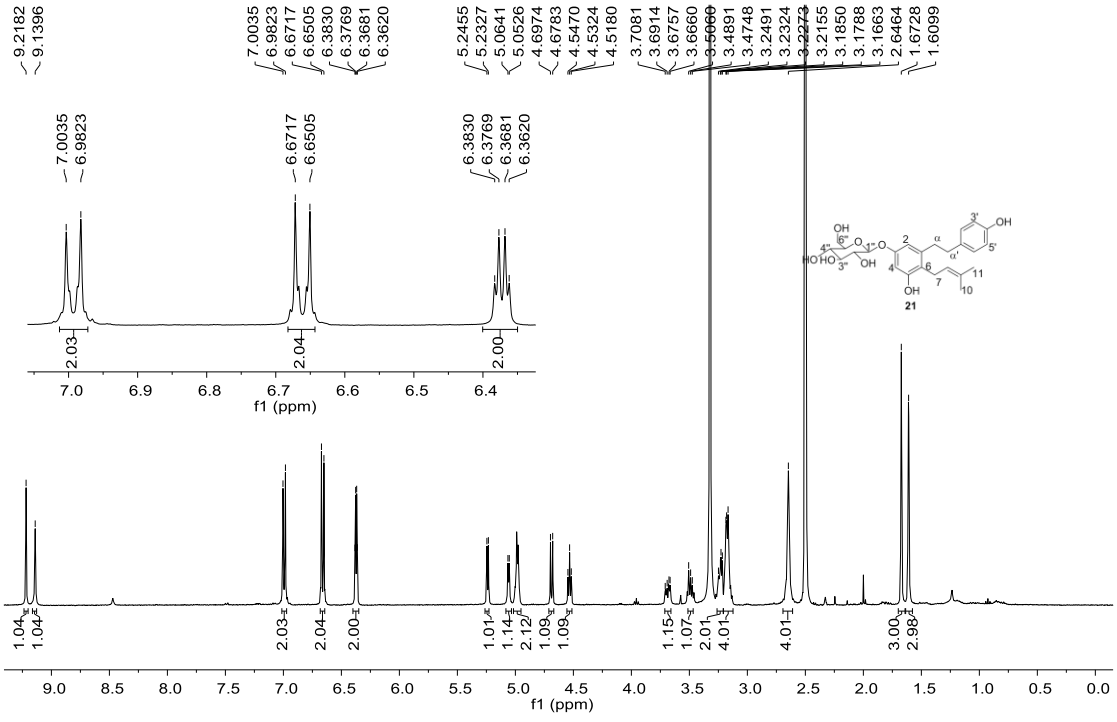

Spectrum S97. ^{1}H NMR spectrum of **21** in DMSO-d_6 at 400 MHz.

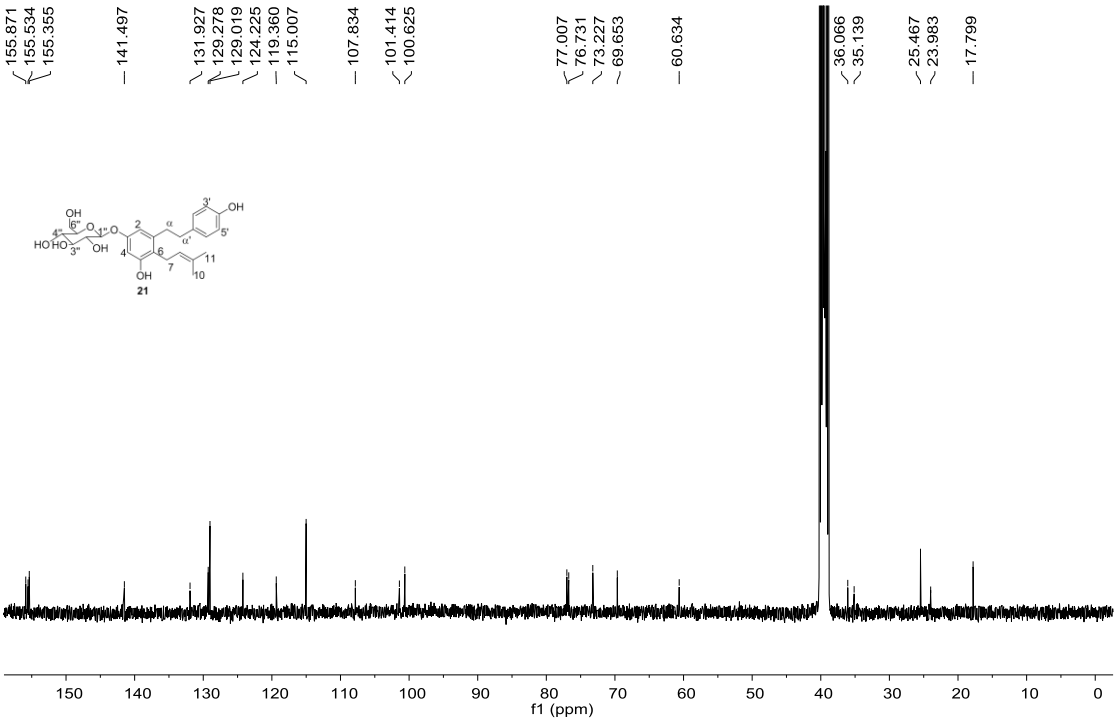

Spectrum S98. ^{13}C NMR spectrum of **21** in DMSO-d_6 at 100 MHz.

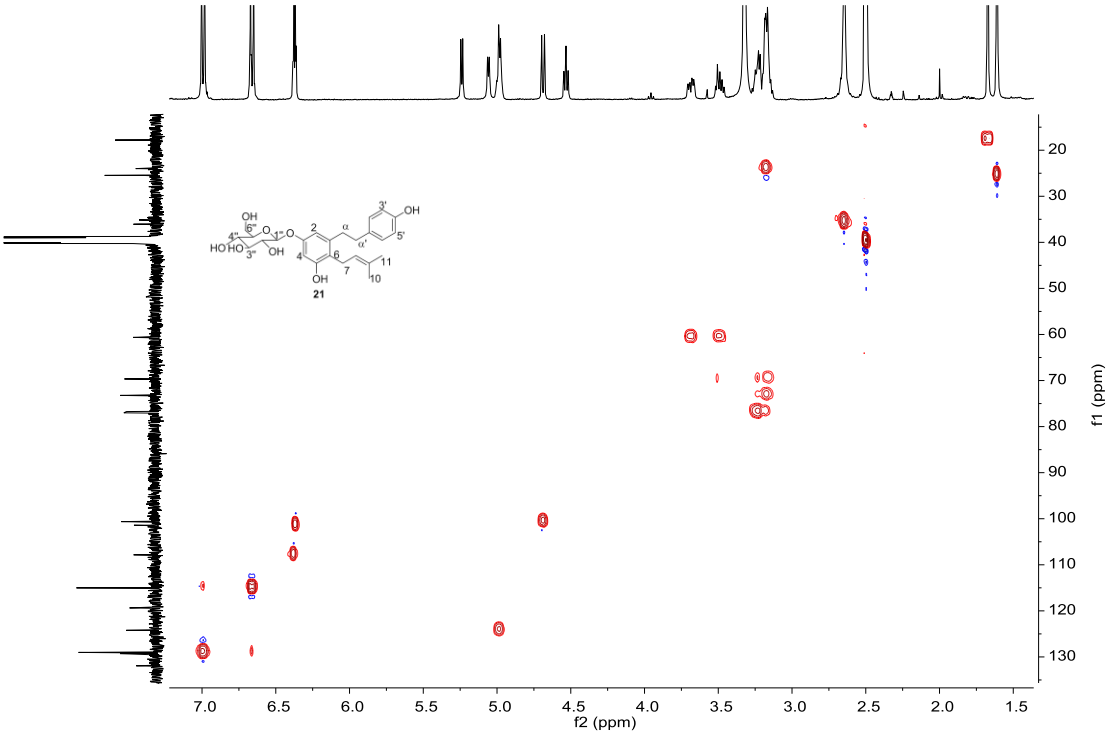

Spectrum S99. HSQC spectrum of **21** in DMSO-d_6.

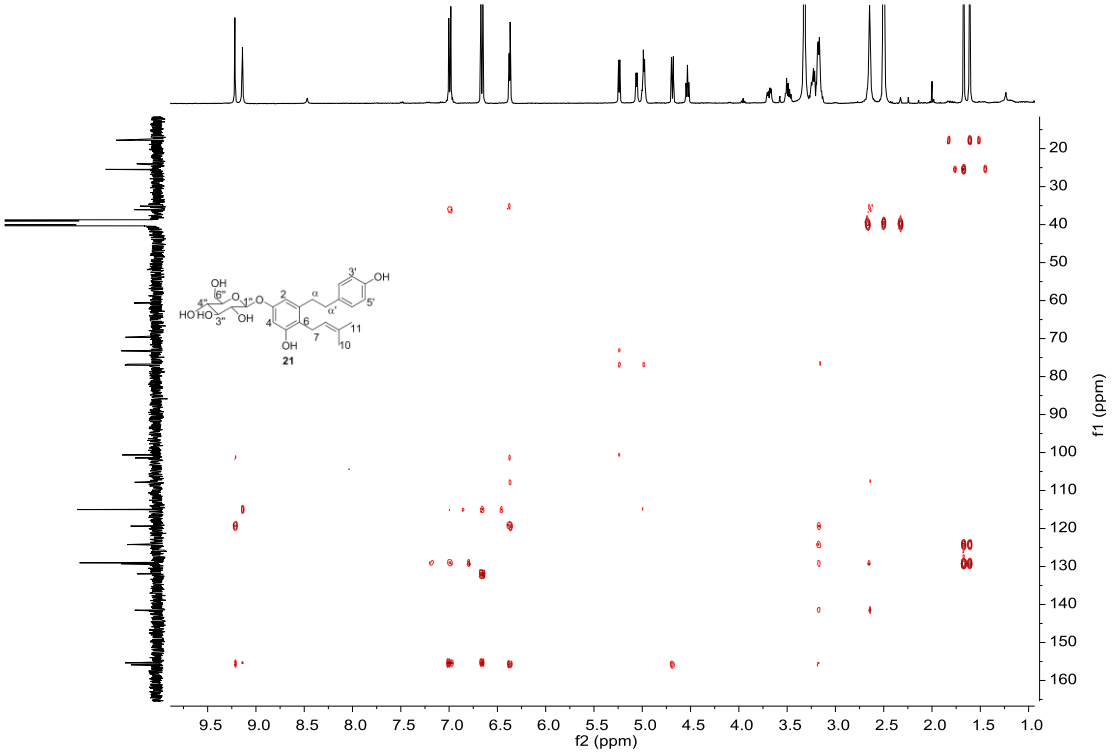

Spectrum S100. HMBC spectrum of **21** in DMSO-d_6.

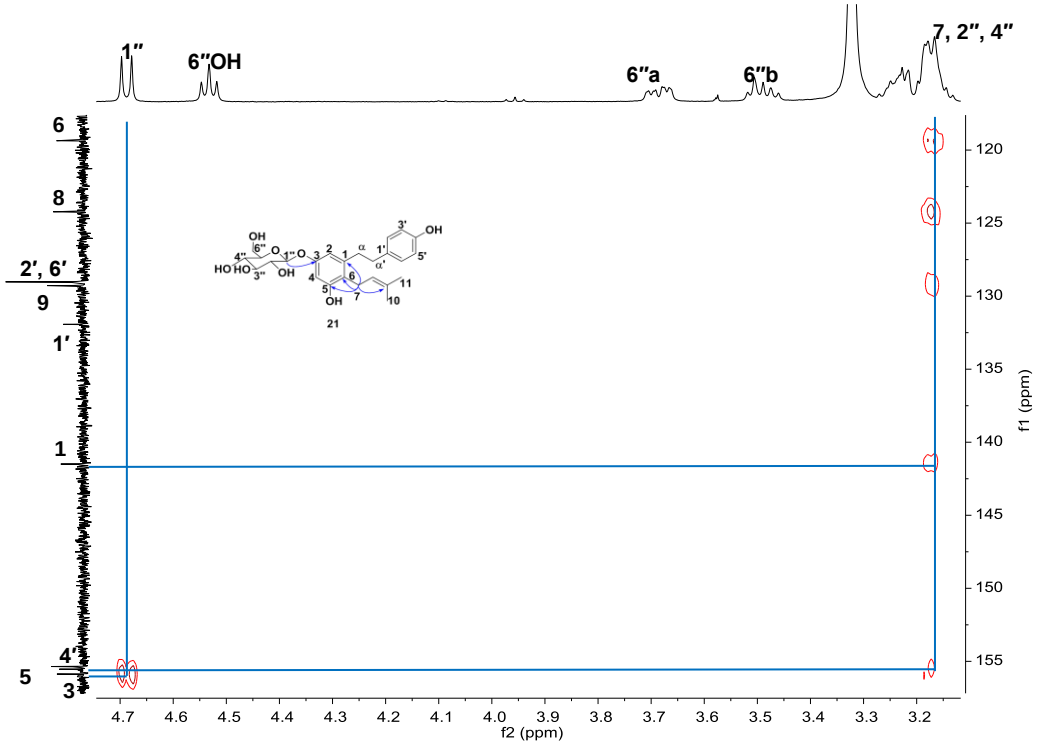

Spectrum S101. The partial enlarged view of HMBC spectrum of **21** in DMSO-d_6.

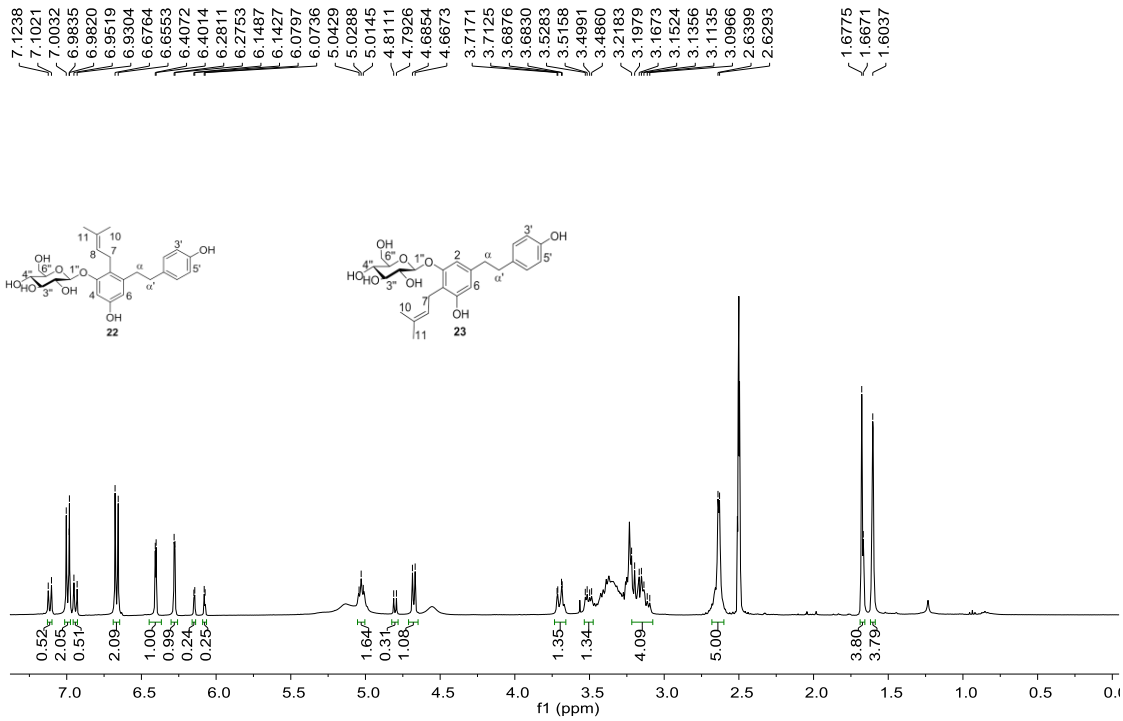

Spectrum S102. ^{1}H NMR spectrum of **22** and **23** in DMSO-d_6 at 400 MHz.

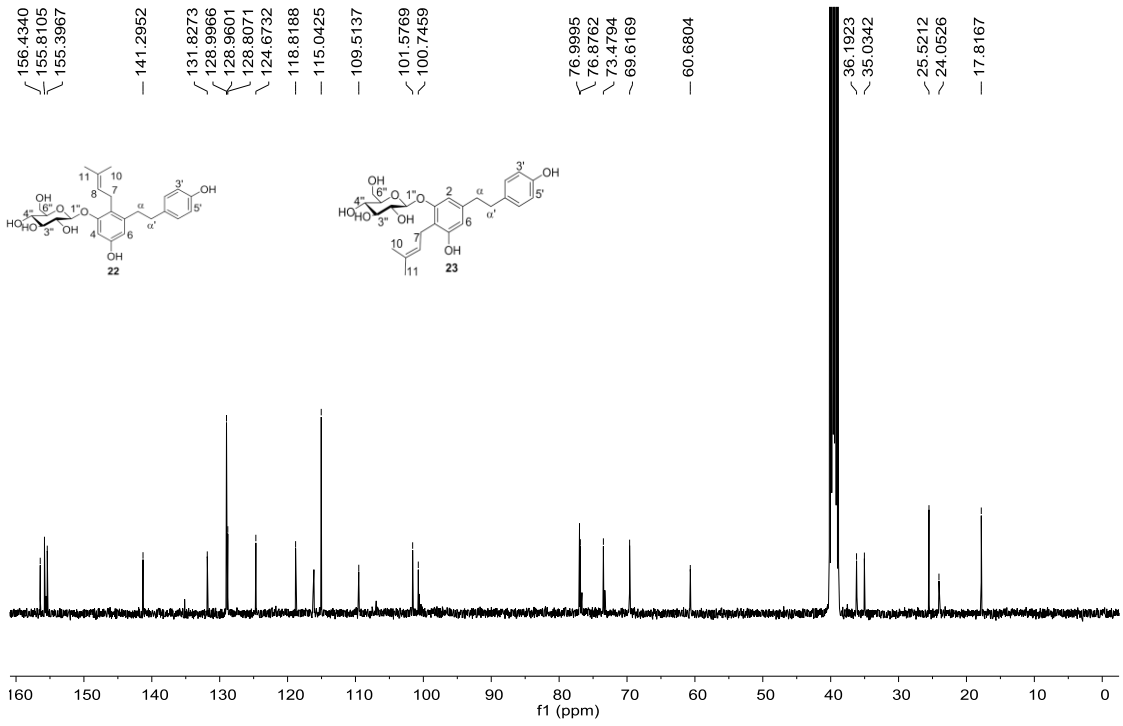

Spectrum S103. ^{13}C NMR spectrum of **22** and **23** in DMSO-d_6 at 100 MHz.

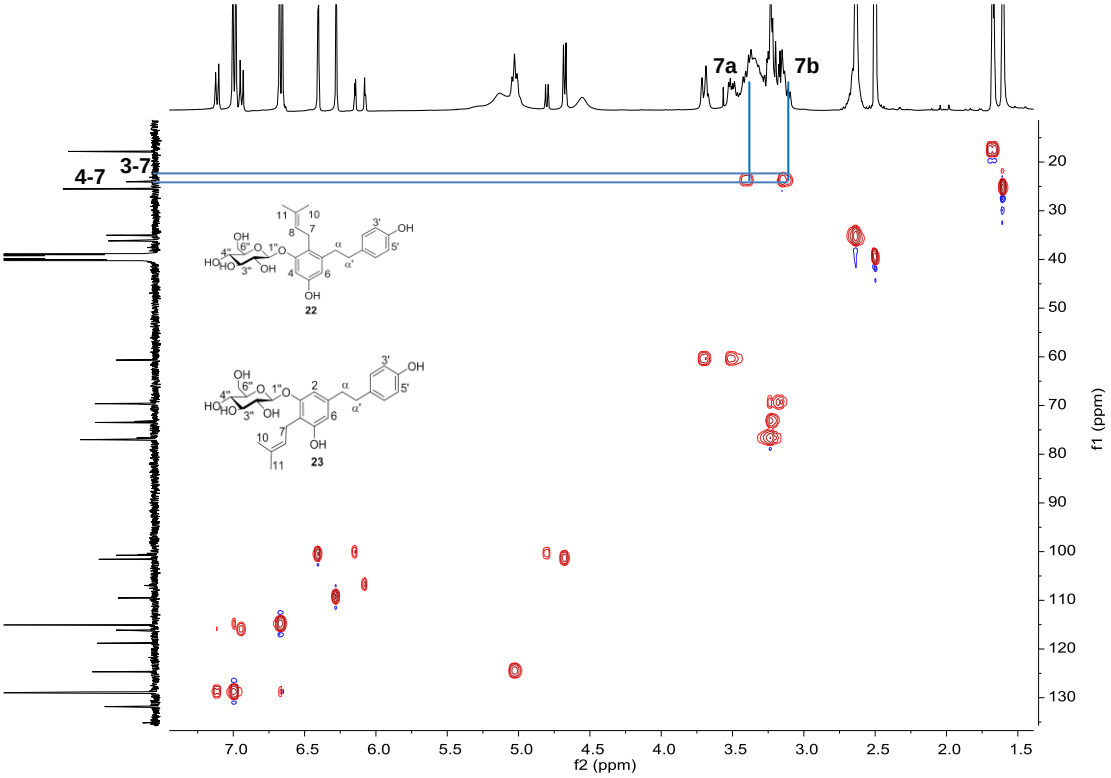

Specrtrum S104. HSQC spectrum of **22** and **23** in DMSO-d_6.

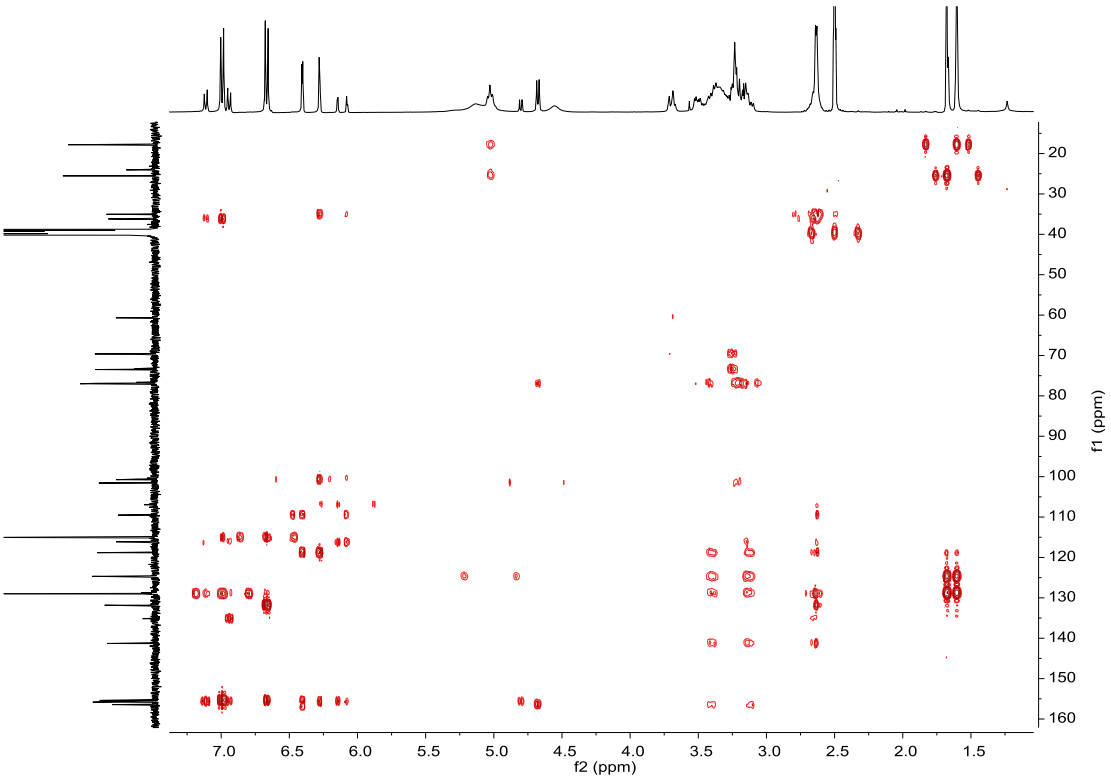

Specrtrum S105. HMBC spectrum of **22** and **23** in DMSO-d_6.

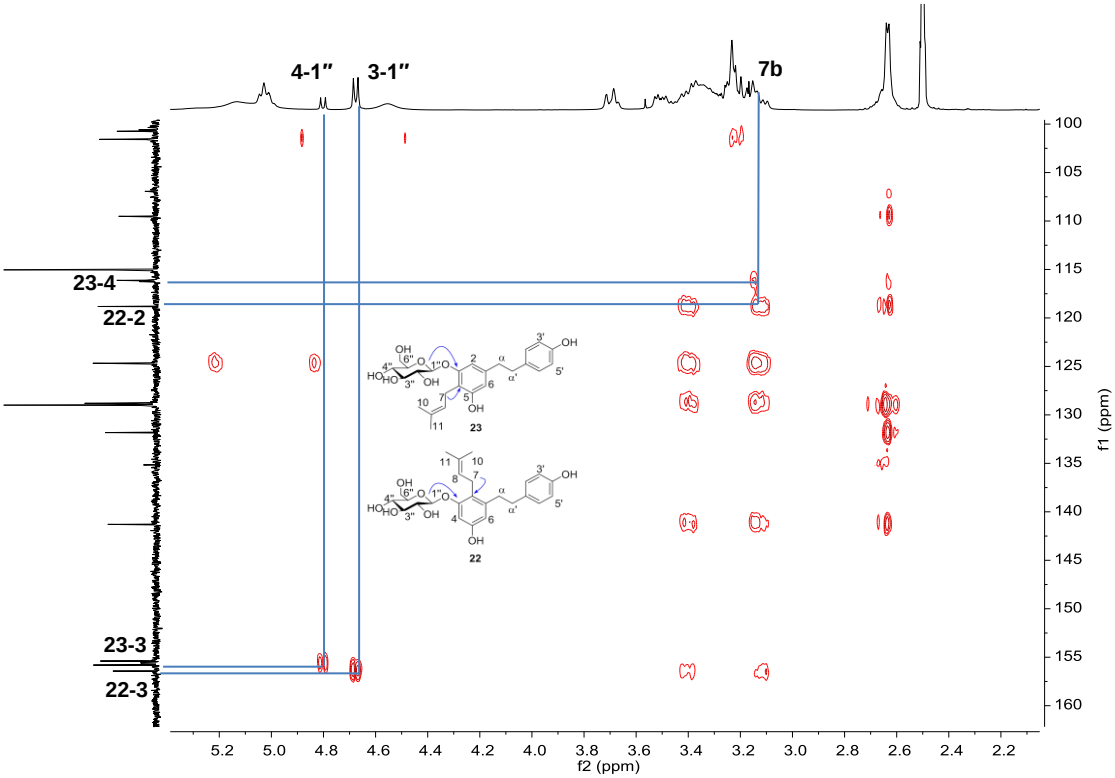

Spectrum S106. The partial enlarged view of HMBC spectrum of **22** and **23** in DMSO-d_6.

References

1. Markham GD, DeParasis J, Gatmaitan J. The sequence of *metK*, the structural gene for *S*-adenosylmethionine synthetase in *Escherichia coli*. *J Biol Chem* 1984;**259**:14505–7.

2. Xie K, Chen R, Chen D, Li J, Wang R, Yang L, et al. Enzymatic *N*-glycosylation of diverse arylamine aglycones by a promiscuous glycosyltransferase from *Carthamus tinctorius*. *Adv Synth Catal* 2017;**359**:603–8.

3. Ehlting J, Büttner D, Wang Q, Douglas CJ, Somssich IE, Kombrink E. Three 4-coumarate: coenzyme A ligases in *Arabidopsis thaliana* represent two evolutionarily divergent classes in angiosperms. *Plant J* 1999;**19**:9–20.

4. Chen H, Kim HU, Weng H, Browse J. Malonyl-CoA synthetase, encoded by acyl activating enzyme 13, is essential for growth and development of *Arabidopsis*. *Plant Cell* 2011;**23**:2247–62.

5. An JH, Kim YS. A gene cluster encoding malonyl-CoA decarboxylase (MatA), malonyl-CoA synthetase (MatB) and a putative dicarboxylate carrier protein (MatC) in *Rhizobium trifolii*: cloning, sequencing, and expression of the enzymes in *Escherichia coli*. *Eur J Biochem* 1998;**257**:395–402.

6. Wang J, Li S, Xiong Z, Wang Y. Pathway mining-based integration of critical enzyme parts for *de novo* biosynthesis of steviolglycosides sweetener in *Escherichia coli*. *Cell Res* 2016;**26**:258–61.

7. Chen R, Gao B, Liu X, Ruan F, Zhang Y, Lou J, et al. Molecular insights into the enzyme promiscuity of an aromatic prenyltransferase. *Nat Chem Biol* 2017;**13**:226–34.

8. Xie K, Chen R, Chen D, Li J, Wang R, Yang L, et al. Exploring the catalytic promiscuity of a new glycosyltransferase from *Carthamus tinctorius*. *Org Lett* 2014;**16**:4874–7.

9. Chen D, Chen R, Wang R, Li J, Xie K, Bian C, et al. Probing the catalytic promiscuity of a regio- and stereospecific *C*-glycosyltransferase from *Mangifera indica*. *Angew Chem Int Ed* 2015;**127**:12869–73.

10. Sui S, Guo R, Xie K, Yang L, Dai J. UGT88B2: A promiscuous *O*-glycosyltransferase from *Carthamus tinctorius*. *Chin Herb Med* 2020;**12**:440–5.

11. Chen D, Fan, S., Chen, R., Xie, K., Yin, S., Sun, L., et al. Probing and engineering key residues for bis-*C*-glycosylation and promiscuity of a *C*-glycosyltransferase. *ACS Catal* 2018;**8**:4917–27.

12. Chen D, Sun L, Chen R, Xie K, Yang L, Dai J. Enzymatic synthesis of acylphloroglucinol 3-*C*-glucosides from 2-*O*-glucosides using a *C*-glycosyltransferase from *Mangifera indica*. *Chem Eur J* 2016;**22**:5873–7.

13. Adesanya SA, Ogundana SK, Roberts MF. Dihydrostilbene phytoalexins from *Dioscorea bulbifera* and *D. dumentorum*. *Phytochemistry* 1989,**28**:773–4.

14. Brand S, Hölscher D, Schierhorn A, Svatoš A, Schröder J, Schneider B. A type III polyketide synthase from *Wachendorfia thyrsiflora* and its role in diarylheptanoid

and phenylphenalenone biosynthesis. *Planta* 2006,**224**:413–28.

15. Mo T, Wang J, Gao B, Zhang L, Liu X, Wang X, et al. Combinatorial synthesis of flavonoids and 4-hydroxy-*δ*-lactones by plant-oringinated enzymes. *Chin J Org Chem* 2015,**35**:1052–9.
16. Akiyama T, Shibuya M, Liu HM, Ebizuka Y. *p*-Coumaroyltriacetic acid synthase, a new homologue of chalcone synthase, from *Hydrangea macrophylla* var. *thunbergii*. *Eur J Biochem* 1999,**263**:834–9.
17. Kettenes-van den BJJ, Salemink CA. Cannabis XIX. Oxygenated 1,2-Diphenylethanes from Marihuana. *Recueil des Travaux Chimiques des Pays-Bas* 1978,**97**:221–2.
18. Hata K, Baba K, Kozawa M. Chemical studies on the heartwood of Cassia garrettiana Craib. II. Nonanthraquinonic constituents. *Chem pharm bull* 1979,**27**:984–9.
19. Edwards RL, Lewis DG, Wilson DV. Constituents of the higher fungi. Part I. Hispidin, a new 4-hydroxy-6-styryl-2-pyrone from *Polyporus hispidus* (Bull.) Fr. *J Chem Soc* 1961:4995–5002.
20. Wang QH, Wang ML, He X, Wang Q. Structural elucidation of two new diphenylethanes from *Artemisia mongolica*. *Chem Nat Compd* 2021,**57**:448–50.
21. Werner SR, Chen H, Jiang H, Morgan JA. Synthesis of non-natural flavones and dihydrochalcones in metabolically engineered yeast. *J Mol Catal B Enzym* 2020,**66**:257–63.
22. Wang J, Liu Y, Liu C, Shi Q. Characterization of the metabolites of gigantol in rat,

dog, monkey, and human hepatocytes using ultra-high-performance liquid chromatography coupled with high-resolution mass spectrometry. *Rapid Commun Mass Spectrom* 2020,**34**:e8810.

23. Majumder PL, Pal S. Cumulatin and tristin, two bibenzyl derivatives from the orchids *Dendrobium cumulatum* and *Bulbophyllum triste*. *Phytochemistry* 1993,**32**:1561–5.

24. Crombie L, Jamieson SV. Dihydrostilbenes of Cannabis. Synthesis of canniprene. *J Chem Soc Perk T 1* 1982:1467–75.

25. Yanagisawa T, Sato S, Maruno M, Nomura T. 5-Lipoxygenase and cyclooxygenase inhibitors for treatment of arachidonate metabolism disorders. Japan, JP07017859 A 1995-01-20.

26. Kyoshi K, Yuka O, Shunji S, Taro N. Cardiovascular agents containing gancaonins and glycerol as Na^+-K^+ ATPase inhibitors, canantagonists, and phosphodiesterase inhibitors. Japan, JP07017857 A 1995-01-20.

27. Zhou B, Wan C. Phenolic constituents from the aerial parts of *Glycyrrhiza inflata* and their antibacterial activities. *J Asian Nat Prod Res* 2015,**17**:256–61.

28. Feng W, Cao X, Kuang H, Zheng X, A new stilbene glycoside from *Dryopteris sublaeta*. *Acta Pharmaceutica Sinica* 2005,**40**:1131–4.